Graz University of Technology

Krump Corinna

From *O*- to *C*-glycoside:

A two-enzyme one-pot conversion

MASTERARBEIT

Zur Erlangung des akademischen Grades einer Diplom- Ingenieurin der Studienrichtung Biotechnologie

erreicht an der

Technischen Universität Graz

Betreuer:

Univ.-Prof. Dipl.-Ing. Dr.techn. Bernd Nidetzky

Dipl.-Ing. Alexander Gutmann

Institut für Biotechnologie und Bioprozesstechnik

2013

EIDESSTATTLICHE ERKLÄRUNG

Ich erkläre an Eides statt, dass ich die vorliegende Arbeit selbstständig verfasst, andere als die angegebenen Quellen/Hilfsmittel nicht benutzt und die den benutzten Quellen wörtlich und inhaltlich entnommenen Stellen als solche kenntlich gemacht habe.

Graz, am …………………………   ……………………………………………..

                                                            (Unterschrift)

STATUTORY DECLARATION

I declare that I have authored this thesis independently, that I have not used other than the declared sources / resources and that I have explicitly marked all material which has been quoted either literally or by content from the used sources.

……………………………   ……………………………………………..

        date   (signature)

ABSTRACT

Catalyzed by UDP-dependent plant glycosyltransferases the glycosylation of flavonoid compounds generates a pool of therapeutically active substances with significant antioxidant activity. However, chemical synthesis of those is cost- intensive and associated with low product yield. In this study, an enzyme- based system for the generation of the antioxidative *C*-glycoside nothofagin is introduced. Phloretin, comprising one of the common phenolic compounds in *Malus sp.*, is converted to phlorizin by the action of *Pc*OGT (*O*-GT from *Pyrus communis*, pear) or to nothofagin via *Os*CGT (*C*-GT from *Oryza sativa*, rice). This system exploits the inherent reversibility of the *O*-glycosyltransferase to generate phloretin and UDP-glucose from phlorizin and UDP, which in turn serve as substrates for the irreversible formation of nothofagin. UDP is regenerated during the formation of the product.

The specific characteristics of both enzymes notably determined the performance of the coupled system, being mainly dictated by pH optima, substrate affinities and stability against the organic solvents. Due to differing pH optima, a reasonable compromise affording sufficient activity of both enzymes was identified. Poor solubility of substrates required the application of organic solvents, the concentration of which strongly influenced enzyme stability; destabilization was avoided by an elevation of the overall protein concentration. Kinetic characterization of *Pc*OGT and *Os*CGT revealed inhibition of both enzymes by high concentration of the aglycon phloretin generated as intermediate product in the *O*-/*C*-glycoside conversion. Usage of high substrate concentrations provoked phloretin accumulation, thereby reducing the overall performance and the final product yield. The *C*-glycosylation reaction was identified to be the most critical parameter.

The described system allows sufficient conversion of the *O*- into the *C*-glycoside associated with the advantages of avoiding expensive sugar-donors and easier product recovery due to the absence of side products. The system performance is strongly governed by the reaction environment regarding pH, solvent, substrate concentration as well as the glycosylation activities. Nevertheless, it was demonstrated that a 75 % yield of nothofagin could be reached employing a fed- batch mode over a longer reaction time.

KURZFASSUNG

Die Glykosylierung von Flavonoid- Verbindungen durch UDP-abhängige, pflanzliche Glykosyltransferasen führt zur Entstehung eines Pools an therapeutisch wirksamen Substanzen mit hoher antioxidativer Aktivität. Allerdings ist die chemische Synthese kostenintensiv und mit niedrigen Ausbeuten verbunden. In der vorliegenden Arbeit wird ein auf Enzymen basierendes System zur Erzeugung des antioxidantischen *C*-Glykosids Nothofagin vorgestellt. Phloretin, eine der häufigsten Phenolverbindungen im Apfel, wird durch *Pc*OGT (*O*-Glykosyltransferase aus *Pyrus communis*, Birne) zu Phlorizin oder durch *Os*CGT (*C*-Glykosyltransferase aus *Oryza sativa*, Reis) zu Nothofagin umgesetzt.

Dieses System nützt die Reversibilität der *O*-Glykosyltransferase um Phlorizin und UDP zu Phloretin und UDP-Glukose umzusetzen, welche wiederum als Substrate für die *C*-Glykosylierungsreaktion zu Nothofagin verwendet werden. UDP wird während der Bildung des Produktes regeneriert.

Die spezifischen Eigenschaften der einzelnen Enzyme bestimmen die Leistung des Systems maßgeblich. Großen Einfluss haben vor allem Parameter wie pH- Optima, Substrataffinitäten und die Stabilität gegenüber organischen Lösungsmitteln. Da *Pc*OGT und *Os*CGT unterschiedliche pH-Optima aufweisen, wurde eine Kompromisslösung gefunden, die ausreichende Aktivität beider Enzyme gewährleistete. Die moderate Löslichkeit der Substrate erforderte den Einsatz von organischen Lösungsmitteln, deren Konzentration großen Einfluss auf die Enzymstabilität zeigte. Eine Verringerung der Destabilisierung bei der Verwendung von hohen Konzentrationen an DMSO wurde durch eine Erhöhung der Konzentration an Gesamtprotein erreicht. Die kinetische Charakterisierung der beiden Enzyme zeigte eine Substrathemmung durch hohe Konzentrationen an Phloretin. Der Einsatz von hohen Substratkonzentrationen führte zur Aufstauung des Aglykons, wodurch die Gesamtleistung und die Ausbeute des Endprodukts reduziert wurden. Die *C*-Glykosylierung wurde als besonders kritischer Parameter identifiziert.

Das beschriebene System erlaubt die erfolgreiche Umwandlung eines *O*-Glykosids in ein *C*-Glykosid, und ist mit den Vorteilen der Vermeidung teurer Substrate und der vereinfachten Produktgewinnung aufgrund der Abwesenheit jeglicher Nebenprodukte verbunden. Die Leistung des Systems wird stark von Reaktionsbedingungen wie pH- Wert, Lösungsmittelkonzentration, Substratkonzentration sowie Enzymeinsatz determiniert. Dennoch konnte eine Ausbeute von 75 % unter Verwendung eines Fed- Batch- Modus über eine längere Reaktionszeit erreicht werden.

TABLE OF CONTENTS

1 INTRODUCTION

1.1 Glycosylation

Glycosylation reactions refer to the transfer of a sugar from an activated donor to different acceptors. This results in the formation of poly-, di- and monoglycosides of non- carbohydrates such as proteins, lipids, steroids and other small molecules and plays an important role in the biosynthesis of natural products, as it leads to an enhancement of their solubility and stability and aids the regulation of their chemical properties and bioactivities (1), (2). Oligosaccharides and glycoconjugates have been demonstrated to be mediators of important biological processes and their high therapeutic potential turned to be one of the "hot" subjects in biochemistry (3).

For example, flavonoids are a highly diverse group of plant natural products with over 7000 known compounds (4) which often exist in glycosylated forms. Thus, there is great interest in the development of chemical and enzymatic tools to diversify natural product glycosylation patterns. Reactive and toxic aglycones are transformed into more stable and non- reactive species and the attachment of hydrophilic sugar moieties to hydrophobic acceptors causes an increase in water solubility.

The vast majority of drug leads are directly derived from or inspired by natural products, most of which are glycosylated (1). Sugar attachments have remarkable influences ranging from modulating pharmacology and pharmacokinetic properties to dictating tissue specificity (5). Although most sugar linkages are achieved through *O*-glycosidic bonds, also *N*-, *C*- and *S*-glycosides are known (6) as shown in Figure 1.
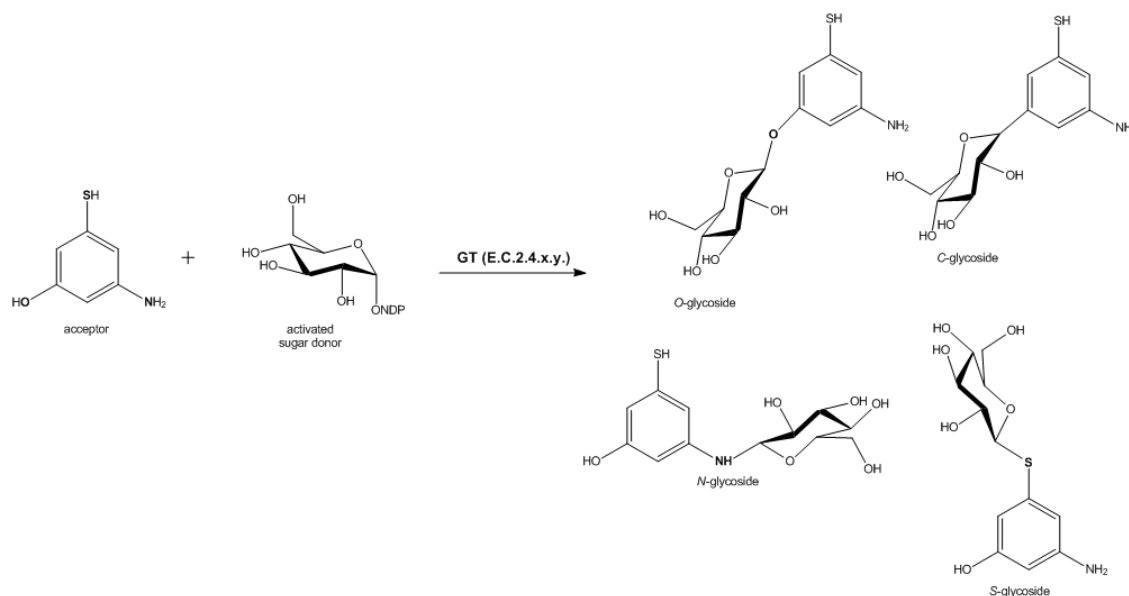
Figure 1: The type of glycosyltransferase is decisive for O-, N-, C- or S-glycosidic bond formation with a suitable acceptor

The reactions are carried out by glycosyltransferases (EC 2.4.x.y.), which are a highly divergent, polyphyletic, multi- gene family (7) classified into 91 different subfamilies according to the degree of primary sequence identity found at the CAZY database (http://www.cazy.org/) (8), (9). Being present in both prokaryotes and eukaryotes, these enzymes generally display high specificity towards the glycosyl donor and the acceptor.

1.2 UDP- dependent plant glycosyltransferases

Belonging to family 1 GTs, UDP-dependent glycosyltransferases (UGTs) catalyze the transfer of a sugar moiety from an activated UDP-sugar to a specific acceptor molecule (7), which often comprises the last step in the biosynthesis of natural plant products (2).

Originally defined by Hughes and Hughes (10), they possess an apparently conserved UGT-defining sequence motif at the C-terminus, namely the PSPG (Putative Secondary Plant Glycosyltransferase) defining motif (7), which is involved in sugar donor binding. It is comprised by 44 amino acids, ten of which are highly conserved among different UGT´s (two α-helices, three β-sheets; see Figure 4), indicating an involvement in UDP-sugar donor recognition (11).
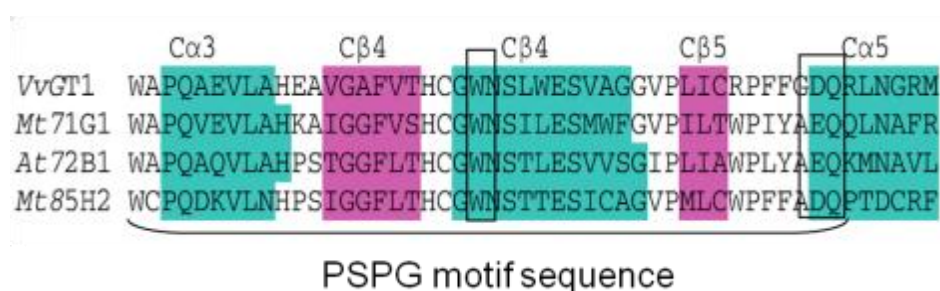
Figure 2: Putative Secondary Plant Glycosyltransferase defining motif sequence Overlay of the conserved sugar interacting residues (W, D/E and Q) from the four solved structures of plant GTs, showing interactions with the sugar part of UDP-sugar donor (11)

UDP-glycosyltransferases that contain the PSPG motif mainly have a share in the synthesis of bioactive natural products, plant growth control and cell homeostasis as well as in detoxification of xenobiotics (2), (12). Substrate specificity of plant UGTs involves regioselective and regiospecific recognition of a sugar acceptor as well as a UDP-sugar donor. The most commonly used sugar is UDP-glucose, although UDP-galactose, UDP-xylose and UDP-glucoronic acid are also used (13); generally a high specificity for the sugar donor is observed (14), (15), (16), (17), (18).

1.2.1 UGT structure

The crystal structure of UGTs has only recently been resolved with the first being *Medicago truncatula* UGT71G1 (19). Additional three plant UGTs have been subsequently crystallized: *Vitis vinifera* anthocyanidin 3-*O*-glucosyltransferase (20), *Medicago truncatula* UGT85H2 (21) and *Arabidopsis thaliana* UGT72B1 (22); a high conservation of secondary and tertiary structures was observed (23).

The folds of glycosyltransferases have been shown to primarily consist of α/β/α-sandwiches, similar to the Rossmann- type fold (six parallel β-sheets with 321456 topology). Two structural families have been described, called GT-A and GT-B (Figure 3).

GT-A fold   **GT-B fold**
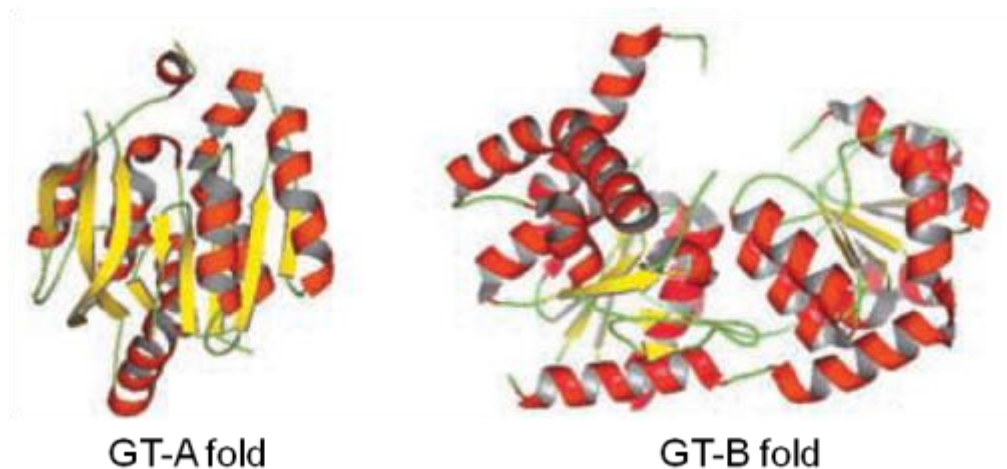
Figure 3: The representative GT protein structures These structures either consist of a single domain with parallel β-strands flanked on either side by α-helices (GT-A fold), or two Rossmann fold- like domains that are separated by a deep cleft (GT-B fold) (24)

The GT-A family enzymes are characterized by the common DxD- motif responsible for the interaction with the nucleotide donor; their activity is dependent on the presence of a divalent cation, being either Mn^{2+} or Mg^{2+} (25), (26).

Proteins belonging to the GT-B fold family are comprised by two separate Rossmann-domains connected via a flexible linker region and have the catalytic site embedded between the domains as a deep narrow cleft. The sugar-donor binding pocket is mainly formed by residues from the C-terminal domain, whereas the N-terminal domain is mainly responsible for binding of the acceptor molecule. One side of the donor binding pocket is flanked by the PSPG motif with the highly conserved Rossmann- fold featuring an α/β/α-structure where residues at the N-terminal end are positioned towards the UDP-sugar donor (11).
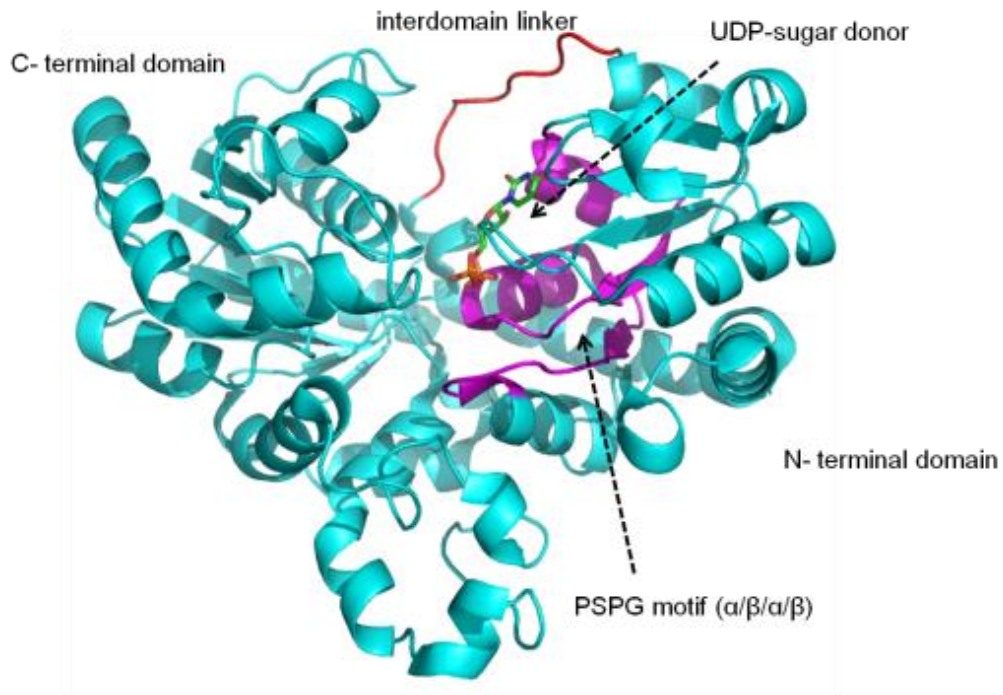
Figure 4: Crystal structure of UGT78G1 (*Medicago truncatula* flavonoid 3-*O*-glycosyltransferase; PDB: 3HBF) The interlinking residues between the two domains are indicated in red; residues comprising the PSPG motif for sugar- donor interaction are shown in purple. The PSPG motif is set up by two repeating α-helix- β-sheet structures. The UDP-sugar donor is shown in atom- color code embedded between residues of the PSPG motif

Up to now, there is no clear evidence of a bound metal ion being associated with catalysis although divalent cations may be required for full activity of enzymes displaying a GT-B fold. Plant UDP-dependent glycosyltransferases commonly adopt the GT-B fold (8).

1.2.2 UGT reaction mechanism

Further classification of GTs is performed according to their reaction mechanism, being either inverting or retaining depending on the configuration of the anomeric carbon atom upon formation of the new glycosidic bond. Inverting glycosyltransferases catalyze group transfer reactions with a net inversion of the stereochemistry at the anomeric reaction center of the donor, whereas retaining glycosyltransferases catalyze group transfer reactions with net retention of the anomeric reaction center (27).
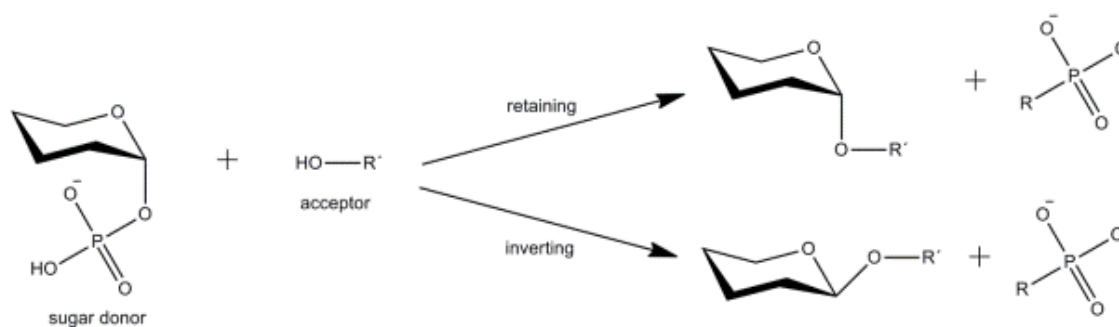
Figure 5: GT´s can be either inverting or retaining with respect to the anomeric configuration of the sugar donor

The plant UDP-dependent glycosyltansferases usually act according to an inverting reaction mechanism, similar to a direct displacement S_N2- like reaction mechanism, where a side chain of a residue located in the active site functions as a base catalyst by deprotonating the incoming nucleophile of the acceptor (27) and thereby activating it for nucleophilic attack on the anomeric carbon of the sugar donor. This is further facilitated by the phosphate leaving group of the sugar donor. Conversion most likely involves the formation of an oxocarbenium- like transition state (Figure 6).
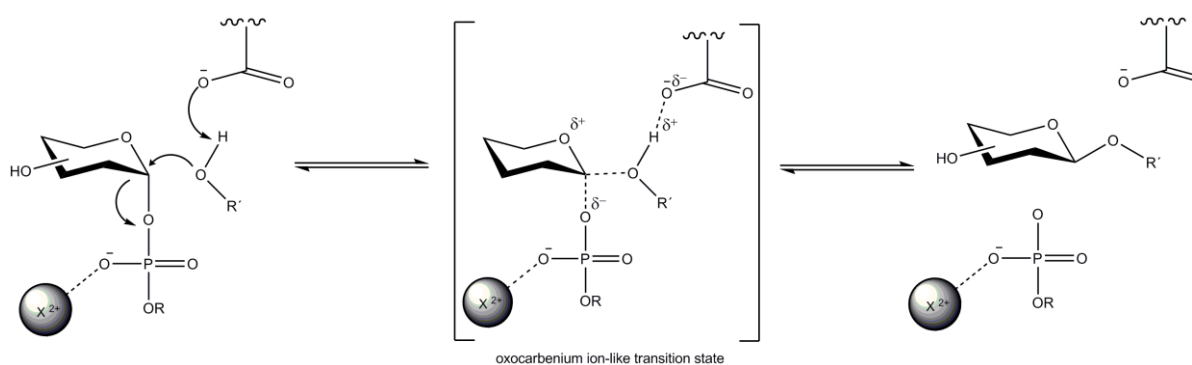
Figure 6: Inverting GT reaction mechanism Inverting glycosyltransferases utilize a direct- displacement S_N2-like reaction that results in an inverted configuration of the anomeric carbon via a single oxocarbenium ion-like transition state (27)

1.3 *O*- vs. *C*-glycosylation reaction

Compared to ubiquitous *O*-glycosyltransferases (*O*-GTs), *C*-glycosyltransferases (*C*-GTs) are very rare and their reaction mechanism is yet poorly elucidated (6). Substrates for *C*- are also available for *O*-glycosylation, albeit no clear *C*-glycosylation motif was identified yet. Based on synthetic chemistry, two possible routes for the enzymatic *C*-glycoside formation can be suggested (28) (29).
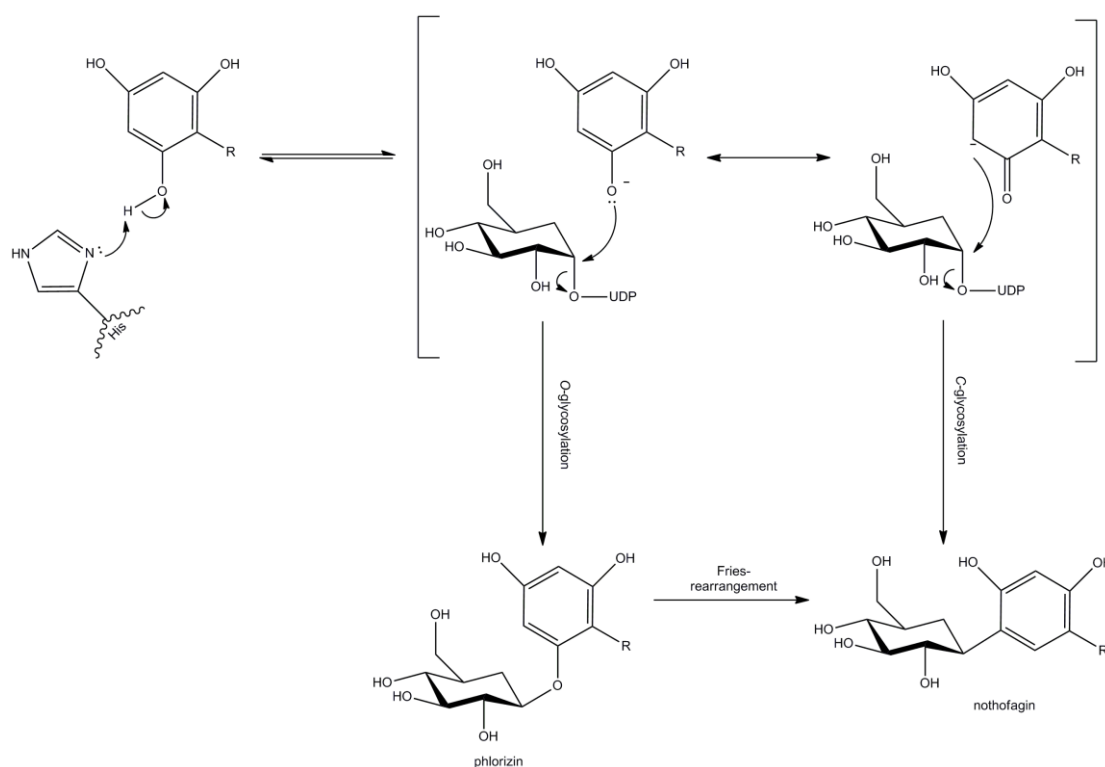
Figure 7: Proposed reaction mechanisms of *O*- and *C*-glycosyltransferases The *C*-glycoside is formed either after activation of the acceptor by deprotonation and rearrangement to a *C*-glycoside via an *O*-glycoside intermediate, or directly via a Friedel- Crafts- like reaction (29)

Both routes (Figure 7) start with the activation of the OH- group through deprotonation by a catalytic base. For *O*-glycosylation it has been demonstrated that the oxyanion attacks the anomeric carbon of the sugar donor in an S_N2- like reaction mechanism leading to the formation of the *O*-glycosidic linkage. This comprises also the first step on the two- strep rearrangement to the ortho- *C*-glycoside. The second route is a single Friedel- Crafts- like mechanism, where the delocalization of the negative charge of the ortho- carbons of the phenoxy ion enables direct formation of the *C*-glycoside via a nucleophilic attack of the carbanion instead of the oxyanion. It can be suggested that eventual differences in the active sites of *O*-GTs and *C*-GTs are not due to different binding of the substrate, but have a mechanistic relevance (29).

1.4 Flavonoids
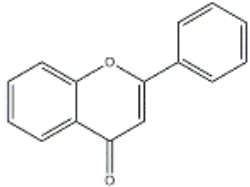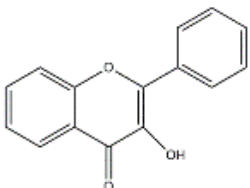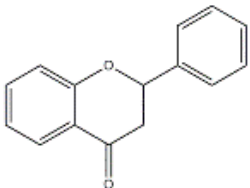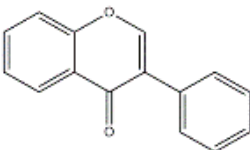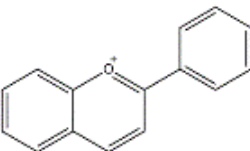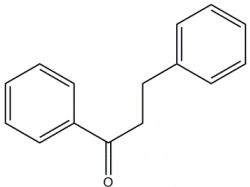
Flavonoids comprise a broad class of low molecular weight secondary plant polyphenols exhibiting significant antioxidant and chelating properties. They are widely recognized as essential health beneficial constituents of nutrition and are abundantly found in green vegetables, fruit, chocolate and tea (see Table 1). Mostly they are glycosylated, whereas 3-*O*-glycosides are most common (30). The most common glycosidic unit is glucose, albeit others like glucorhamnose-, galactose- and arabinose-links also exist (31).

Dietary flavonoids are diverse and vary according to hydroxylation pattern, conjugation between aromatic rings, glycosidic moieties and methoxy groups. Polymerization of the nuclear core structure yields tannins and other complex species occurring in red wine, grapes and black tea (31).

According to their structure, flavonoids are to be classified into different categories, such as chalcones (1,3-diaryl-2-propen-1-ones), which lack a heterocyclic C- ring and dihydrochalcones, which lack an α-β- double bond. The category of dihydrochalcones comprises substances such as phloretin [β-(4-hydroxyphenyl)-1-(2,4,6-trihydroxypropiophenone)] and its glycoside phlorizin (phloretin-2-β-D-glucose).

The ability of a flavonoid to inhibit free-radical mediated events is governed by its chemical structure. Multiple hydroxyl groups confer substantial antioxidant, chelating and prooxidant activity to the molecule. Double bonds and carbonyl functions in the heterocycle or polymerization of the nuclear structures increases the activity by affording a more stable flavonoid radical through conjugation and electron delocalization (32).

Table 1: Classification, structure, food sources of dietary flavonoid antioxidants (33)

general structure	flavonoid	dietary sources	effect
flavones			
	chrysin apigenin rutin luteolin & glycosides	fruit skins red wine red pepper	antioxidant
flavonol			
	kaempferol quercetin myricetin	black tea onion tomatoes berries olive oil	antioxidant (inhibition of CYP450 activity)
flavanone (dihydroflavone)			
	naringin naringenin taxifolin hesperidin	red wine citrus fruits	antioxidant; reduction of atherosclerotic plaques, reduction of carcinogenesis
isoflavone			
	genistin genistein daidzin daidzein	soybean	reduction of carcinogenesis; cardio protection (reduction of LDL cholesterol)
Anthocyanidin			
	agigenidin cyanidin	colored fruits	antioxidant; protection against UV- light; scavenging of free radicals
dihydrochalcones			
	nothofagin phloretin aspalathin	apples, rooibos tea	antioxidant

1.4.1 Flavonoids as antioxidants

The generation of reactive species of oxygen *in vivo* largely contributes to the development of various human diseases, such as cancer, cardiovascular as well as pulmonary and neurological diseases (34). Hence, substances that can act as protective agents against these reactive species may be useful for therapy. According to this, it is suspected that the positive health effects of flavonoids and derivatives thereof can be attributed to their antioxidant activity (33). The ability of flavonoids to transfer electrons and free radicals and chelate metal catalysts (35) is ascertained to cardio protective effects (36), (37), for example the oxidation of LDL can be inhibited.

Although it was reported (38) that with increasing number of glycosidic moieties the antioxidant activities of flavonol glycosides seems to decrease, the attachment of sugar residues to flavonoid compounds is advantageous in terms of stability and bioavailability.

For the glycosylated dihydrochalcones nothofagin and aspalathin from rooibos extracts it was shown that these substances exhibit high antioxidant capacities when compared to commercially available substances (Trolox®; Hoffman- LaRoche, CAS-Nr: 53188-07-1). It was confirmed, that a hydroxyl group at the 2´- position of the A- ring of dihydrochalcones, which is formed by reducing the flavanone C-ring, is essential for radical scavenging properties (39). Chemically, dihydrochalcones can be prepared by catalytic hydrogenation under alkaline conditions from flavones.

1.4.2 Phloretin

Phloretin (3-(4-hydroxyphenyl)-1-(2,4,6-trihydroxyphenyl)propan-1-one) is a product of the phenylpropanoid pathway (40); derivatives thereof comprise more than 90 % of the soluble phenolic compounds in leaves of *Malus x domestica* (41). Various mono- and diglycosides of phloretin with the sugar moiety being attached either at position 2´or 4´ have been described from different *Malus* species (42), (43).
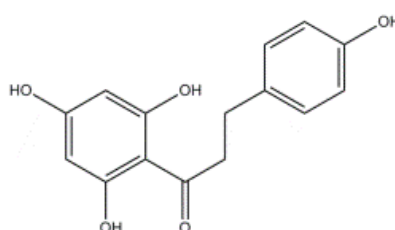

Figure 8: Structure of the dihydrochalcone phloretin

Rezk et al (34) proposed that the antioxidant activity of phloretin is likely due to a stabilization of the radical that is formed after hydrogen abstraction. This reaction is also suspected to involve a keto- enol tautomeric transformation of the carbonyl group.

The benefits of phloretin derivatives for human health are well documented by various publications and patents; most of which relate to diabetes, stress hyperglycemia, obesity and antioxidative activity. The substances also serve as longevity- extending agents in foods, beverages, food additives, pharmaceuticals and cosmetics (44), (45).

Phloretin is commercially available as pharmaceutical for the treatment of oxidative skin aging ("Phloretin CF" Laboratories SkinCeuticals). SkinCeuticals combined vitamins C and E with phloretin and ferulic acid and thereby developed a potent agent against light- induced formation of thymine- dimers leading to skin wrinkle formation and acts protective for ceratinocytes, melanocytes and fibroblasts against oxidative damages by free radicals.

1.4.3 Flavonoid *O*-glycoside: Phlorizin
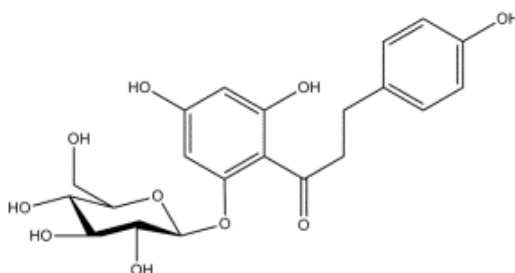
Figure 9: Structure of phlorizin, the main *O*-glycoside of phloretin

The most prominent phloretin 2´-*O*- glycoside (phlorizin) is generated by the glycosylation of phloretin at position 2´ in the presence of uridine-5-diphosphate-glucose catalyzed by a dihydrochalcone 2´-*O*-glycosyltransferase shown in Figure 10 (46). It has attracted high scientific interest by its use as a pharmaceutical and by being a tool for human renal physiology research. Its major pharmaceutical function is the production of renal glycosuria and the blockage of intestinal glucose adsorptions (47).

Phlorizin is highly abundant in apple trees (*Malus domestica*), while other species accumulate only low amounts of phlorizin. The closely related *Pyrus sp.* (pear) does not accumulate phloretin derivatives (48). This could be explained by the fact, that the cDNAs encoding for enzymes involved in phlorizin biosynthesis in apple are not all present in pear.
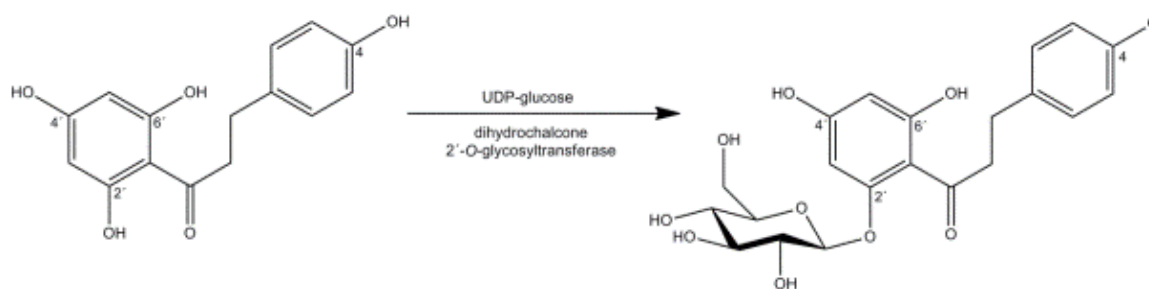
Figure 10: Phlorizin is formed by glycosylation at the 2´- position of phloretin by a dihydrochalcone 2´-O-glycosyltransferase (e.g. *Pc*OGT)

Since phlorizin was isolated in the early 1800s for the first time, it plays an important role in diabetes and renal physiology research (49). It was suspected to affect renal glucose transporters and thereby offer a new attempt for the treatment of hyperglycemia. Along with the examination of phlorizin effects, SGLT2s (sodium- dependent glucose transporters 2) were identified as being responsible for glucose reabsorption from the urine. Analogs of phlorizin with a *C*-glycosidic linkage have been developed that circumvent bioavailability and biostability problems of phlorizin, namely dapaglioflozin and canaglioflozin (49), and are in use for diabetes therapy.

## 1.4.4 Flavonoid *C*-glycosides: Nothofagin and Aspalathin

Nothofagin and aspalathin, two *C*-linked dihydrochalcone glycosides related to phlorizin, are the principal flavonoid constituents in green rooibos (50). Aspalathin differs from nothofagin (the 3´-*C*-β-ᴅ- glycoside of phloretin) by its additional hydroxyl- group at position 3 (Figure 11). Due to their preeminent stability to spontaneous and enzyme- catalyzed hydrolysis, *C*-glycosides are outstanding in the class of flavonoid dihydochalcones. Therefore, these substances have aroused particular interest for medicinal use as isofunctional analogues of the corresponding *O*-glycosides; they potentially offer the important advantage of improved *in vivo* half- life (29).

Nothofagin was first isolated from the heartwood of *Nothofagus fusca*, at present the only natural source of nothofagin besides *Aspalathus linearis* (rooibos) (51). It belongs to the group of dihydrochalcones and serves as phenolic antioxidant (52). Nothofagin, compared to aspalathin, shows slightly less potential to act as antioxidant in aqueous solution (53) and is suspected to exhibit a slightly lower protecting effect against Fe(II)- induced lipid peroxidation (54).

The differences in their antioxidant effects in hydrophobic or hydrophilic environments could be explained by differences in the conformation of aspalathin and nothofagin, as well as by the absence of a catechol moiety in the nothofagin molecular structure (54).

Contributing factors to their antioxidant activity are mainly the C-2´- and C-6´- hydroxyl group as well as the keto- enol tautomerism (54). Krafcyz et al (53) demonstrated radical cation scavenging activity and inhibition of LDL oxidation by nothofagin and aspalathin. Both substances can be considered as direct precursors of various other biologically interesting *C*-aryl flavonoid natural products (55).
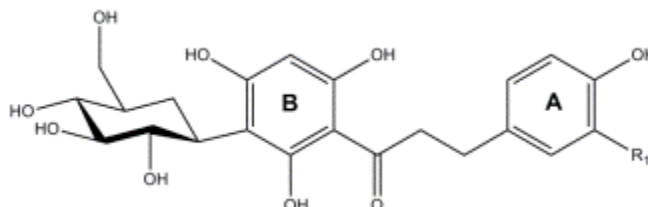

Figure 11: Structure of dihydrochalcones (e.g. nothofagin with R_1= H, aspalathin with R_1= OH)

Chemically, the natural glycosyl flavonoids can be synthesized in eight steps from tribenzyl glucal, tribenzylphloroglucinol and 4-(benzyloxy)phenyl acetylene or 3,4-bis(benzyloxy)phenyl acetylene. The key step in the reaction is the coupling of 1,2-di-*O*-acyl-3,4,6-tribenzylglucose with tribenzylphloroglucinol utilizing a highly stereoselective Lewis acid, which then gives rise to the corresponding β-*C*-aryl-glycosides. With this system the natural glycosyl flavonoids nothofagin and aspalathin can be synthesized with about 28 % and 20 % overall yield (56), respectively.

Nothofagin is hardly commercially available and its chemical synthesis is associated with high costs and low product yield; therefore enzymatic synthesis from available natural starting materials would be beneficial for the investigation of this substance and its effects on human health.

1.5 Reversible glycosyltransferases

Generally, glycosyltransferases are perceived as unidirectional enzymes driving the formation of glycosidic bonds from nucleotide disphosphate sugar (NDP-sugar) donors and glycon acceptors (57). Glycosyltransfer reversibility may be utilized for the synthesis of valuable rare NDP-sugars, for the exchange of a sugar moiety for another on core scaffolds or for the transfer of sugars between different scaffolds, thereby increasing the diversity of natural products. This suggests GT- catalysis being of greater versatility and utility than was previously appreciated (58).

1.5.1 Reverse glycosylation

Zhang and coworkers (58) introduced four GTs from two different natural biosynthetic pathways (calicheamicin and vancomycin) possessing ability to catalyze reversible reactions and thereby easily exchanging sugars and aglycons.

GalG1 and GalG4 (calicheamicin) and GtfD and GtfE (vancomycin), respectively, were shown to catalyze three novel reactions: (i) the synthesis of exotic NDP-sugars from natural glycosides (Figure 12, A) , (ii) the exchange of natural glycosides with exogenous carbohydrates present as NDP-sugars (Figure 12, B), and (iii) the sugar- transfer from one product backbone to a different natural- product scaffold (Figure 12, C).
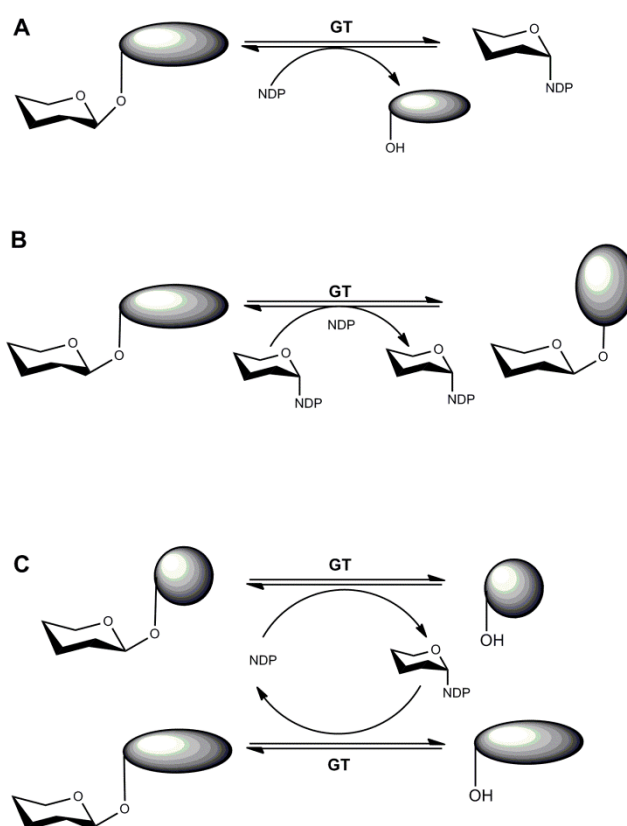
Figure 12: Schematic representation of reverse glycosyltransferase catalysis (A) NDP-sugar synthesis via reverse glycosyltransfer, (B) GT- catalyzed sugar exchange reaction to exchange native natural product sugar appendages with alternative sugars supplied as exogenous NDP-sugars, (C) generalized scheme for aglycon exchange reaction wherein a sugar is excised from one natural product (as an NDP-sugar) and subsequently attached to a distinct aglycon acceptor. The interchange of aglycones from different compounds requires multiple GTs, whereas the interchange of aglycones from a single natural product class is generally accomplished via one GT.

One application of reversing the glycosyltransfer constitutes the use of natural glycosylated products as source of activated sugars or the interdependent change of aglycones by combining of two GTs. The basis for this application is that most glycosyltransferases act also in a

reversible manner, meaning that they are able to catalyze both the forward and backward reaction.

Using this approach, NDP-sugars can be harvested from glycosylated natural products by employing the corresponding glycosyltransferase and can be attached to a second natural product utilizing a different GT. This is of great importance, since various activated sugars involved in natural product biosynthesis are difficult to obtain synthetically (59).

Minami and co- workers (60) postulated a new aglycon switch approach composed of two reactions: the in- situ generation of NDP-sugar from natural glycoside by reverse reaction, which subsequently transfers simultaneously the transient NDP-sugar to a targeted acceptor by itself.

In this scenario, supplementation of an appropriate NDP is necessary as a chemical initiator (Figure 13).
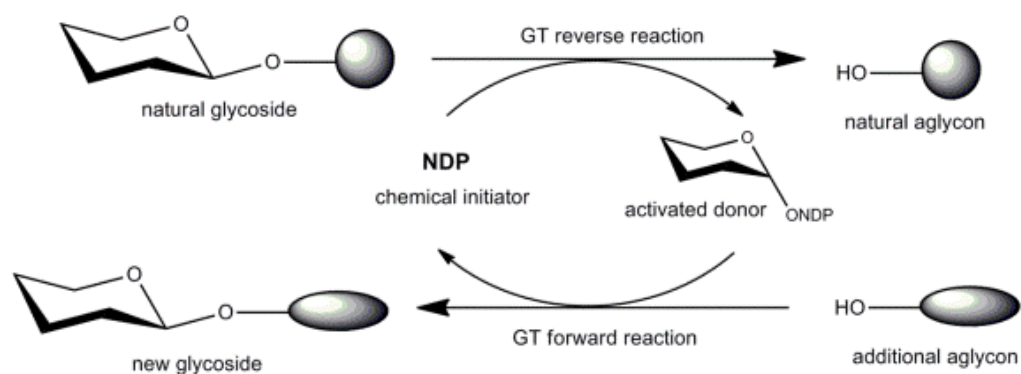

Figure 13: Aglycon switch New enzymatic aglycon switch approach using natural glycoside, NDP, and additional aglycon in a strict stereo- and regioselective manner without previous NDP-sugar synthesis and recovery of the glycosyl donor (60)

1.5.2 Glycorandomization

Apart from conventional chemical synthesis, natural product chemical diversity can be further increased via glycorandomization, allowing the generation of libraries of compounds only differing in their glycosyl substituent. Chemoenzymatic glycorandomization is dependent upon the substrate promiscuity of enzymes to activate and attach sugars to natural products (5).

By employing inherent or engineered substrate promiscuous nucleotidyltransferases, chemoenzymatic glycorandomization provides a short activation pathway for the synthesis of nucleotide diphosphosugar (NDP-sugar) donor libraries. These activated donor libraries, in turn, serve as substrates for natural product glycosyltransferases, thereby providing rapid chemoenzymatic means to diversify natural product- based scaffolds (61). Such multi- enzyme, single- vessel reactions offer an attractive alternative to the extensive synthetic manipulation typically required for chemical glycosylation strategies (61).
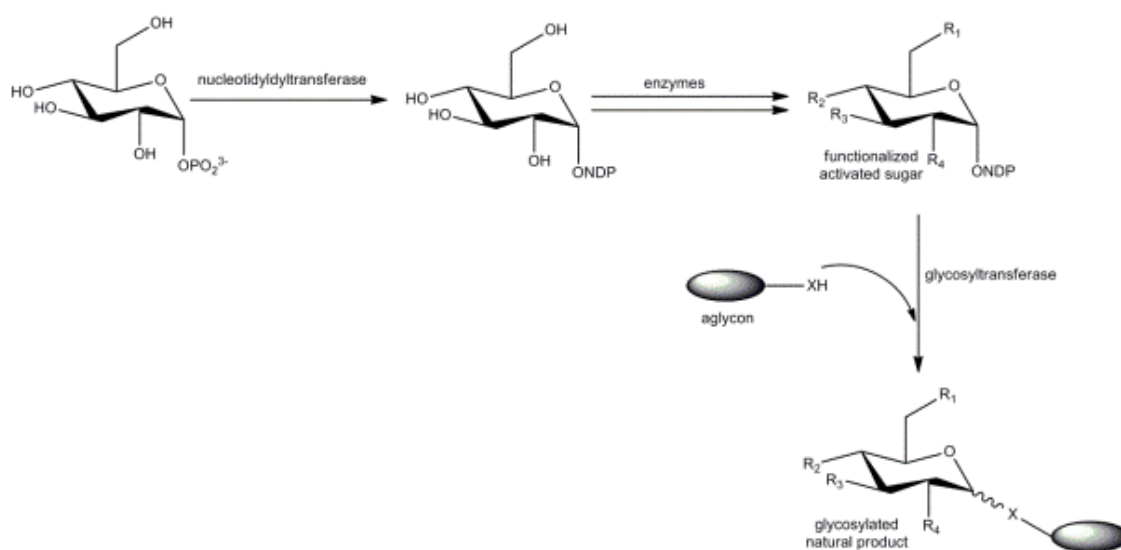
Figure 14: Chemoenzymatic glycorandomization General biosynthetic strategy initiated by NDP-sugar formation (via nucleotidyltransferases) and followed by multi- enzyme functionalization before glycosyltransferase- catalyzed glycosylation (5)

Williams and co- workers (62) presented the application of glycorandomization employing recombinant *E.coli* strains to allow production of a range of small molecule glycosides. Their strategy based on engineered promiscuity of three enzymes, an anomeric kinase, a sugar-1-phosphate nucleotidyltransferase and a glycosyltransferase, and on the assumption of small molecules being able to freely diffuse into bacterial cells.
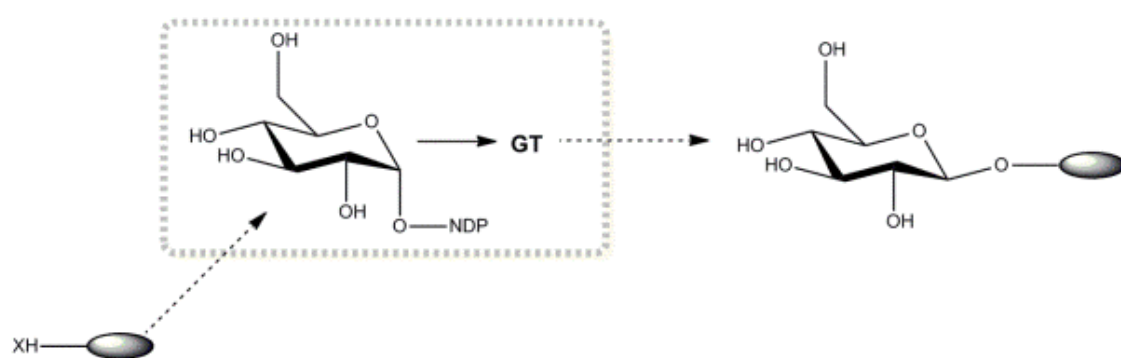
Figure 15: *In vivo* glycorandomization employing bacterial host systems Aglycones are fed into engineered bacterial host cells expressing a glycosyltransferase that is able to use endogenous dTDP/UDP-glucose as glycosyl donor (62)

In vitro glycorandomization provides a powerful tool for altering the glycosylation patterns of natural products and therapeutics. The advantages of the *in vivo* system are given by means of high permeability of small molecule acceptors and sugars of engineered *E.coli*, rendering the system amenable to standard large scale fermentation. The corresponding secretion of novel glycoside products greatly relieves the purification of the desired products (62).

1.6 Glycosyltransferases used in this thesis

Two family 1 inverting plant glycosyltransferases with GT-B fold were used in this study. Both enzymes readily catalyze the glycosylation of the dihydrochalcone acceptor phloretin using UDP-glucose as sugar donor. Both enzymes, however, differ in the type of glycosidic bond formation. Whereas *Os*CGT (*C*-glycosyltransferase from *Oryza sativa* – rice) catalyzes the formation of the 3'-*C*-β-D-glucoside nothofagin (Figure 18), *Pc*OGT (*O*-glycosyltransferase from *Pyrus communis* – pear) forms the 2'-*O*-β-D-glucoside phlorizin (Figure 20). In contrast to the *O*-glycosylation by *Pc*OGT, the *C*-glycosylation of *Os*CGT is not reversible.

As for most family 1 plant GTs, the enzymatic activity is based on a catalytic dyad of His and Asp/Ile, for *Pc*OGT and *Os*CGT, respectively. An alignment of the two enzymes revealed a sequence similarity of 30 %, and it was suggested that the arrangement of catalytic residues is mainly responsible for distinguishing between *O*-and *C*-glycoside formation.

Figure 16: Arrangement of the catalytic dyad in *Pc*OGT and *Os*CGT For both enzymes the catalytic histidine at position 24 is conserved, whereas the aspartate and isoleucine occupy different positions in *Os*CGT and *Pc*OGT sequence.

A sequence alignment (Figure 16) verified the suggested great importance of His24 for catalytic activity, whereas positions 120 and 121 are not conserved. As the position of Asp and Ile differs in both active site sequences, one can suggest these positions being discriminatory for the type of glycosidic bond formed. The activation of His by Asp seems to be essential for *O*-glycosidic bond formation whereas *C*-glycosylation is favored when Ile occupies the place of Asp in the active site. Precise positioning of the acceptor substrates seems to define the generation of either *O*- or *C*-glycosidic linkages (29).

Mutational studies on *Pc*OGT showed that a disruption of the His- Asp dyad almost completely eliminated *O*-glycoside formation and the *C*-glycoside nothofagin was the main product. These findings enforce the theory that disrupting the conserved catalytic dyad could be the specificity- discriminating feature of plant glycosyltransferases (29).

1.6.1 *Oryza sativa C*-glycosyltransferase

*Os*CGT, from rice (*Oryza sativa spp. Indica*), catalyzes the UDP-glc-dependent *C*-glycosylation of 2-hydroxyflavanone precursors of flavonoids (63). It is a 49.43 kDa family 1 glycosyltransferase comprised by 471 amino acid residues and is related to known *O*-glycosyltransferases.
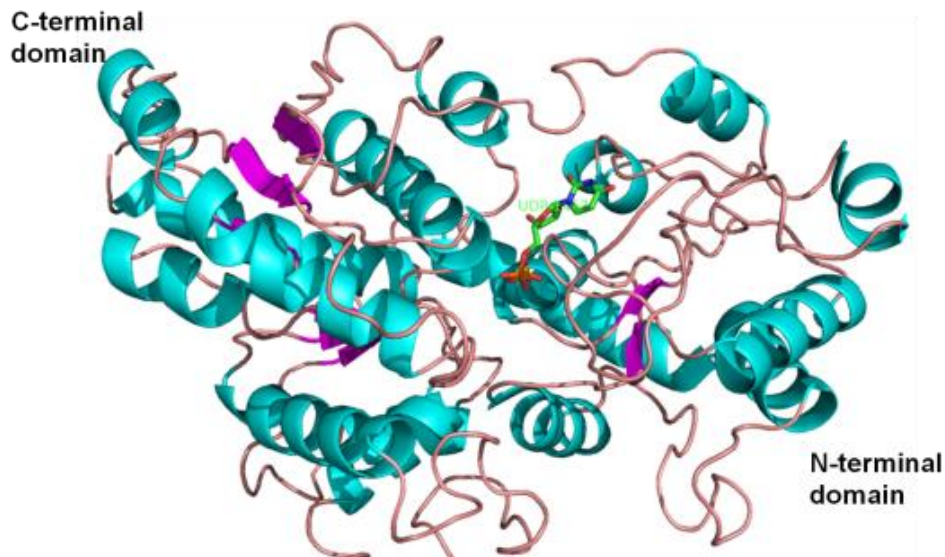

Figure 17: Proposed structure of *Os*CGT Ribbon diagram of *Os*CGT (I-TASSER; template structure *Vv*GT1, PDB: 2C1Z) showing the 3D folding of elements of the secondary structure with α-helices shown in cyan, β-sheets in magenta and connecting loops in wheat. Bound UDP from *Vv*GT1 is shown as stick model in green/orange.

The protein structure of *Os*CGT was predicted by homology. This revealed the overall folds of the two β/α/β-Rossmann domains being clearly conserved in the two proteins, with a few smaller insertions or deletions in the loop regions. There were also no obvious differences in the conformation of the active site residues detected, that could be responsible for the unusual *C*-conjugating activity of *Os*CGT or the potential of the enzyme to use sugar donors other than UDP-glucose in the plant secondary product GT binding domain (11); *Os*CGT is an obligate *C*-glycosyltransferase.

Figure 18: Reaction catalyzed by _Os_CGT _Oryza sativa C_-glycosyltransferase catalyzes the reaction of phloretin with UDP-glucose to give the corresponding _C_-glycoside nothofagin and UDP in a non- reversible reaction mechanism.

In _C_-glycosidic bond formation, the negative charge of the hydroxyl group gets displaced to the C_3-atom of the acceptor substrate, allowing C_1 of the sugar ring of UDP-glucose to directly bind to the acceptor.

1.6.2 _Pyrus communis O_-glycosyltransferase

Pyrus communis 2´-_O_-glycosyltransferase (UGT88F2) is set up by 483 amino acid residues, comprises a molecular mass of 53.53 kDa and shows high sequence similarity (99.4 %) with _Malus x domestica_ UDP-glucose:phloretin 2'-_O_-glycosyltransferase UGT88F1 (GenBank accession no. ABY73540).
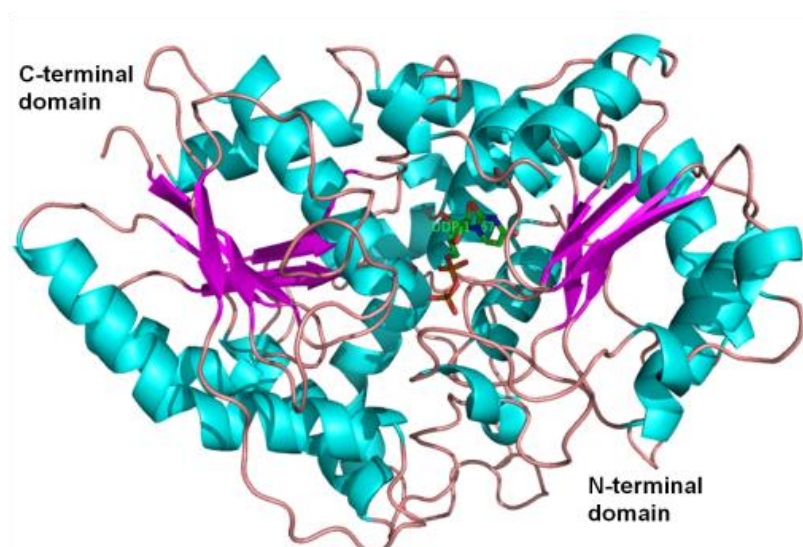

Figure 19: Proposed structure of _Pc_OGT Ribbon diagram of _Pc_OGT (I-TASSER; template structure _Vv_GT1, PDB: 2C1Z) showing the 3D folding of elements of the secondary structure with α- helices shown in cyan, β-sheets in magenta and connecting loops in wheat. Bound UDP from _Vv_GT1 is shown as stick model in green/ orange.

The N-terminal domain of the protein was shown to possess lower sequence identity than the C-terminal domain, which includes the 44 residue PSPG- motif (46).

_Pc_OGT catalyzes the glycosylation of phloretin at position 2' to form phlorizin (46).
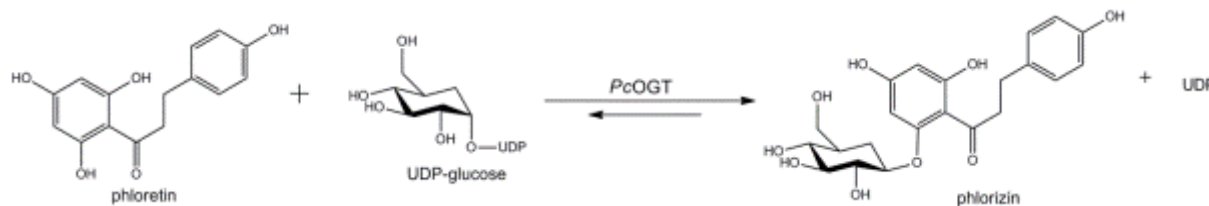
Figure 20: Reaction mechanism of *Pyrus communis O*-glycosyltransferase *Pc*OGT catalyzes the reaction of phloretin with UDP-glucose to give the corresponding *O*-glycoside phlorizin and UDP. Also the reverse reaction from phlorizin to phloretin at the expense of UDP with the generation of UDP-glucose is catalyzed, albeit with lower efficiency.

UGT88F2 was shown to exclusively glycosylate phloretin with strict regioselectivity for position 2'; no activity was detected towards other substrates such as naringenin, butein, cinnamic acid or caffeic acid. As phloretin and its derivatives are not present in the genus *Pyrus*, it was suggested, that a phenolic substance other than phloretin represents the native substrate, although it was not identified yet (46).

In *Pc*OGT catalysis, His acts as catalytic base and abstracts a proton from the acceptor substrate provoking its activation. H^+- abstraction causes a slight negative charge at the acceptor´s reacting hydroxyl- group, which then nucleophilically attacks the UDP-sugar donor and the glycosidic linkage between O^- and the C_1 of the glucose ring structure can be established. Asp stabilizes the charge of His, thereby facilitating successful bond formation.

*Pc*OGT is able to catalyze the reverse reaction, the conversion of phlorizin to phloretin at the expense of UDP, thereby generating UDP-glucose, albeit this reaction route occurs with lower efficiency than the common forward reaction.

1.7 Aim of this thesis

The goal of this thesis was to establish a two- enzyme- system for the efficient synthesis of the *C*-glycoside nothofagin from the *O*-glycoside phlorizin. Basing on the approach of reversing GT- catalyzed reactions, this set-up is suggested to circumvent the common drawbacks of high costs of aglycones and the impaired availability of donor substrates.

In the coupled- enzyme system, not the aglycon phloretin but its more common *O*-glycoside phlorizin is used as starting material. The ability of *Pc*OGT to also catalyze the reverse reaction, i.e. the cleavage of the *O*-glycosidic linkage to produce phloretin and UDP-glucose, is exploited to generate the required aglycones and sugar donor substrates for further synthesis. *Os*CGT is then used to convert these intermediary products via an irreversible reaction to the final *C*-glycoside.
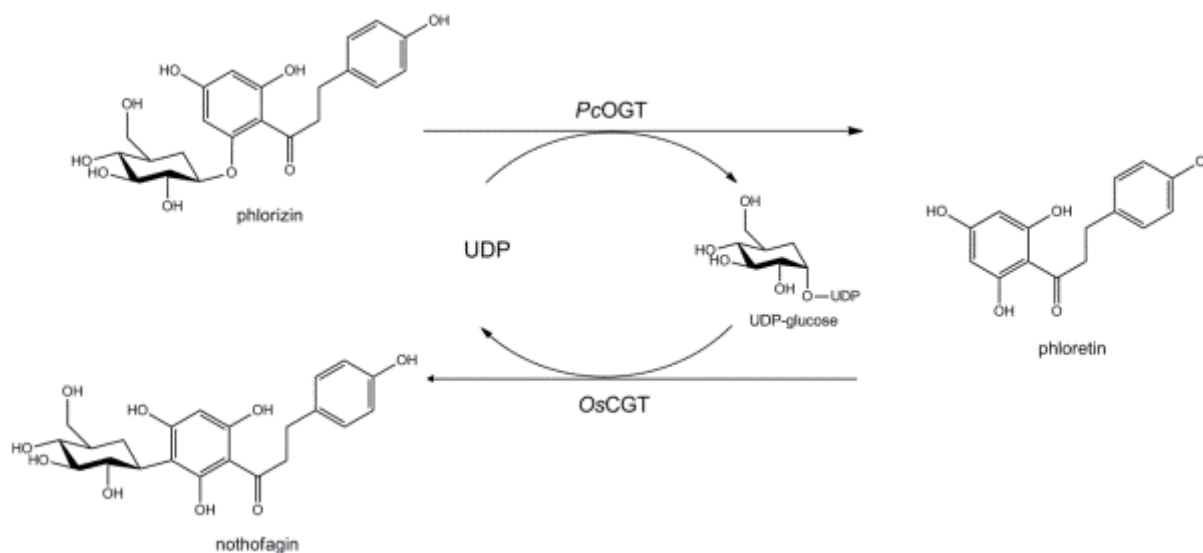

Figure 21: Coupled reaction of *Pc*OGT and *Os*CGT Phlorizin is converted to phloretin and UDP-glucose by *Pc*OGT´s reverse reaction using UDP; phloretin is then transformed to nothofagin by *Os*CGT using the before generated UDP-glucose and regenerating UDP.

This "two-enzymes one-pot" system allows the formation of nothofagin by using only catalytic amounts of UDP, as it is regenerated during product formation. The overall costs in this synthesis mode could be reduced as expensive sugar donors do not need to be fed to the system since phloretin and UDP-glucose are generated via the first reversible *O*-glycosylation reaction.

As for the final *C*-glycosylation no ability of catalyzing a reverse reaction was detectable a quantitative conversion is possible and the purification and processing of the final product is eased due to the absence of any side products.

2 MATERIALS AND METHODS

2.1 Materials and Instruments

All chemicals were of highest purity available and obtained from Roth (Karlsruhe, Germany) and Sigma Aldrich (St. Louis, MO, USA) if not otherwise mentioned. Phloretin (98%) was purchased from AK Scientific, Inc. (CA, USA), uridine diphosphate (≥96%) was from Sigma Aldrich and phlorizin dihydrate (≥98%) was from Roth. Materials for SDS- PAGE were from Amersham BioSciences (Uppsala, Sweden) and BioRad (Vienna, Austria). Enzymes for DNA modification were obtained from MBI Fermentas (Flamborough, ON, Canada) and PCR primers were purchased from Life Technologies. Phusion® High- fidelity DNA polymerase was from New England Biolabs. Strep-Tactin® Sepharose and desthiobiotin for Step- tag affinity chromatography were from IBA. The BCA assay kit was purchased from Thermo Scientific. The used instruments are listed in Table 2.

Table 2: Used instruments and manufacturers

Instrument	Manufacturer
DU®800 Spectrophotometer	Beckman Coulter
PCR Thermo Cycler	BioRad iCycler iQ™
FLUOStar Omega plate reader	BMG Labtech
Shaker Certomat® BS-1	Sartorius
Sorvall®RC-5B refrigerated superspeed centrifuge	DuPont Instruments
French Pressure cell press	American Instrument Company, Division of Travenol Lab, Inc.
Centrifuge 5804R	Eppendorf
SDS PAGE	BIO-RAD PowerPac™ Basic
HPLC	Agilent 1200 series
HPLC column	Chromolith®RP-18C column (100- 4.6 mm)

2.2 Strain construction

2.2.1 *Escherichia coli* strains

The gene encoding *Os*CGT (GenBank: FM179712.1) was provided by the group of Robert Edwards (Centre for Bioactive Chemistry, Durham University, United Kingdom). It was supplied in a pET-Strp3 vector, a custom- made derivative of pET-24d vector, allowing protein expression with an N-terminally fused Strep- tag II (29).

The *Pc*OGT gene (UGT88F2; GenBank: FJ854496.1) was received from the group of Karl Stich (Institute of Chemical Engineering, Technical University Vienna, Austria) in a pYES2.1/V5-His-TOPO vector. Internal restriction sites for *Nde*I and *Xho*I were removed by OE-PCR before cloning the gene into the pET-Strp3 vector for expression as N-terminally Strep- tagged fusion protein.

Three fragments of *Pc*OGT were amplified with the primers given in Table 3 and linked via OE-PCR along with the introduction of flanking restriction sites. Upon purification via agarose gel electrophoresis and terminal digestion with *Nde*I and *Xho*I, the gene was ligated into the respective sites of the pET-Strep3 vector as well as into pET28a for expression with an N-terminal His- tag (29).

Table 3: Primers used for *Pc*OGT_Strep OE-PCR

PcOGT overlap-extension PCR middle fragment

forward primer: *Pc*OGT_*Nde*I_fw	5´-TAA CCA TAT GGG AGA CGT CAT TGT ACT GTA CGC-3´
reverse primer: *Pc*OGT_*Xho*I_rem_rv	5´-GCT AGG TGG CTC CAG CTC TTC GAA CGT GTT G-3´

PcOGT overlap- extension PCR 5´- fragment

forward primer: *Pc*OGT_*Xho*I_rem_fw	5´-CAC GTT CGA AGA GCT GGA GCC ACC TAG CGT C-3´
reverse primer: *Pc*OGT_*Nde*I_rem_rv	5´-CAT TCC TGT TCA TGT GCT GCT CCG CGT AAA GC-3´

PcOGT overlap- extension PCR 3´- fragment

forward primer: *Pc*OGT_*Nde*I_rem_fw	5´-ACG CGG AGC AGC ACA TGA ACA GGA ATG TTC-3´
reverse primer: *Pc*OGT_*Xho*I_rv	5´-GGT GCT CGA GCT ATG TAA TGC TAC TAA CAA AGT TGA CCA AG-3´

Mismatching base pairs are underlined

The described plasmids were used for transformation of electro- competent *E.coli* BL21- Gold (DE3) cells. 5 µL of desalted, purified plasmid- DNA were mixed with 70 µL of cells and exposed to 1.8 kV for 4.8 msec and incubated with pre-warmed SOC- medium prior cultivation on selective LB- kanamycin plates. The correct sequence of the complete genes was verified by sequencing (LGC Genomics, Berlin, Germany).

2.2.2 *Saccharomyces cerevisiae* strain for *Pc*OGT expression

Saccharomyces cerevisiae CEN.PK2-1C was transformed with the originally received pYES2.1/V5-His-TOPO vector containing the *Pc*OGT gene.

Untransformed yeast cells were cultivated on standard YPD- agar plates (10 g/L yeast extract, 20 g/L peptone, 20 g/L glucose, 20 g/L agar) for 48 h. A single colony was used for the preparation of competent cells for transformation with pYES2.1/V5-His-TOPO plasmid encoding *Pc*OGT_His. Therefore cells were incubated in liquid YPD- culture medium (10 g/L yeast extract, 20 g/L

peptone, 20 g/L glucose) for 24 h at 30 °C. Upon reaching the desired optical density of 2.0 at 600 nm, cells were harvested by centrifugation (5 min, 3.000 g, 4 C) and washed with 25 mL sterile H_2O prior another round of centrifugation. The resulting pellet was resuspended in 1 mL of sterile H_2O. Transformation was performed by the LiAc/ single- stranded carrier DNA/PEG-method (64).

Table 4: Components of transformation mix

reagents	volume (µL)
PEG 3500 50% w/v	240
LiAc (1.0 M)	36
Boiled ss-carrier DNA	50
Plasmid DNA + water	34
total	**360**

100 µL of competent cells were mixed with 360 µL of the transformation mix Table 4 and incubated at 42° C for 40 min at 600 rpm. The transformation mix was removed employing centrifugation and the transformed cells were resuspended in 1 mL sterile H_2O before cultivation on selective SGI- plates (1 g/L peptone, 6.7 g/L yeast nitrogen base without amino acids, 20 mg/L *L*-tryptophane, 2 g/L glucose, 20 g/L agar) at 30 °C for 60 h.

2.3 Enzyme Expression

2.3.1 *Escherichia coli* expression: LB-medium

Recombinant *Os*CGT_Strep or *Pc*OGT_Strep cells were cultivated in 1 L baffled shaking flasks at 37 °C and 110 rpm using 300 mL Luria- Bertani medium (10 g/L peptone, 5 g/L NaCl, 5 g/L yeast extract) containing 50 µg/mL kanamycin. Pre-cultures of 70 mL were inoculated with 40 µL glycerol stock (50 % glycerol, recombinant cells) and incubated for 15 h at 37 °C in standard LB-medium containing kanamycin. Main cultures were then inoculated to OD_{600} values of 0.08 to 0.1 depending on optical density of the pre-culture. As the main cultures reached an optical density of 0.8- 1.2 at 600nm, protein expression was induced by the addition of 0.5 mM isopropyl β-D-1-thiogalactopyranoside (IPTG) and the temperature was lowered to 25 °C. After 18 h of incubation, the cells were harvested by centrifugation (30 min, 4 °C, 5.000 rpm), resuspended in water and stored at -70 °C.

2.3.2 *Escherichia coli* expression: ZYM 5052-medium

Recombinant cells with pET28a-*Pc*OGT plasmid were cultivated in auto- inducible ZYM 5052 medium (65) in order to reach high cell densities resulting in high expression levels of target protein. Detailed composition of solution M, trace element stock and solution 5052 of the complex medium are given in the appendix.

Table 5: Components of complex, auto inducible ZYM 5052 Medium

component	concentration
peptone	10 g/L
yeast extract	5 g/L
solution M	20 mL
trace elements	0.2 mL
1 M MgSO$_4$	2 mL
solution 5052	20 mL

Peptone with yeast extract (solution Z), solution M, solution 5052, M$_g$SO$_4$ and trace elements were prepared separately and sterilized by autoclaving, except for trace element solution which was sterilized by filtration through a syringe filter (0.2 µM pore size). Media components were mixed after sterilization to the final composition listed in Table 5 and aliquots of 300 mL containing 50 µg/mL kanamycin were separated into prior sterilized baffled cultivation flasks. Inoculation was performed from pre-cultures in LB- medium to an OD$_{600}$ of 0.1. Cultivation was initially done for 4 h at 37 °C (110 rpm) to maximize cell growth. Protein expression was induced by glucose depletion and metabolic switch to lactose consumption. Induction was further aided by temperature change from 37 °C to 16 °C and further incubation for 60 h with shaking (110 rpm). The temperature change was done automatically without monitoring glucose depletion or cell growth. Cell harvest was performed by centrifugation (5.000 rpm, 30 min, 4 °C) and the cells were resuspended in sterile water prior storage at -70 °C.

2.3.3 *Saccharomyces cerevisiae* expression

For expression of *Pc*OGT in *Saccharomyces cerevisiae*, a single colony of transformed cells was used for inoculation of 50 mL pre-culture in SGI- medium (1 g/L peptone, 6.7 g/L yeast nitrogen base without amino acids, 20 mg/L *L*-tryptophane, 20 g/L glucose) and incubated for 15 h at 30 °C until an OD$_{600}$ of 2.0- 4.0 was reached. Main cultures (250 mL) of YPGE- medium (5 g/L glucose, 10 g/L peptone, 10 g/L yeast extract, 3 Vol% ethanol) were then inoculated from pre-cultures to a starting OD$_{600}$ of 0.2- 0.4 and incubated in 1 L sterile baffled flasks at 30 °C with shaking (110 rpm) until OD$_{600}$ reached values of 0.8– 1.2. Induction of protein expression was performed by the

addition of sterile galactose solution (21.6 g/L in final culture medium) and incubation was continued for another 15 h at 30 °C. Cell harvest was performed by centrifugation (5.000 rpm, 30 min, 4 °C) and the cells were resuspended in sterile water prior storage at -70 °C

2.4 Purification

2.4.1 Purification via Strep-tag affinity chromatography

Cell lysis was performed by repeated passage through a cooled French Press (100 bar). Cell debris was removed by centrifugation at 13.200 rpm at 4 °C for 45 min and the supernatant was used for purification upon two-fold dilution with buffer (100 mM Tris/HCl (pH 8.0), 150 mM NaCl, 1 mM EDTA) and filtration through a 1.2 µm cellulose- acetate filter. *Os*CGT_Strep and *Pc*OGT_Strep enzyme purification was performed by Strep- tag affinity chromatography on a gravity flow Strep- Tactin® Sepharose® column (3 mL column volume; Pierce, Rockford, USA) as recommended by the manufacturer (IBA BioTAGnology; Göttingen, Germany). After column equilibration with 3 CVs (column volume) of washing buffer (100 mM Tris/HCl (pH 8.0), 150 mM NaCl, 1 mM EDTA) the protein sample was applied. Following washing with 5 CVs of washing buffer, bound proteins were eluted with 3 CVs of elution buffer (100 mM Tris/HCl (pH 8.0), 150 mM NaCl, 1 mM EDTA, 2.5 mM desthiobiotin), whereas the first 0.5 CVs were discarded and the rest was collected and pooled. Column regeneration was performed by applying 15 CVs of regeneration buffer (100 mM Tris/HCl (pH 8.0), 150 mM NaCl, 1 mM EDTA, 1 mM HABA) followed by equilibration with 10 CVs of washing buffer. The enzymes were concentrated and the buffer was exchanged to 25 mM HEPES, pH 7.0 using centrifugal concentrators (VivaSpin tubes) with a molecular weight cut- off of 10 kDa. Aliquots of the enzymes were stored at -20 °C. Atween the purification of different enzymes the column was washed with 6 M guanidine/HCl to eliminate cross- contaminations.

2.4.2 Purification via Ni^{2+}- metal chelate affinity chromatography

*Pc*OGT was expressed with an N-terminal His-tag in *E.coli* BL21Gold (DE3) as well as in *Saccharomyces cerevisiae* CEN.PK2-1C. Again cell lysis was performed by repeated passage through a cooled French Press (100 bar). Cell debris was removed by centrifugation at 13.200 rpm at 4 °C for 45 min and the supernatant was used for purification upon two-fold dilution with buffer (20 mM Tris/HCl (pH 7.4), 500 mM NaCl, 20 mM imidazole) and filtration through a 1.2 µm cellulose- acetate filter.

A 5 ml HiTrap^{TM} Chelating FF column (5 mL, Amersham Biosciences, GE- Healthcare) was loaded with Ni^{2+}. A flow rate of around 5 ml/min was applied manually using a syringe. Purification was done at 4 °C. The column was first equilibrated by washing with 5 CVs of buffer W (20 mM Tris/HCl (pH 7.4), 500 mM NaCl, 20 mM imidazole) at a flow rate of 5 mL/min. Upon washing, the cell extract was loaded, followed by further application of 5 CVs of buffer W. Elution of His-tagged enzymes was performed in two steps using 4 CVs buffer E1 (20 mM Tris/HCl (pH 7.4), 500 mM NaCl, 250 mM imidazole) and 5 CVs of buffer E2 (20 mM Tris/HCl (pH 7.4), 500 mM NaCl, 500 mM imidazole), respectively. Most tagged *Pc*OGT eluted with 250 mM imidazole. Fractions were pooled and concentrated in 25 mM HEPES (pH 8.0) using 20 mL Vivaspin concentrator tubes. Before storage at 20 % EtOH the column was washed by 7 CVs of water.

2.5 Determination of protein concentration

Concentration of protein was measured by the BCA protein assay (Thermo Scientific, Rockford, IL, USA). Thereby, the formation of Cu^{2+} by the Biuret complex with proteins is photometrically determined using bicinchoninic acid (BCA). The reaction is separated into two steps: the first reaction occurs at lower temperatures and is the result of the interaction of copper and BCA with cysteine, tryptophane and tyrosine residues in the protein. At elevated temperatures, the protein peptide bonds are additionally responsible for color development.

25 µL of protein solution were incubated with 200 µL of BCA solution in 96- well micro- plates at 37 °C for 30 min and the absorption at 562 nm was determined by a plate reader (FLUOstar Omega plate reader, BMG Labtech). The concentrations were calculated using BSA standards from 0 to 2000 µg/mL.

2.6 SDS PAGE analysis

Sodium dodecyl sulphate polyacrylamide gel electrophoresis was used to evaluate enzyme purity. Samples were incubated with equal volumes of SDS dissociation buffer (20 mM KH$_2$PO$_4$, 6 mM EDTA, 6 % SDS, 10 % glycerol, 0.05 % bromophenol blue) at 95 °C for 10 min. Denatured protein samples were applied and protein fragments were separated on the gel (nUView Precast Gels; NuSep Tris- Glycine NB 4- 20 %; NuSep Ltd., Australia) by the application of 150 V for 60 min. Staining of protein bands was accomplished with Coomassie brilliant blue dye (0.1 % Coomassie R-

250, 40 % EtOH, 10 % HAC) for 60 min, followed by destaining (30 % EtOH, 10 % HAC) for two times 30 min.

2.7 HPLC Activity measurements

Initial rate measurements were performed at 30 °C with an HPLC based assay. Under standard conditions UDP-glucose and phloretin were used as substrates in 25 mM Tris/HCl (pH 7.0) containing 13 mM MgCl$_2$, 50 mM KCl, 0.13 % BSA and 5 % or 20 % organic solvent (DMSO, EtOH). Rate measurements of *Pc*OGT reverse reaction were done as described for forward reactions but using phlorizin and UDP instead of phloretin and UDP-glc as substrates. The reactions were started by the addition of *Pc*OGT and *Os*CGT, respectively, and samples were taken by mixing an aliquot with equal amounts of acetonitrile causing the reaction to be stopped. Precipitated protein was removed by centrifugation at room temperature at 13.200 rpm for 20 min.

10 µL of the samples were used for analysis on an Agilent 1200 HPLC equipped with a Chromolith® Performance RP- 18C end capped column (100- 4.6 mm) from Merck. The column was thermostatically controlled at 35 °C and the separation of sample components was monitored at 288 nm via UV detection. Separation of phloretin and its glycosides phlorizin and nothofagin (Figure 22) was achieved by a method using water containing 0.1 % TFA as buffer A and acetonitrile with 0.1 % TFA as buffer B, respectively. A 7.5 min long linear gradient from 20 to 47.5 % B (1 mL/min) was used for product separation. This step was followed by 0.05 min of a linear gradient from 47.5 to 100 % B (1 mL/min) and 1.45 min of isocratic flow at 100 % B (1.5 mL/min) to wash off any hydrophobic compounds. After a 0.05 min linear gradient from 100 to 20 % B (1.5 mL/min) an isocratic flow of 2.45 min at 20% B (1.5 mL/min) was applied to equilibrate the column.
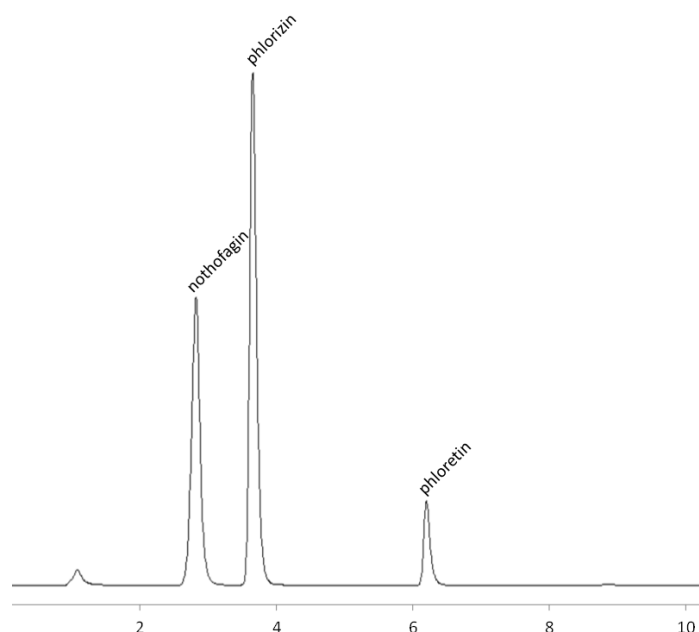
Figure 22: HPLC chromatogram of phloretin and its glycoside derivatives The *C*-glycoside nothofagin was detected at a retention time of 3.2 min, the *O*-glycoside phlorizin eluted with a retention time of 3.8 min and the aglycone phloretin was detected at a retention time of 6.1 min.

For the specific enzymatic activity, the linear initial rates were evaluated. The actual concentrations of the respective products were calculated from standard curves. Calibration curves for phloretin and phlorizin were determined for a standard series containing 10- 5000 µM of both substances. The quantities of products and/ or substrates were calculated from the peak areas using the respective response factors of the standards.

2.7.1 Data analysis

Substrate and product concentrations were calculated via internal standards from the respective peaks areas upon HPLC analysis, as mentioned before.

The theoretical initial concentration of substrate was used as reference for the calculation of the overall conversion and the final product yield. For the conversion the percentage of remaining substrate at the end of the reaction was subtracted from the initial concentration. The final yield was determined by converting the final product concentration into the percentage of transformed initial substrate given in percent. The internal mass balances were determined by summarizing all concentrations at the first analyzed reaction time point (t= 0 min) and comparing this to the theoretically used concentration of substrate. Deviations from the mass balances were then calculated using Equation 1.

$$\% \; deviation = \left(\frac{c_{substrate+product} - c_{substrate,theor.}}{c_{substrate,theor.}} \right) * 100$$

Equation 1: Calculation of mass balance deviation The concentration of substrate and product at the end of the reaction was determined by summarizing phlorizin, nothofagin and phloretin and compared to the theoretically employed phlorizin concentration

Reactions, that showed a deviation exceeding a value of 25 % from the theoretical mass balance were not used for analysis and are not given in this thesis.

2.7.2 Determination of specific activity of purified fractions

The specific enzymatic activity of *Os*CGT and *Pc*OGT was determined by incubating different concentrations of enzyme with 0.1 mM phloretin and 600 µM UDP-glc in 25 mM Tris/HCl buffer (pH 7.0) in final reaction volumes of 500 µL. Samples of 100 µL were taken every 20 min over a time period of 1 h and the reaction was stopped by the addition of 100 µL acetonitrile. Precipitated protein was removed by centrifugation (13.200 rpm, 20 min, RT) and the supernatant was used for analysis. The amount of produced *O*-glycoside phlorizin and *C*-glycoside nothofagin was then related to the specific activity of *Pc*OGT and *Os*CGT, respectively.

2.8 Characterization of single enzymes

The activity of *Pyrus communis O*-glycosyltransferase was examined with respect to the forward as well as the reverse reaction, i.e. the conversion of phloretin and UDP-glucose to phlorizin and UDP and vice versa. For *Oryza sativa C*-glycosyltransferase only the reaction with phloretin and UDP-glucose to yield nothofagin and UDP was investigated. For all measurements employing the single enzymes, buffer containing 50 mM KCl, 13 mM MgCl$_2$, 0.13 % BSA (w/v) and a final concentration of DMSO of 5 % was set as standard condition, if not otherwise mentioned. Measurements were done with HPLC as described.

2.8.1 Influence of organic solvents on stability and activity

As phloretin and phlorizin are barely water- soluble, the use of organic solvents was essential to enhance the availability of the substrate in the reaction mixture. To determine influences of the concentration of organic solvent on enzyme activity and stability, both *Os*CGT and *Pc*OGT were incubated in separate reaction mixtures with different concentrations of DMSO and EtOH (5-30 % in 5 % steps), with 0.1 mM phloretin, 600 µM UDP in buffer (25 mM Tris/HCl, pH 7.0). The

reactions proceeded for 1h and samples were taken every 20 minutes. The production of phlorizin and nothofagin by *Pc*OGT and *Os*CGT, respectively, was determined with HPLC.

The influences on the stability were evaluated by incubating the enzyme in reaction solutions lacking UDP-glc with different solvent concentrations for 20 h at 30 °C and the reaction was then started by the addition of the sugar donor. Activities were evaluated via product concentrations of phlorizin and nothofagin, respectively.

2.8.2 Cation dependency of *Pc*OGT

An eventual dependency of *Pc*OGT activity on the presence of divalent cations was evaluated by using buffer (20 mM HEPES, pH 7.0) containing either $MnCl_2$ or $MgCl_2$ (13 mM final concentration). Buffer (20 mM HEPES, 50 mM KCl, 0.13 % BSA (w/v)) without further ions was used as control. The enzymatic activity was measured as described by regular sampling over 60 min. All measurements were performed in duplicate using enzyme concentrations of 0.5 µg and 0.125 µg, respectively, in a final reaction volume of 500 µL.

2.8.3 pH profiles of *O*-glycosylation reactions

For characterization of the *O*-glycosyltransferase the specific enzymatic activities at different pH were determined as described. Optimal pH conditions for the conversion of phloretin to phlorizin by *Pc*OGT were identified by measuring the product concentration. The standard protocol for activity measurements was modified by using citrate, Tris/HCl or CAPS buffer (25 mM final concentration) of the respective pH. Buffers were prepared from pH 5.0 to 11.0 in steps of 0.5 pH units and the used enzyme concentration was adjusted according to the expected activity (Table 6).

Table 6: Used enzyme concentrations for the pH profile of *Pc*OGT forward reaction

pH range	enzyme concentration (µg/mL)
5.0- 5.5	0.060
6.0- 6.5	0.030
7.0- 9.0	0.015
9.5- 10.0	0.030
10.5- 11.0	0.060

*Pc*OGT was incubated in a final reaction volume of 1000 µL with 0.1 mM phloretin and 600 µM UDP-glc in buffer. Proceeding of the reaction was monitored for 1 h by sampling every 20 min and the enzymatic activity was monitored with HPLC upon sample preparation as described before. The actual pH in the reaction solution was determined by measuring the pH at

the start and the end of the reaction; the mean thereof was used for evaluations. Also the optimum pH for the reverse reaction of *Pc*OGT, the conversion of phlorizin and UDP to phloretin and UDP-glc, was evaluated using citrate and Tris/HCl buffer in the range of pH 3.0- 9.5 in steps of 0.5 pH units. 0.06 µg of *Pc*OGT were incubated with 1 mM phlorizin and 2 mM UDP in a final volume of 1000 µL.

As for the forward reaction, the progress of conversion was monitored over 1 h with sampling every 20 min. Subsequently the final conversion was determined after further addition of 5 µg enzyme and prolonged incubation for 12 h. The concentration of produced phloretin was measured with HPLC and corresponded to the specific activity of the enzyme at different pH conditions. Evaluation of results was performed as described for the forward reaction.

The preference of the reaction direction of *Pc*OGT with varying pH conditions was determined by comparing the ratio of forward and backward activities at the corresponding pH. The ratio was calculated using Equation 2.

$$ratio_{forward/reverse} = \frac{k_f}{k_r}$$

Equation 2: Calculation of the ratio_{forward/reverse} for *Pc*OGT forward and reverse reaction (k_f... rate of forward reaction in mU/mg, k_r... rate of reverse reaction in mU/mg)

2.8.4 Alternative sugar donors

It was tried to replace the donor substrate UDP-glucose with UMP and glucose-1-phosphate in *O*- and *C*-glycosylation and the production of phlorizin and nothofagin, respectively, was to be detected. *Pc*OGT and OsCGT were incubated with 5 mM phloretin, 20 mM UMP and 20 mM G-1-P in a final volume of 1000 µL with buffer (25 mM Tris/HCl, pH 7.0). The enzyme concentration was increased by factor ten compared to reactions employing the common sugar donor UDP-glc.

2.8.5 Kinetic characterization of *Pc*OGT and *Os*CGT

Kinetic parameters for *Pc*OGT and *Os*CGT were determined by incubating the single enzymes with different concentrations of one substrate while keeping the concentrations of the second substrate constant. Final volumes of 700 µL containing buffer (see Table 7 and Table 8), were used. Samples were taken regularly over a time period of 180 min and the reactions were stopped by the addition of acetonitrile. Initial reaction rates were calculated via the increase of product concentrations measured.

The Michaelis- Menten parameters were then calculated from a plot of the reaction velocities against substrate concentrations using the hyperbolic curve fit function of SigmaPlot 9.0.

2.8.5.1 *Pyrus communis O*-glycosyltransferase

Michaelis- Menten parameters of *Pc*OGT were determined for substrates (phloretin, phlorizin, UDP-glucose, UDP, UDP-galactose) in the single- enzyme reaction set-up. The used concentrations and buffers are listed in Table 7.

Measurements for phloretin and UDP-glucose were performed via a discontinuous spectrophotometric assay. Pure enzyme (0.42 µg) was incubated at different substrate concentrations in buffer containing, 13 mM HEPES (pH 7.0), 50 mM KCl, 13 mM $MnCl_2$, 0.13 % BSA and 5 % EtOH in a final reaction volume of 1000 µL. Typically 4 samples of 150 µL were taken and the reaction was stopped by heating for 10 min at 95°C followed by cooling on ice. Upon centrifugation (20 min, RT, 13.200 rpm) to remove eventually precipitated protein, 100 µL of the samples were mixed with 400 µL measuring solution (0.225 mM NADH, 0.875 mM PEP, 5 % EtOH) and the absorbance at 340 nm was evaluated. 0.5 µL of PK/LDH (0.4 U PK, 0.6 U LDH) were added to each sample followed by incubation for 45 min at 37 °C prior another absorbance measurement. The difference in absorbance before and after PK/LDH addition was then used for the calculation of the initial rates of *Pc*OGT at different substrate concentrations. Exact calculations of Michaelis- Menten parameters were then again performed employing SigmaPlot 9.0 as described.

Table 7: Substrate concentrations for kinetic characterization of *Pc*OGT

parameters	acceptor concentration (µM)	sugar donor concentration (µM)	buffer
phloretin	5- 750	2000	HEPES (pH 7.0)
UDP-glc	250	25- 3750	HEPES (pH 7.0)
UDP-gal	200	0- 10000	Tris/HCl (pH 7.0)
phlorizin	10- 5000	2000	Tris/HCl (pH 7.0)
UDP	5000	5- 2000	Tris/HCl (pH 7.0)

2.8.5.2 *Oryza sativa C*-glycosyltransferase

Michaelis- Menten kinetics of *Os*CGT were determined for the substrates phloretin and UDP-glucose as described.

Table 8: Substrate concentrations for kinetic characterization of *Os*CGT

parameters	acceptor concentration (µM)	sugar donor concentration (µM)	buffer
phloretin	0- 5000	2000	Tris/HCl (pH 7.0)
UDP-glc	1000	5- 2000	Tris/HCl (pH 7.0)

2.9 Coupled reactions

In coupled reactions, the degylcosylation of phlorizin to phloretin by *Pc*OGT and the reglycosylation of phloretin by *Os*CGT yielding nothofagin were monitored with HPLC as described before. Enzymatic activities for both *Pc*OGT and *Os*CGT were defined for the glycosylation of phloretin under standard conditions (1 mM phloretin, 600 µM UDP-glc). A two-fold excess of *Pc*OGT was applied to account for the lower deglycosylation rate and to ensure sufficient substrate supply for *C*-glycosylation. 25 mM Tris/HCl at pH 7.0 was defined as the standard buffer. The buffer additionally contained 50 mM KCl, 13 mM $MgCl_2$ and 0.13 % BSA (w/v) and a final DMSO concentration of 20 %, if not otherwise mentioned.

Typically 2 mM UDP and 5 mM phlorizin were used when both *Pc*OGT and *Os*CGT were incubated if not elsewise described. The progress of the reaction was monitored by regular sampling over a defined time, with more narrow time spans between samples at the beginning of the reaction. The conversions were stopped by mixing the samples with equal volumes of acetonitrile. After removal of precipitated protein by centrifugation, the supernatant was subjected to HPLC analysis as described for the activity measurements of the single enzymes. The concentrations of the product nothofagin, the intermediate phloretin and remaining substrate phlorizin were then determined based on retention times and peak area, and used for calculating the enzymatic activities.

2.9.1 Variation of glycosylation activities

The glycosylation activities of *Pc*OGT and *Os*CGT were varied with constant concentrations of substrates phlorizin (25 mM), UDP (2 mM) and buffer (25 mM Tris/HCl, pH 7.0) in a final reaction volume of 300 µL. Used enzyme activities are given in Table 9 below:

Table 9: Variation of glycosylation activities in coupled assay

reaction no	*Pc*OGT : *Os*CGT	*Pc*OGT (mU/mL)	*Os*CGT (mU/mL)
1	2:1	100	50
2	2:1	200	100
3	1:2	25	50
4	1:1	25	25
5	1:2	12.5	25
6	1:1	12.5	12.5
7	2:1	10	5

The conversion of substrate and formation of nothofagin was monitored over 24 h with regular sampling and analyzed by HPLC. Samples (20 µL) were diluted fivefold with buffer (10 %

buffer, 20 % DMSO) to a final volume of 100 µL. The reaction was stopped by adding 100 µL AcN. After centrifugation, the supernatant was used for concentration determination by HPLC.

2.9.1.1 Increase of *C*-glycosylation activity

To increase the yield of the final product nothofagin and to examine any limiting influence of *C*-glycosylation in the coupled reaction set- up the enzymatic activity of *Os*CGT in the reactions was varied while the activity of used *Pc*OGT was kept constant at 100 mU/mL. The enzymes were incubated in a final reaction volume of 700 µL containing 10 mM phlorizin, 2 mM UDP and 25 mM Tris/HCl (pH 7.0). Samples of 100 µL (sample dilution 1:5) were taken regularly over 24 h and the reaction was stopped by the addition of equal volumes of acetonitrile prior analysis of the generated product concentration by HPLC.

Table 10: Enzymatic activities used for analysis of *C*-glycosylation reaction

*Pc*OGT: *Os*CGT	*Os*CGT(mU/mL)	*Os*CGT (µg)	*Pc*OGT (mU/mL)	*Pc*OGT (µg)
1 : 2	50	34.6	100	11.9
1 : 1.5	150	51.9	100	11.9
1 : 2	200	68.6	100	11.9
1 : 3	300	103.8	100	11.9
1 : 5	500	174.2	100	11.9

2.9.2 Variation of organic solvents

Similar to the studies on single enzymes, the effect of EtOH and DMSO on the coupled conversions was analyzed. 100 mU/mL *Pc*OGT and 50 mU/mL *Os*CGT, respectively, were incubated in 25 mM Tris/HCl (pH 7.0) and varying organic solvent concentrations of 5- 20 % (steps of 5 %) in final reaction volumes of 1000 µL. The reaction was monitored over 24 h with regular sampling and analysis was performed according to the described activity assay using HPLC. The final substrate as well as the initial rate of product formation was evaluated against the actual concentration of organic solvent.

2.9.3 Optimization of pH conditions

From single pH profiles of *Pc*OGT reverse reaction and *Os*CGT forward reaction, the optimum pH for the coupled conversion was estimated. To verify this, the efficiency of the coupled system was examined by incubating both enzymes with HEPES buffer at different pH in the range of 6.0- 8.5 in steps of 0.5 pH units. Both enzymes were incubated along with 5 mM phlorizin, 2 mM UDP in a final reaction volume of 1000 µL containing 25 mM buffer. The actual pH

in the reaction mixtures were determined by measuring it after addition of all components. The reaction was monitored over 24 h by regular sampling and analyzed via HPLC as described.

2.9.4 Variation of substrate concentration: Kinetic characterization of the coupled system

For better description of the coupled system and comparison with the kinetic characteristics of the single enzymes, apparent Michaelis- Menten parameters were also determined for phlorizin and UDP in the coupled reaction set- up. Therefore UDP (5- 2000 µM) or phlorizin concentrations (0- 5000 µM) were varied while keeping the second substrate constant at 5mM phlorizin and 2mM UDP, respectively.

Reaction mixtures contained 100 mU/mL *Pc*OGT (23.3 µg protein) and 50 mU/mL *Os*CGT (27.8 µg protein), 10 % buffer (25 mM Tris/HCl, pH 7.0), in a final reaction volume of 1 mL for UDP and 700 µL for phlorizin variation, respectively.

Samples of 10 % of the initial reaction volume (100 µL for UDP, 70 µL for phlorizin) were taken at regular times and concentrations of produced nothofagin and phloretin were measured via HPLC as described upon reaction stop by acetonitrile addition. The time dependent increase in concentrations of both reaction products (phloretin and nothofagin were summarized) was evaluated and the increase thereof was plotted against the applied UDP/ phlorizin concentrations. Exact calculations of Michaelis- Menten parameters were done with SigmaPlot 9.0 as mentioned.

2.9.5 Increase of initial substrate concentration

To increase the final yield of nothofagin, the initial concentration of phlorizin was increased up to 100 mM with constant concentrations of UDP (2 mM) and buffer (25 mM Tris/HCl, pH 7.0) and glycosylation activities in a 2:1 ratio (100 mU/mL *Pc*OGT and 50 mU/mL *Os*CGT). Samples were taken regularly over 24 h and the degree of conversion of phlorizin to phloretin and nothofagin, respectively, was measured by HPLC as previously described.

2.9.6 Fed batch conversion

To achieve higher yields of nothofagin, the conversion of the *O*-glycoside was performed in a fed- batch mode where one sample (S1) was fed solely with substrate upon its depletion and a second sample (S2) was fed with substrate and additional enzyme.

The reactions were started with 10 mM phlorizin, 1 mM UDP, enzymatic activities of 500 mU/mL *Pc*OGT (83.6 µg protein) and 250 mU/mL *Os*CGT (174.2 µg protein) in a reaction

volume of 1500 µL containing 25 mM Tris/HCl (pH 7.0), 50 mM KCl, 13 mM MgCl$_2$, 0.13 % BSA and 20 % DMSO and were incubated for 70 h. Feeding was performed with 10 mM phlorizin upon its complete depletion and 25 % of the initially added enzymatic activities (125 mU/mL PcOGT, 62.5 mU/mL OsCGT), while keeping the concentration of organic solvent constant at 20 %. A third sample (S3) containing all buffers and substrates, but lacking enzymes was incubated for detection of eventual precipitation of product or substrate due to the prolonged incubation time. For exact measurements, samples (10 µL) were diluted ten-fold (10 % buffer, 20 % DMSO) to a final volume of 100 µL prior reaction stop with 100 µL of acetonitrile. Product formation and substrate depletion was analyzed using HPLC.

As complete substrate use- up was not reached in the expected time frame, additional OsCGT/ PcOGT was fed to the reaction to accelerate substrate conversion. After 4 h of reaction 10 µL of both enzymes (280 mU/mL PcOGT, 50 mU/mL OsCGT) were added to each sample, resulting in an increase of the overall protein concentration to 325 µg.

Substrate feed for S1/ S3 and substrate/ enzyme feed for S2 was performed after 4h, 25 h and 52 h of incubation, where after 52 h only enzymes were added. To one sample (S1) additional 50 µL OsCGT (185.3 µg) and 15 µL PcOGT (43.4 µg) were added, while to the second sample (S2) only additional OsCGT but no PcOGT were fed, in order to evaluate any possible limitations of the system by the C- glycosylation reaction.

3   RESULTS AND DISCUSSION

Upon expression and purification, *Pc*OGT and *Os*CGT were characterized in separate reactions with respect to specific activity, behavior at different pH conditions and with varying concentrations of organic solvents. Their ability of utilizing alternative sugar donors was evaluated followed by their detailed kinetic characterization via the determination of their respective Michaelis- Menten parameters for both substrates. The findings from single enzyme characterization were then partly employed for the set- up of the coupled reaction system coupling *Pc*OGT and *Os*CGT for the conversion of the *O*-glycoside phlorizin into the *C*-glycoside nothofagin via the intermediate aglycon phloretin. The behavior of the coupled reaction system was investigated and optimized with regard to optimal pH conditions, organic solvent concentrations, sufficient glycosylation activities and concentration of substrates. The determined optimal parameters were then used for increasing the final product yield via a fed-batch conversion reaction.

3.1   Expression and Purification

3.1.1 Expression with Strep-tag

Purification of *Os*CGT_Strep and *Pc*OGT_Strep was performed by Strep- tag affinity chromatography employing a gravity flow Strep- Tactin® Sepharose® column. The concentration of purified protein was measured by BCA assay and was determined to be about 3.7 mg for *Os*CGT and 18.8 mg for *Pc*OGT per liter cultivation medium. Purity of samples was verified by SDS PAGE as given in Figure 23.
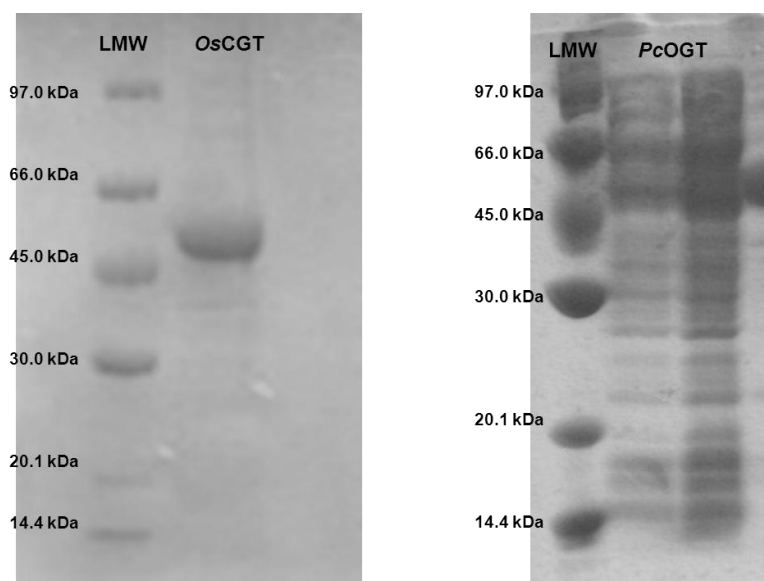
Figure 23: SDS PAGE of purified *Os*CGT_Strep and *Pc*OGT_Strep Prominent bands representing both enzymes at a molecular weight of 49.4 kDa for *Os*CGT and 53.5 kDa for *Pc*OGT (applied in duplicate with 10 µg and 20 µg), respectively, are visible.

SDS PAGE analysis of *Os*CGT fractions verified high expression and high purity of samples, whereas *Pc*OGT samples still showed significant levels of impurities. However, no interference with the specific *O*-glycosylation activity was found and therefore further purification was not required for this study.

3.1.2 Expression with His-tag

His-tagged constructs of *Pc*OGT expressed in *E.coli* in LB- and ZYM 5052 medium, as well as yeast- expressed enzyme was purified via Ni^{2+}- affinity chromatography. The protein concentrations were determined to be 3.3 mg/L culture from three rounds of expression in LB-medium, 17 mg/L culture for ZYM 5052-expressed and 2.3 mg/L culture for yeast- expressed enzyme were determined.
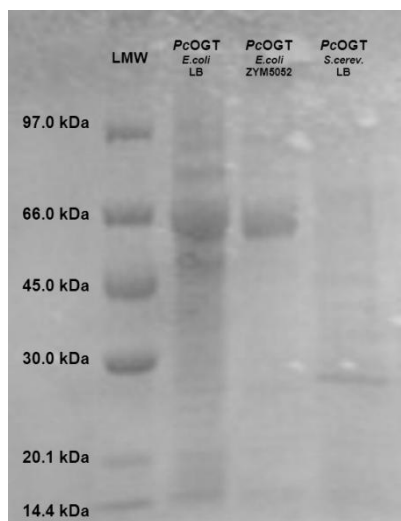
Figure 24: SDS PAGE of purified *Pc*OGT_His from different cultivation approaches After expression in *E.coli* using either LB- or ZYM 5052 medium strong bands at 55.5 kDa corresponding to *Pc*OGT were visible. Yeast expression did not lead to a prominent band, which is corresponding to the low protein concentration and activity measured.

No clear band corresponding to the molecular mass of *Pc*OGT was detectable for the fractions generated from yeast expression, which was consistent with the low measured protein concentration and specific activity. For proteins expressed in *E.coli* strong signals were detected, although purity of LB- expressed was less than for ZYM 5052- expressed samples. No interference of impurities with the specific activity of *Pc*OGT was found and therefore further purification was not required. His- tagged *Pc*OGT from LB- cultivation was used for characterization of the *O*-glycosyltransferase as well as for coupled reaction assays.

3.1.3 Determination of specific activity of purified proteins

Specific enzymatic activities from all purified fractions were measured with HPLC and for calculation of the initial linear rates of product formation at least 3 points were used. Calculated values are given in Table 11.

Table 11: Specific activities of purified *Os*CGT and *Pc*OGT fractions

enzyme fraction	no of cultivation	average yield (mg/L medium)	activity (mU/mg)	average activity (mU/mg)
*Os*CGT_Strep	1	3.7	6217	**7394**
	2		8571	
*Pc*OGT_Strep	1	18.0	6843	**6843**
*Pc*OGT_His (LB)	1	3.5	20234	**17606**
	2		16742	
	3		15842	
*Pc*OGT_His (ZYM 5052)	1	17.0	38220	**38220**
*Pc*OGT_His (yeast)	1	2.0	4	**4**

For *Pc*OGT, the highest specific activity was measured for fractions purified from ZYM 5052- cultures, which was corresponding to the higher protein concentrations resulting from higher cell densities. A higher concentration of the target protein could help to saturate the Ni^{2+}- column and therefore reduce unspecific binding of other proteins which resulted in a higher specific activity.

Protein expression levels in *Saccharomyces cerevisiae* were very low and therefore hardly any activity was detected. Generally the specific activity as well as the average protein yield for *Pc*OGT after different cultivations and purifications was very reproducible.

3.2 Characterization of single enzymes

3.2.1 Influence of organic solvents on stability and activity

Limited solubility of phloretin and its glycosides in aqueous solution required the use of organic co-solvents. Therefore, the resistance of *Pc*OGT and *Os*CGT against solvent- induced loss of activity and/or stability was evaluated for ethanol and DMSO concentrations from 5 to 30 % in the final reaction volume containing 0.1 mM phloretin and 2 mM UDP-glucose. The impact on stability was measured after incubating the single enzymes in the reaction mixture containing solvent for 20 h, whereas the influence on activity was measured directly after addition of enzymes to the reaction mixture.

The effect of increasing solvent concentrations on the initial activities was determined via calculating the reduction in activity with increasing solvent concentrations, using the activity at the lowest used solvent concentration (5 %) as a reference. The influence on stability was evaluated by comparing the activity after 20 h of incubation with values obtained from direct activity measurements without prior incubation at corresponding organic solvent concentrations.
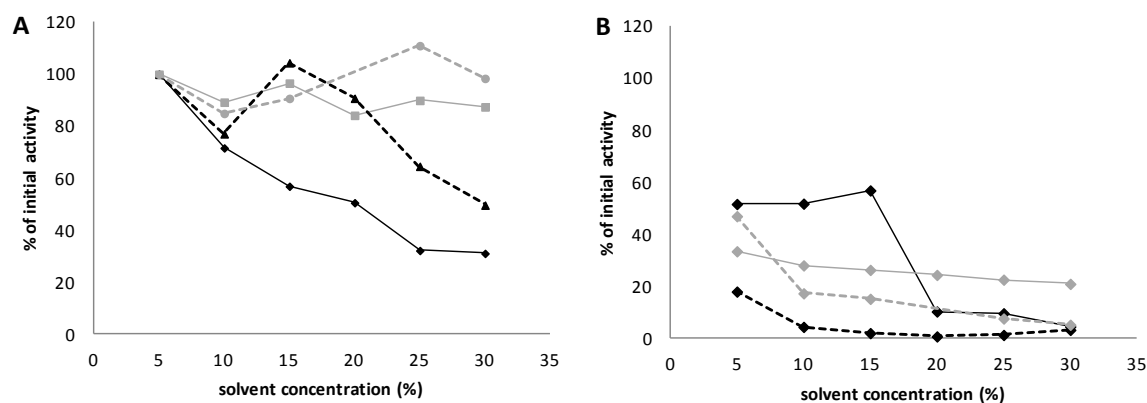
Figure 25: Influence of organic solvents on activity and stability of *Pc*OGT and *Os*CGT (A) Influence of organic solvent concentration on activity of *Pc*OGT and *Os*CGT (Influence on activity was measured directly upon addition of the enzymes to the reaction mixture, the activity at 5 % organic solvent was used as reference); (B) Influence of organic solvent concentration on enzymatic stability of *Pc*OGT and *Os*CGT (Impact on stability was measured upon incubation of the enzymes for 20 h in the reaction mixture containing EtOH/ DMSO, initial activity without incubation at corresponding solvent concentrations was used as reference)
*Pc*OGT is shown in black: continuous line represents EtOH, dashed line shows DMSO
*Os*CGT is shown in grey, continuous line represents EtOH, dashed line represents DMSO

Activities determined upon enzyme addition at 5 % organic solvent were used as reference and the decrease thereof with increasing solvent concentration was monitored. Incubating the *O*-glycosyltransferase with DMSO did not cause a decrease of the activity for concentrations up to 15 %; with 30 % DMSO about half of the activity was lost. The rate of inactivation with increasing solvent concentrations was more significant for EtOH, leading to a 70 % loss of activity for the highest solvent concentration tested.

*Os*CGT showed less inactivation for both solvents over the whole evaluated concentration range. For a six-fold increase of the EtOH concentration only 13 % of the activity was lost. DMSO did not lead to a significant reduction in enzymatic activity, a recovery for concentrations higher than 15 % was even observed.

Upon incubation of both enzymes in different concentrations of organic solvents for 20 h the activity was measured and compared to the activities at corresponding solvent concentrations without prior incubation. For all samples at least 50 % of the initial activity was lost by incubation due to destabilization of the enzymes. As observed for the prior experiment, EtOH exhibited less negative effects on *Pc*OGT. Ethanol concentrations higher than 15 % caused massive inactivation; 30 % EtOH provoked complete destabilization of the enzyme displayed by total activity loss. Half of the initial *O*-glycosylation activity was lost by incubation with 5 % EtOH, whereas the same concentration of DMSO reduced the initial activity by 80 %. For both solvents high concentrations (> 20 %) led to a complete inactivation of the enzyme.

For *Os*CGT it was observed that the initial activity was more reduced by incubating with 5 % EtOH than with the same concentration of DMSO. Albeit the activity of *Os*CGT at 5 % solvent concentration in presence of EtOH was about 10 % lower than for DMSO, the further decrease in stability with increasing EtOH concentrations occurred with moderate rate. DMSO led to complete enzyme inactivation with concentrations of 30 %, whereas for the same concentration of EtOH a remaining activity of 20 % of the initial was determined.

From this experiment one could conclude that for the *C*-glycosyltransferase DMSO would be the solvent of choice, whereas in the low concentration range the *O*-glycosyltransferase showed better performance with EtOH. DMSO caused an acceptable activity loss of *Pc*OGT, therefore this solvent was used for further experiments.

3.2.2 Cation dependency of *Pc*OGT

The specific activity of *Pc*OGT was determined upon incubation in buffer with and without divalent cations and the activity was determined by HPLC measurement of substrate and product concentrations. The activities were determined with substrate concentrations of 0.1 mM phloretin and 2 mM UDP-glc, respectively.

Table 12: *Pc*OGT activity in buffer containing different divalent cations

	buffer (pH)	$MnCl_2$ (mM)	$MgCl_2$ (mM)	KCl (mM)	BSA (%)	activity (mU/mg)
A	HEPES (7.0)	130	0	500	13	1417.8
B	HEPES (7.0)	0	130	500	13	1504.1
C	HEPES (7.0)	130	0	500	13	1152.3
D	HEPES (7.0)	0	0	500	13	1272.5

Since in all conditions enzymatic activity was clearly observable, a strict dependency of *Pc*OGT on divalent cations could be excluded. Slight differences in activity were not necessarily fully caused by effect of the cation but could also be due to minor differences in pH. This was most likely the cause for different activities using buffer B, C and D. Whereas buffer A contained $MnCl_2$, KCl and BSA those were separately added to reaction B,C and D from stock solutions whereby the pH could have changed. As it was expected generally for enzymes comprising the GT-B fold, *Pc*OGT was shown to act independently of divalent cation presence (8).

3.2.3 pH profiles of *O*-glycosylation reactions

For the determination of the optimum reaction conditions for the coupled system, the specific activities of *Pc*OGT forward and reverse reaction were determined at different pH. A pH

favoring the reverse reaction from phlorizin to phloretin and approving sufficient *Os*CGT activity was then chosen for experiments employing the coupled set- up. The substrate concentrations were adapted to the beforehand determined specific activities in the forward and reverse reaction (0.1 mM phloretin, 2 mM UDP-glc for the forward reaction; 1 mM phlorizin and 2 mM UDP for the reverse reaction).
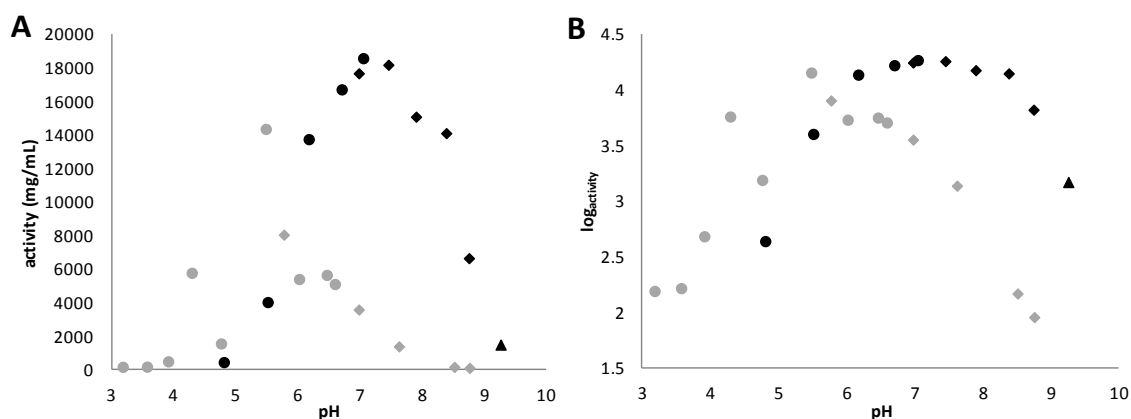
Figure 26: pH profile of *Pc*OGT forward and reverse reaction Forward reaction: conversion of phloretin and UDP-glucose to phlorizin and UDP; Reverse reaction: conversion of phlorizin and UDP to phloretin and UDP-glucose (A) Representation of exact data of *Pc*OGT forward and reverse reaction, (B)Logarithmic representation of forward and reverse reaction activities depending on pH
Forward reaction is shown in black, reverse reaction is represented in grey; circles indicate citrate buffer, diamonds represent Tris/HCl buffer, triangles show CAPS buffer

3.2.3.1 Forward reaction

The concentration of formed *O*-glycoside at varying pH- conditions was monitored to calculate the specific enzymatic activity at the respective condition.

Table 13: pH- profile of *Pc*OGT forward reaction

buffer	pH	activity (mU/mg)	$log_{activity}$
citrate	4.81	435.1	2.64
	5.51	4019.8	3.60
	6.17	13751.3	4.14
	6.70	16723.6	4.22
	7.05	18585.8	4.27
Tris/HCl	6.98	17683.3	4.25
	7.45	18191.8	4.26
	7.89	15090.6	4.18
	8.38	14109.4	4.15
	8.75	6642.9	3.82
CAPS	9.26	1482.6	3.17

Highest specific activity of *Pc*OGT forward reaction measured for pH from 7.0 to 7.5 in citrate or Tris/HCl buffer. pH values higher than 9.5 led to a more than ten-fold decrease of enzyme activity when compared to physiological pH.

A pH lower than 5.0 did not lead to any product formation suggesting that this pH condition caused complete inactivation of the enzyme by a false positioning of the acceptor in the active site, thereby rendering the enzyme inactive due to structural changes. As phloretin possesses three hydroxyl groups available for deprotonation, three different binding modes could be suggested; one to be favored depending on pH (29).

3.2.3.2 Reverse reaction

Upon incubation of *Pc*OGT with phlorizin and UDP, the concentration of the formed aglycon was monitored and related to the enzymes specific activity of catalyzing the reverse reaction.

Table 14: pH profile of *Pc*OGT reverse reaction

buffer	pH	activity (mU/mg)	$\log_{activity}$
citrate	3.18	154.6	2.19
	3.57	163.9	2.22
	3.91	480.9	2.69
	4.29	5766.1	3.77
	4.76	1547.3	3.19
	5.48	1436.1	3.16
	6.02	5395.9	3.73
	6.46	5641.1	3.70
	6.59	5097.8	3.71
Tris/HCl	5.77	8042.6	3.91
	6.98	3573.9	3.55
	7.62	1372.9	3.14
	8.51	146.8	2.17
	8.76	89.9	1.95

The highest specific activity was determined for citrate buffer at pH 5.5. An increase of the pH led to a decrease of the overall enzymatic activity; at pH 9.5 only 0.6 % of the activity could be regained when compared to pH 5.5. At physiological pH, the activity of the reverse reaction was determined to be 56 % of the highest measured value. Almost complete absence of phlorizin formation at high pH would suggest a destabilization of the enzyme at these conditions.

From *Pc*OGT pH profiles of the forward and the reverse reaction (Figure 26) it was assumed that the optimal conditions for the *O*-glycosylation reverse reaction are between pH 5.5 and 6.5, whereas the forward reaction is favored at pH 7.0- 7.5.

3.2.4   pH profile of *C*-glycosylation

The pH profile of *C*-glycoside synthesis was clearly distinct from the corresponding pH profile of *O*-glycoside synthesis (Alexander Gutmann, TU Graz; unpublished data) utilizing substrate concentrations of 0.1 mM phloretin and 2 mM UDP-glucose.
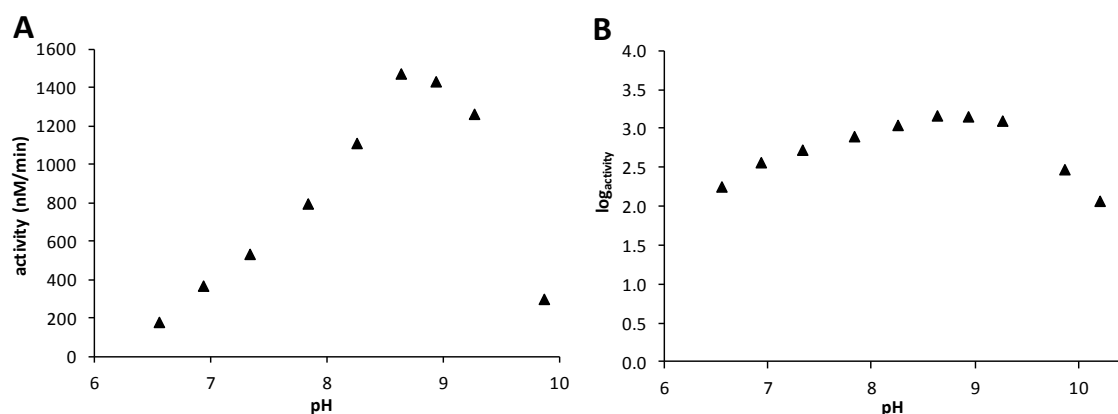
Figure 27: pH profile of *Os*CGT reaction Reaction from phloretin and UDP-glucose to nothofagin and UDP. (A) Representation of exact data, (B) Logarithmic representation of *Os*CGT pH profile

For *Os*CGT, the optimum pH for *C*-glycoside formation was determined to be 8.5- 9.0. It could be suggested that at higher pH values an additional hydroxyl- group of phloretin was present in its deprotonated form, thereby easing its transformation into nothofagin by *Os*CGT.

The optimum pH for *Pc*OGT reverse reaction and *Os*CGT, respectively, were used to preset the optimal conditions for further coupled reactions assays. Tris/HCl buffer (pH 7.0) was chosen as standard condition. It was expected that this pH should afford acceptable conditions for both enzymes and thereby satisfying catalysis of both reactions in the coupled system.

3.2.5   Preference of *Pc*OGT reaction direction

By comparing the rates of the forward and the reverse reaction of *Pc*OGT at different pH values it was observed that with increasing pH, the activity ratio increased with benefit on the forward reaction. From pH 5.5 to 7.0 the ratio was calculated to be 2.6, whereas at pH 9.0 it was determined to be around 40.0. This indicated that with higher pH the reaction from phloretin with UDP-glc to phlorizin and UDP is favored over the reaction of phlorizin and UDP to phloretin and UDP-glc.

Table 15: Calculation of ratio$_{forward/reverse}$ for *Pc*OGT forward and reverse reaction

pH	buffer	activity$_{forward}$ (mU/mg)	activity$_{reverse}$ (mU/mg)	ratio$_{forward/reverse}$
5.5	citrate	4019.8	1463.1	**2.7**
6.0	citrate	13751.3	5395.9	**2.5**
6.5	citrate	16723.6	5641.1	**3.0**
7.0	Tris/HCl	18585.8	8042.6	**2.3**
7.5	Tris/HCl	18191.8	3573.9	**5.1**
8.0	Tris/HCl	15090.6	1312.2	**11.5**
9.0	Tris/HCl	6642.9	146.8	**43.5**
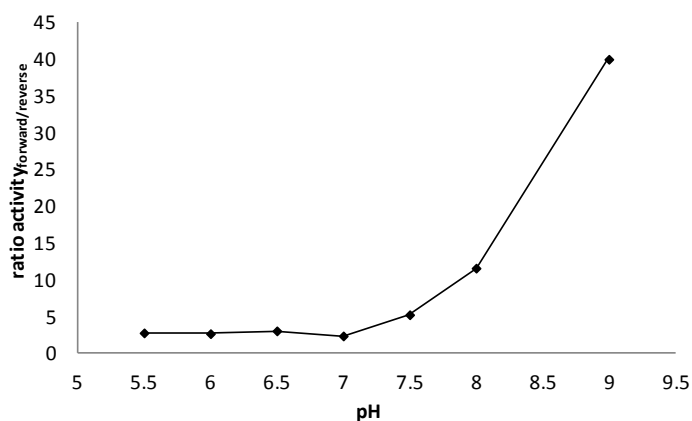
Figure 28: Ratio$_{forward/reverse}$ of *Pc*OGT glycosylation reactions The ratio was determined by comparing the activities of the forward and the reverse reaction at corresponding pH (exact data are given in Table 15)

From Figure 28 one can derive that with increasing pH the ratio of the forward and reverse reaction of *Pc*OGT dramatically increased, peaking at pH 9.0. This indicated that the ability of *Pc*OGT of catalyzing the conversion of phlorizin to the aglycon was strongly inhibited by increasing pH. This result was constituent with the beforehand determined optimal pH conditions, being pH 7.0 to 8.0 for the forward, and pH 6.0- 6.5 for the reverse reaction, respectively. At acidic pH (<5.0) the reverse reaction is much favored over the forward reaction, presumably due a wrong binding mode of the acceptor into the active site. One could also suggest that the higher activity in the reverse direction was possible due to the complete absence of the forward reaction at low pH.

3.2.6 Alternative sugar donors

The replacement of UDP-glucose with UMP and glucose- 1- phosphate (G1P) was performed in order to test it as an opportunity to utilize alternative sugar donors for the generation of *O*- or *C*-glycosides by *Pc*OGT and *Os*CGT, respectively. The substrate concentrations were set to 5 mM phloretin, 20 mM UMP and 20 mM G-1-P for both enzymes.
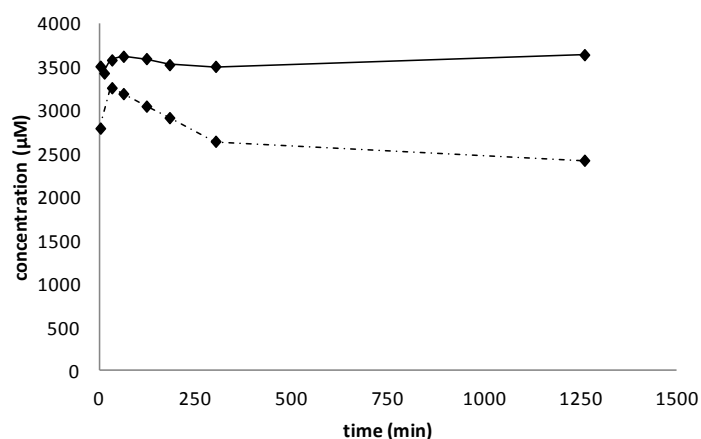
Figure 29: Conversion of phloretin by *Pc*OGT and *Os*CGT in presence of UMP and G-1-P as alternative sugar donors No conversion of substrate or product formation was detectable for both enzymes, which is represented by a constant concentration of phloretin (continuous line: *Pc*OGT, dashed line: *Os*CGT)

For both, *Pc*OGT and *Os*CGT, no conversion of phloretin into the corresponding *O*-or *C*-glycoside was detectable using UMP and G-1-P instead of UDP-glucose as cofactor, albeit the enzyme concentrations were increased tenfold compared to normal reaction conditions. Phloretin concentrations did not decrease over time for both enzymes and no formation of phlorizin or nothofagin, respectively, was observable.

3.2.7   Stabilization of activity via BSA

It was determined that a high concentration of organic solvent ($\geq 10\,\%$) induced inactivation of both *Pc*OGT and *Os*CGT. For the coupled system it was necessary to increase the overall concentration of organic solvent in order to be able to increase the used amount of substrate. To evaluate any eventual stabilization via a higher protein concentration by coupling the enzymes, both *Pc*OGT (23.3 µg) and *Os*CGT (7.4 µg) were incubated with BSA in the single enzyme reaction set-up with increasing concentrations of DMSO (0.1 mM phloretin and 2 mM UDP-glc final substrate concentrations). Additional 100 µg BSA were added to the standard buffer, which already contained a concentration of 0.13 %. The final protein concentration was about 250 µg and 230 µg for the *O*-glycosyltransferase and *C*-glycosyltransferase reactions, respectively.

Table 16: Stabilization of enzymatic activity via BSA addition

enzyme	reaction	$k_{product}$ (µM/min)	activity (mU/mg)
*Pc*OGT	phloretin + UDP-glc → phlorizin + UDP	0.83	3320
*Pc*OGT	phlorizin + UDP → phloretin + UDP-glc	0.77	3080
*Os*CGT	phloretin + UDP-glc → nothofagin + UDP	0.84	3360

Due to the commonly higher protein concentration in the final reaction the specific activity of both enzymes was stabilized even at high solvent concentrations. A decrease was observed when comparing the activities with values from initial measurements of the specific activities using 5 % DMSO, nevertheless, it was demonstrated that up to 30 % DMSO were possible to be applied if protein- stabilizing agents were added. Employing a solvent concentration of 5 % DMSO resulted in an enzymatic activity of about 7394 mU/mg for *Os*CGT and about 38220 mU/mL for *Pc*OGT, respectively. Evaluating the level of activity decrease even in presence of stabilizing agents, one could assume the *O*-glycosyltransferase to be more sensitive to higher solvent concentrations.

3.2.8 Kinetic characterization (Michaelis- Menten kinetics)

Kinetic parameters (K_m, k_{cat}, k_{cat}/K_m) were determined for both enzymes by measuring the initial reaction rate using different concentrations of one substrate and a constant concentration of the second. The formation of the respective products was monitored over time.

3.2.8.1 *Pyrus communis O*-glycosyltransferase

Michaelis- Menten parameters for phloretin and UDP-glucose/ UDP-galactose of the *O*-glycosylation forward reaction and for phlorizin and UDP of the reverse reaction were calculated employing SigmaPlot 9.0 by from the initial reactions rates dependent on different substrate concentrations.

Table 17: Michaelis- Menten parameters for *Pc*OGT catalysis

	v_{max} (µM/min)	K_m (µM)	K_i (µM)	k_{cat} (s^{-1})	k_{cat}/K_m (s^{-1}µM^{-1})
phloretin	3850 ± 4470	311 ± 425	60 ± 80	2.70	0.0090
UDP-glucose	8850 ± 250	56 ± 7	/	6.30	0.1100
UDP-galactose	825 ± 57	1220 ± 280	/	0.25	0.0002
phlorizin	3435 ± 150	18 ± 5	/	1.02	0.0600
UDP	3005 ± 170	470 ± 76	/	0.90	0.0020

Kinetic parameters for *Pc*OGT forward reaction were determined by varying the initial phloretin concentration (0- 750 µM) and keeping UDP-glucose concentration (1 mM) constant or by varying UDP-glucose concentration (0- 3750 µM) at a constant phloretin concentration (250 µM). The initial reaction rates were determined via HPLC; exact data are given in the appendix.

A K_m for phloretin of about 310 µM was determined, with a maximum reaction rate of about 3850µM/min and a turnover number of 2.7 s^{-1}. It was observed that with progress of the reaction and the related decrease of substrate concentration also the enzymatic activity decreased. The decrease in the reaction rate could be explained by the decrease of the phloretin and an increase of the phlorizin concentration, thereby providing more substrate for the reaction in the reverse direction. Generally, the reaction was observed to slow down as it approximated the equilibrium between the forward and the reverse direction. The enzyme showed substrate inhibition for concentrations higher than 100 µM phloretin (K_i~ 60 µM).

For varying the concentration of UDP-glucose while keeping phloretin concentration constant, there was also no relation of the decrease of the concentration of UDP-glc and an increase/ decrease of the enzymatic activity observable. A Michaelis- Menten constant of *Pc*OGT for UDP-glucose of about 60 µM was measured, beside a maximum reaction rate of about 8850 µM/min and a turnover of 6.3 s^{-1}. Saturation of the enzyme was achieved for UDP concentrations higher than 1200 µM.

Determinations of kinetic parameters for the alternative sugar donor UDP-galactose for the *O*-glycosylation reaction were performed using different concentrations of UDP-galactose (0-10000 µM) while keeping the concentration of phloretin (200 µM) constant. Initial reaction rates at different concentrations were then used to calculate Michaelis- Menten parameters and are given in the appendix (Table 32, Table 33 and Figure 60). A Michaelis- Menten constant of about 1220 µM, a maximum reaction rate of about 825 µM/min and a turnover number of 0.25 s^{-1} were determined. Complete saturation of the enzyme was not achieved with any of the used UDP-galactose concentrations.

The kinetics of *Pc*OGT reverse reaction were examined by incubating pure enzyme with different concentrations of phlorizin (10- 5000 µM) and constant UDP concentration (1 mM) or varying UDP concentrations (5- 2000 µM) and constant phlorizin concentrations (5 mM). Exact results are given in the appendix (Table 34, Table 35, Table 36, Table 37 and Figure 61, Figure 62). For phlorizin in the *Pc*OGT reverse reaction a K_m- value of about 18 µM, a maximum reaction rate of 3440 µM/min and a turnover of 1.02 s^{-1} was measured. Saturation of the enzyme was achieved for phlorizin concentrations higher than 500 µM. For UDP the half- saturation constant was determined to be about 470 µM and the enzyme showed a maximum reaction rate of about 3000 µM/min and a turnover of 0.9 s^{-1}. Saturation of the enzyme with UDP could be suggested to be reached for concentrations higher than 1600 µM.

For all tested substrates, no inhibition was detectable apart from phloretin, probably due to the beforehand mentioned different binding behavior of the substrate. For high concentrations

of phloretin it could be suggested that inappropriate binding due to active site occupation by already bound phloretin rendered the enzyme inactive.

3.2.8.2 *Oryza sativa C*-glycosyltransferase

Apparent Michaelis- Menten parameters for phloretin and UDP-glucose were determined by incubation of the *C*-glycosyltransferase with various concentrations of one substrate and keeping the concentration of the second substrate constant. Initial reaction rates were then used for the calculation of kinetic parameters.

Table 18: Michaelis- Menten parameters for *Os*CGT catalysis

	v_{max} (µM/min)	K_m(µM)	K_i (µM)	k_{cat} (s^{-1})	k_{cat}/K_m ($s^{-1}µM^{-1}$)
phloretin	9830 ± 590	9 ± 3	1540 ± 400	22.1	2.4
UDP-glucose	7770 ± 315	22 ± 5	/	14.5	0.8

*Os*CGT showed a Michaelis- Menten constant of about 9 µM with a maximum reaction rate of about 9800 µM/min and a turnover number of 22 s^{-1} for phloretin. Substrate inhibition by phloretin was measured to occur for high concentrations, reflected in an inhibition constant of about 1500 µM. Inhibition could be explained by unfavorable binding of the substrate into the active site thereby provoking a reduction in the enzymatic activity.

*Os*CGT was determined to be completely saturated with UDP-glc concentrations higher than 100 µM, reflected in a K_m- value of about 22 µM. The maximum reaction rate was measured to be about 7770 µM/min with a turnover of 14 s^{-1}. The exact data are given in the appendix.

Comparing the Michaelis Menten parameters for phloretin and UDP-glucose of *Pc*OGT and *Os*CGT, one can assume that the *C*-glycosylation reaction of phloretin occurs with a higher efficiency than the *O*-glycosylation, which is reflected by a 2.5-fold lower K_m and a ten-fold higher k_{cat}. The maximum reaction rate with phloretin was also determined to be higher for the *C*-glycosyltransferase than for the *O*-glycosyltransferase by factor 2.5. The same conclusion could be drawn from the kinetic parameters for UDP- glucose, albeit the maximum reaction rate of *Pc*OGT was determined to exceed that of *Os*CGT. The half- saturation constant of *Os*CGT was half that for *Pc*OGT, indicating a lower substrate affinity. The higher maximum reaction rate is represented by a twice as high turnover number for the *C*- than for *O*-glycosylation.

3.3 O-/ C-glycoside conversion

Following characterization of the single enzymes, *Pc*OGT and *Os*CGT were combined in a one-pot reaction system to synthesize nothofagin from phlorizin. The reversibility of the *O*-glycosylation reaction was exploited to transform phlorizin and UDP to the intermediate products phloretin and UDP-glucose, which in turn served as substrates for the *C*-glycosylation reaction to finally yield nothofagin and UDP. The influence of various parameters such as the ratio of the two glycosylation activities, the concentration of organic solvents, pH conditions and substrate concentrations was determined and used for optimization of the system. Upon identification of the optimal reaction conditions, an increase of the final product yield was compassed via prolonged conversion in a fed-batch mode.

3.3.1 Variation of glycosylation activities

To determine the optimal ratio of enzymes for the efficient conversion of phlorizin to nothofagin the employed *O*- and *C*-glycosylation activities were varied with respect to each other. It was pursued to evaluate the required *Pc*OGT activity providing sufficient substrate (phloretin and UDP-glucose) for the *C*-glycosylation reaction in order to avoid substrate limitation of product formation. *Pc*OGT and *Os*CGT activities in the final reaction mixtures were varied as given in Table 19. The deviation of the summarized concentration from the theoretical concentration was determined to be about 22 %, which was higher for reactions employing higher concentrations of protein (highest deviation for reaction 1)

Table 19: Variation of *O*- and *C*-glycosylation activities

reaction no	*Pc*OGT (mU/mL)	*Os*CGT (mU/mL)
1	200.0	100.0
2	100.0	50.0
3	25.0	50.0
4	25.0	25.0
5	12.5	25.0
6	12.5	12.5
7	10.0	5.0
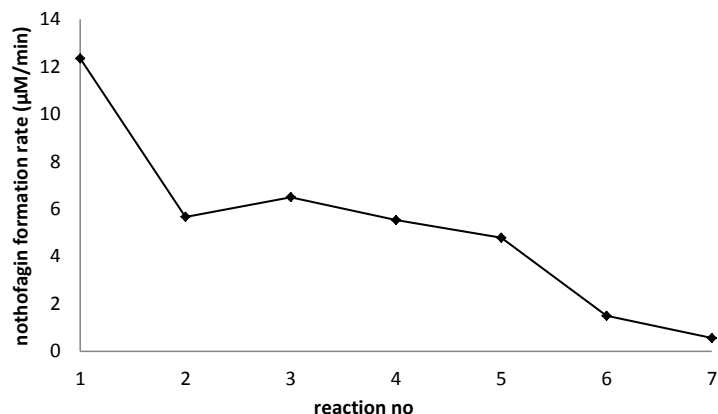
Figure 30: Nothofagin formation rate depending on enzyme activities Initial reaction rates were used for evaluation (The used glycosylation activities for reaction 1-7 are listed in Table 19). Substrate concentrations were set to 25 mM phlorizin and 2 mM UDP.

The maximum product formation rate was observed for reaction 1 (200 mU/mL *Pc*OGT and 100 mU/mL *Os*CGT), whereas for all other reactions where either one or both enzyme activities were reduced, a decrease in the nothofagin formation rate was observed. From reactions 3- 5 one could assume, that the decrease of the *O*-glycosylation activity exhibited less impact on the overall conversion, than a decrease of the *C*-glycosylation activity as shown for reactions 6 and 7.
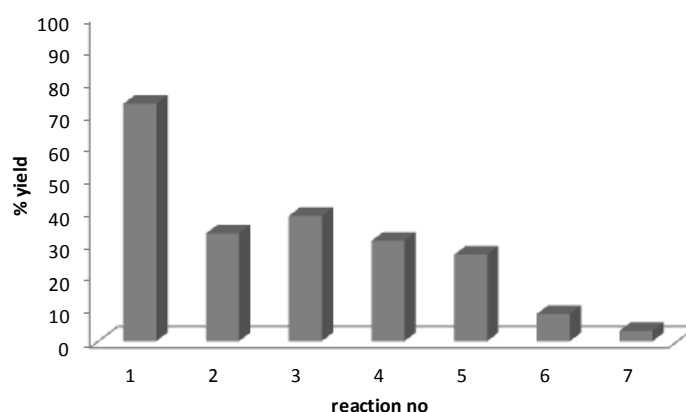
Figure 31: Final yield of nothofagin depending on different enzyme activities The yield was determined after 24 h of incubation and is given in percentage of the maximally obtainable yield (initial concentration of substrate was used as reference) calculated from the initial phlorizin concentration of 25 mM phlorizin.

Reaction 1 (200 mU/mL *Pc*OGT, 100 mU/mL *Os*CGT) led to nearly 90 % of substrate conversion, whereas a subsequent reduction of used enzyme activities led to a decrease of conversion, which was also consistent with the obtained overall product yield (Figure 31). Doubling of both glycosylation activities caused an exact doubling of the final nothofagin yield. For other reactions, there was no linear decrease of substrate conversion or product formation with decreasing enzyme activity detectable.
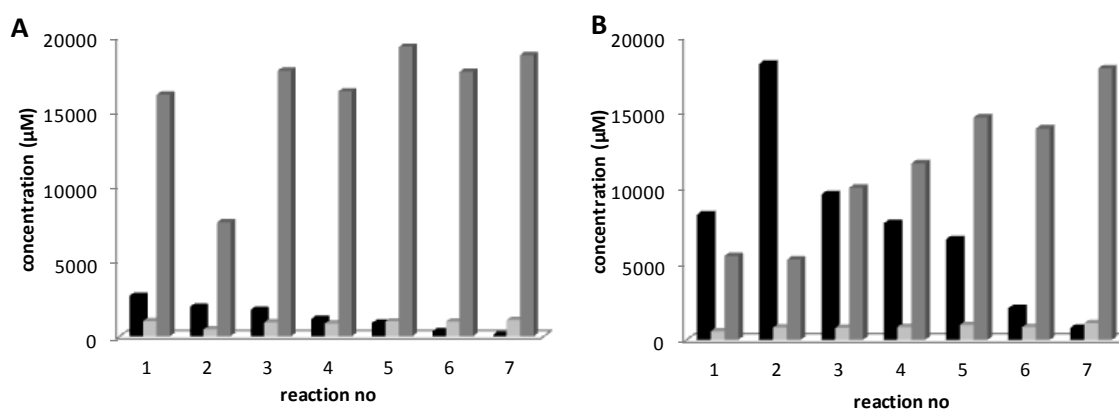
Figure 32: Concentrations of nothofagin, phloretin and phlorizin after 2 h and 24 h of reaction (A) Concentrations after 2 h of reaction, (B) Concentrations after 24 h of reaction (nothofagin is shown in black, phloretin is shown in light- grey, phlorizin is shown in dark- grey).

*Os*CGT activities lower than 25 mU/mL did not lead to a sufficient conversion of the intermediate phloretin into nothofagin, indicating the reaction being partly determined/ limited by the *C*-glycosyltransferase activity. Phloretin concentrations seemed to be constant for all reactions tested, indicating a high *O*-glycosylation activity even for low enzyme concentrations. The phloretin content slightly increased with reduction of the *C*-glycosylation activity as its further conversion into nothofagin was limited. This displayed limitation of the system by *Os*CGT.

Generally, it could be stated that the 2:1 relation of *Pc*OGT and *Os*CGT activities were to be used to allow efficient conversion of phlorizin into nothofagin by providing sufficient amounts of substrates for the *C*-glycosylation reaction. Although both enzymes were varied to different extends no clear conclusion about *Pc*OGT or *Os*CGT being a limiting factor could be drawn from this experiment, although decreasing of *Os*CGT concentration led to a more significant decrease of the final product yield. For further experiments an excess of the *O*-glycosylation activity was employed to avoid limitations of substrate for the *C*-glycosylation, which could be due to changes of the reaction environment caused by progress of the reaction.

3.3.1.1 Increase of *C*-glycosylation activity

To verify eventual limitations of *O*- to *C*-glycoside conversion by the *C*-glycosylation reaction, the enzymatic activity of *Os*CGT was increased whilst keeping *Pc*OGT activity constant. The employed substrate concentrations were 10 mM phlorizin and 2 mM UDP, respectively. The final concentrations of products and substrates were determined after a reaction time of 24 h via HPLC. Deviations from the theoretical mass balance were determined to be about 20 %.

Table 20: Rate of nothofagin formation with different *Os*CGT activities used

reaction no	*Pc*OGT : *Os*CGT (mU/mL)	initial reaction rate (µM/min)
1	1 : 0.5	16.9
2	1 : 1.5	22.4
3	1 : 2	22.8
4	1 : 3	25.7
5	1 : 5	29.9
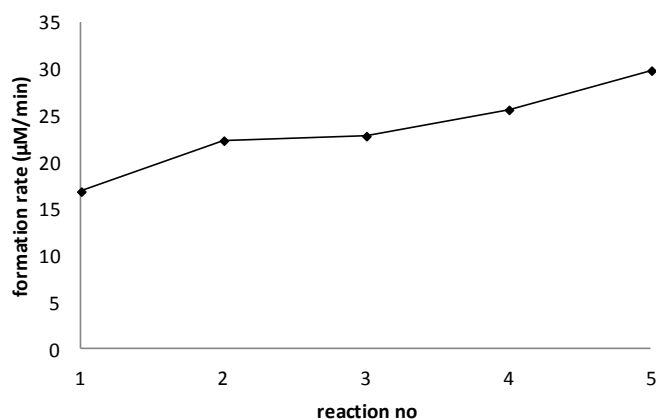
Figure 33: Increase of the nothofagin formation rate depending on increasing *Os*CGT activity Enzymatic activities used in reactions 1- 5 are listed in Table 20

The rate of nothofagin formation was observed to generally increase with increasing *C*-glycosyltransferase activity, although with lower emphases than expected; a ten-fold increase of used *Os*CGT activity, merely led to an increase of the formation rate by factor 1.7.
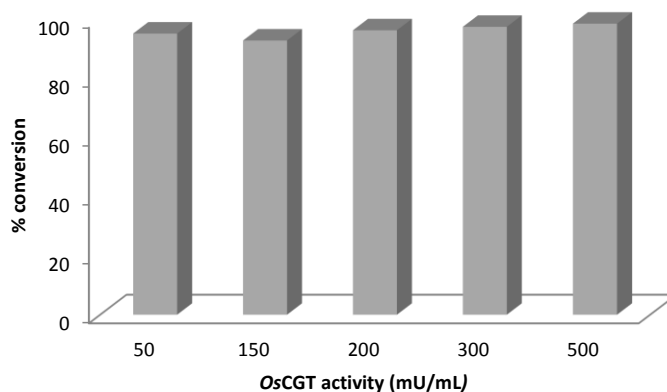
Figure 34: Overall substrate conversion with increasing *Os*CGT but constant *Pc*OGT activity Percentage of conversion was determined after 180 min of reaction by using the initial concentration of substrate as reference (10 mM phlorizin, 2 mM UDP).

For all samples an almost complete conversion of phlorizin (>98 %) was achieved, independently of the used *C*-glycosyltransferase activity. The nearly complete overall conversion

of the substrate phlorizin and relatively high concentrations of the intermediate product phloretin were detected for all different *Os*CGT concentration; it could be assumed that *Pc*OGT did not exhibit limiting influence on the general reaction set- up.

As it was expected, the final concentration of phloretin was decreasing with increasing *C*-glycosyltransferase activity. An increase of the used *Os*CGT activity by factor 10 reduced the final concentration of the intermediate product by half (Figure 35).
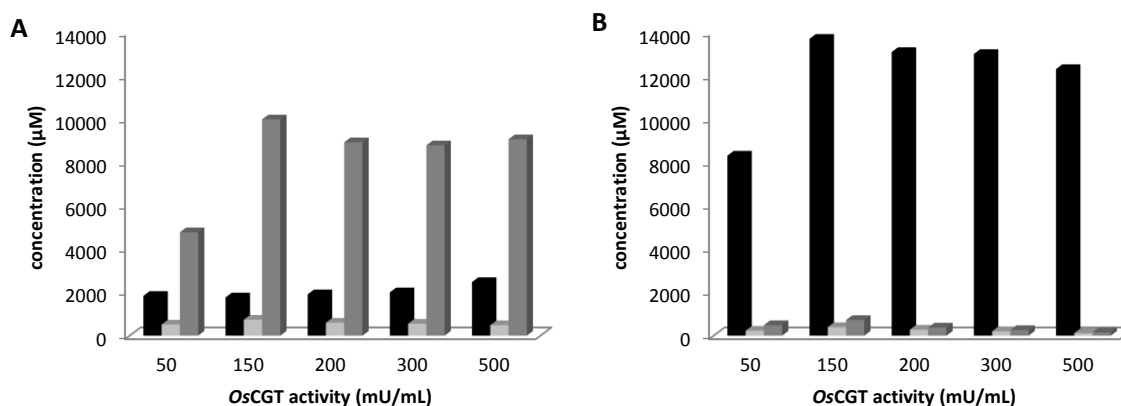
Figure 35: Concentrations of nothofagin, phloretin and phlorizin at different times of incubation (A) Concentrations after 1 h of incubation, (B) Concentrations after 24 h of incubation (nothofagin is shown in black, phloretin is shown in light- grey, phlorizin is shown in dark grey)

An elevation of the used activity of *Os*CGT caused an improvement of the overall conversion and the concentration of achieved final product nothofagin, albeit no linear relation was determined; a two-fold increase of enzymatic activity did not lead to twice the amount of final product. This again suggested other factors having limiting influence on the overall reaction system besides the *C*-glycosylation reaction, albeit *Os*CGT was identified to have a major impact on the overall conversion performance of the system.

3.3.2 Variation of organic solvent concentrations

The concentration of DMSO and EtOH in the final reaction was varied from 5-20 % to evaluate the maximum usable substrate concentration (initial concentrations of 5 mM phlorizin and 2 mM UDP). Substrate conversion and final product yield were evaluated over time depending on the used organic solvent concentrations. The deviation from the theoretical mass balance was determined to be about 10 %.
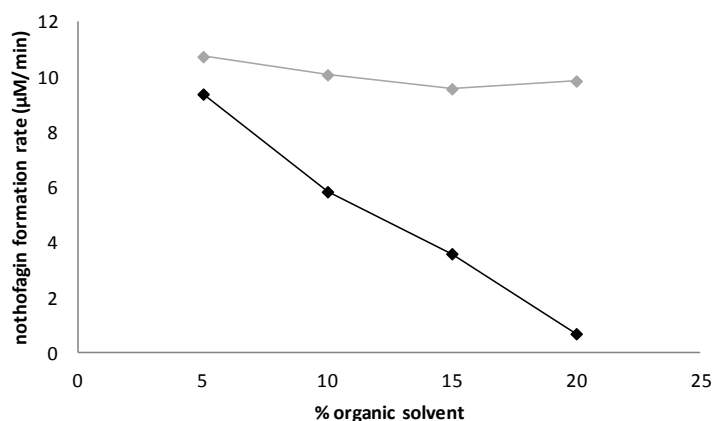
Figure 36: Rate of nothofagin formation in dependence of solvent concentration The linear increase of product, i.e. first 300min of reaction, was evaluated (DMSO is shown in grey, EtOH is shown in black)

The specific ratio of product and substrate concentration (maximally 1.0) after 24 h of reaction was determined to be constant for DMSO (0.85- 0.90), whereas for EtOH it was significantly decreasing. Consistent with the observed yield of the final product nothofagin (Figure 37), the rate of product formation decreased with increasing EtOH concentrations; increasing the content of DMSO in the final reaction volume did not exhibit negative influence on the product formation rate.
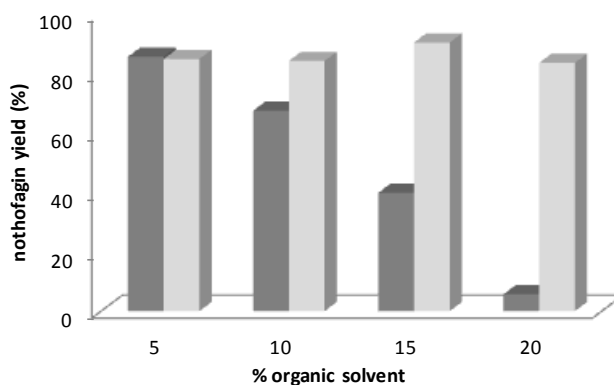
Figure 37: Final yield of nothofagin depending on different concentrations of organic solvent The final yield was evaluated after 24 h of reaction by comparing the final concentrations of the product nothofagin with the initially used substrate concentrations of 5 mM phlorizin and 2 mM UDP (EtOH is shown in dark-grey, DMSO is shown in light- grey)

Evaluating the overall conversion of phlorizin, it could be assumed that high concentrations of EtOH caused inactivation of enzymes resulting in a decrease in conversion, whereas higher concentrations of DMSO did not cause enzyme destabilization. The formation rate of nothofagin was determined to be constant for all concentrations of DMSO, which correlates with the full conversion of substrate at the respective conditions. For EtOH, the product formation

rate was linearly decreasing with increasing concentration; this was also reflected by a constant decrease in the overall yield.

The inactivation of enzymes by EtOH could be explained by the protic nature of the solvent, provoking abstraction of protons from the enzymes and thereby changing their overall structure. DMSO is declared as not possessing protic characteristics, thereby not changing the structure of the enzyme and avoiding their inactivation. Interestingly, the activity of both enzymes was stable at high concentrations of DMSO (20 %) in the coupled reaction assay, albeit it was determined that comparably high solvent concentrations caused inactivation of the single enzymes. As determined from characterizing the single enzymes, *Os*CGT showed a higher stability in presence of 20 % DMSO when compared to *Pc*OGT. As the *O*-glycosylation activity was employed in excess, destabilization due to the organic solvent could be presumably excluded from being the limiting factor, which is also reflected by the overall sufficient product yield for samples with EtOH. Both *Pc*OGT and *Os*CGT activities are drastically reduced in presence of EtOH when incubated as single enzymes; this could also explain the massive reduction of product generation for samples using EtOH. A concentration of 20 % of the solvent caused a reduction of 70 % and 80 % of the *C*- and *O*-glycosyltransferase activity, respectively. This indicated higher enzyme stability and justified DMSO as the solvent of choice for further experiments.
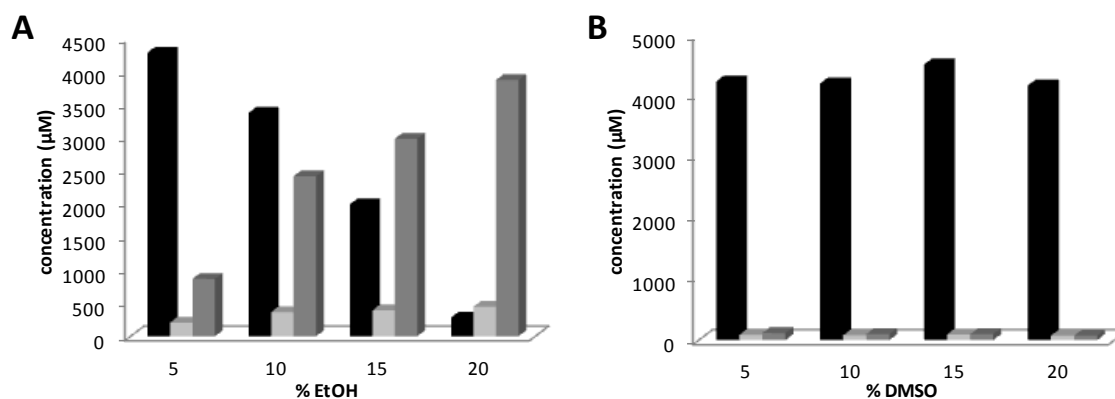
Figure 38: Concentration of substrate and products depending on different concentrations of organic solvents Concentrations were determined after 24 h of reaction by comparing them to the initial substrate concentrations of 5 mM phlorizin and 2 m UDP. The final product nothofagin is shown in black, phloretin is shown in light grey and phlorizin is given in dark grey.

The concentration of the intermediate product was determined to be higher with elevated concentrations of EtOH, whereas the concentration of phloretin of samples containing different concentrations of DMSO was determined to be at a constantly lower level (Figure 38). A higher intermediate concentration in ethanol- containing samples could be explained by a higher inactivation of *Os*CGT compared to *Pc*OGT leading to phloretin accumulation. The overall

conversion of the initial substrate phlorizin also decreased with increasing EtOH concentrations but remained constant with different concentrations of DMSO. The moderate decrease of the enzymatic activity of both, *Pc*OGT and *Os*CGT, was also suggested to be due to the overall higher concentration of protein in the reactions. A stabilizing effect of BSA and higher protein content in the reaction mixture was demonstrated in section 3.2.7.

3.3.3 Optimization of pH conditions

HEPES buffer of different pH (6.0 -8.0) was used to determine the optimum conditions for the combination of *Pc*OGT and *Os*CGT in the one-pot reaction. The conversion of substrate and yield of product from the initially used substrate (5 mM phlorizin and 2 mM UDP) was compared for different pH values. The mass balance deviation was calculated to be around 8 %.
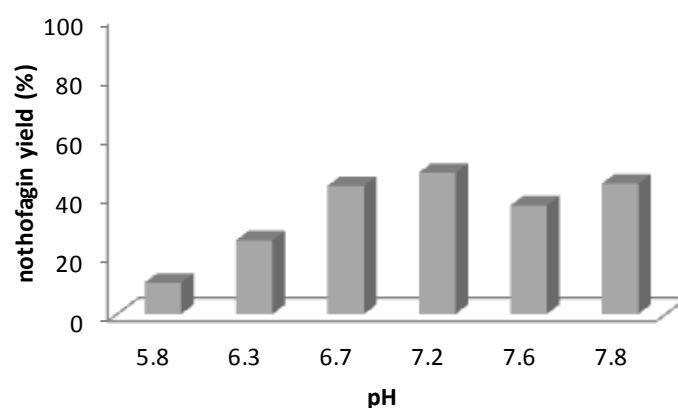
Figure 39: Final yield of nothofagin depending on pH The final yield of nothofagin was determined after 3 h of reaction by comparing the final concentrations of product with the initial concentration of substrate (5 mM phlorizin, 2 mM UDP)

The highest conversion of phlorizin (60 %) was reached at pH 7.2 with a conversion to nothofagin of 50 %; also the ratio of product to substrate (formed nothofagin from initially used phlorizin) was determined to be the highest for pH 7.2 (0.48).

Comparably high nothofagin concentrations were also detected for pH 7.6, which related to *Os*CGT pH optimum of pH 8.0- 8.5. At low pH- values (5.8) comparably high concentrations of phloretin were measurable, corresponding to the optimum pH of 6.0-6.5 of *Pc*OGT reverse reaction. The relatively high concentrations of phlorizin at pH 7.2 are most likely due to low reverse activity of *Pc*OGT at pH higher than 7.0. Complete conversion of phlorizin to nothofagin was not achieved as the reactions were stopped upon 3 h of incubation. This allowed focusing on the initial conversion rate and thereby guaranteed visibility of minor differences of the reactions.

Evaluation of concentrations after completion of conversion presumably would have masked small differences of the reactions.
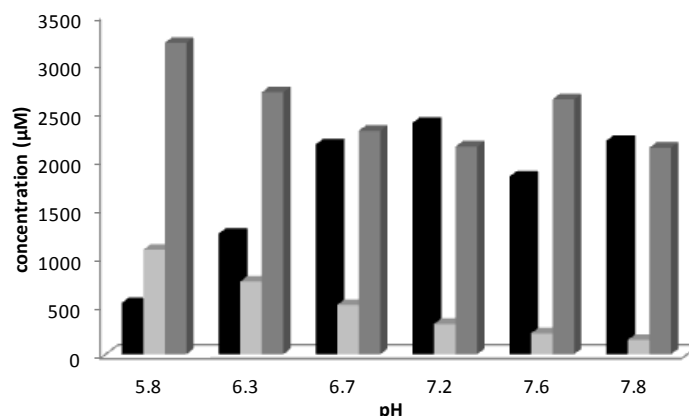
Figure 40: Concentrations of nothofagin, phloretin and phlorizin depending on pH Concentrations were determined after 3 h when the reaction was stopped and compared to the initial 5 mM phlorizin and 2 mM UDP (Nothofagin is shown in black bars, phloretin is shown in light grey and phlorizin is represented by dark grey bars)

It can be seen from Figure 40 that the concentration of phloretin decreased with increasing pH, which was suggested to be due to a higher *C*-glycosyltransferase activity at higher pH; at higher pH the nothofagin formation is enhanced. The concentration of nothofagin was observed to remain generally constant for pH values higher than 6.7.

At lower pH, a notably higher concentration of phloretin was measured due to the favoring of the *Pc*OGT reverse reaction (optimum pH 5.5- 6.5). The *C*- glycosylation reaction did not occur with maximum rate at low pH, thereby entailing the accumulation of the intermediate phloretin.

It was demonstrated recently (29), that a change in pH strongly affected the specificity of *Os*CGT mutant enzymes for the acceptor hydroxyl group to become glycosylated, meaning that a change in pH presumably alters the preferred mode of substrate binding to the enzyme. As the optimum pH for the *C*-glycosyltransferase was determined to be higher than the applied 7.0, one could suggest wrong binding of phloretin into the active site to be responsible for a decreased nothofagin yield in the lower pH range, which was shown for mutated enzymes. The increase in concentration of the final product at elevated pH strengthens the hypothesis of pH- induced acceptor positioning.

It could be suggested that at higher pH at least one hydroxyl group of phloretin is already present in its deprotonated form (pKa ~7.0) causing a higher degree of activation of the substrate. An already deprotonated substrate OH-group would ease the conversion of phloretin into nothofagin by the *C*-glycosyltransferase.

3.3.4 Variation of substrate concentrations: Kinetic characterization of the coupled system

The apparent kinetic parameters for phlorizin and UDP in the coupled reaction of *Pc*OGT and *Os*CGT were determined by varying the concentrations of one substrate and constant concentrations of the second substrate.

Table 21: Kinetic studies on the coupled reaction system under variation of substrate concentrations

	v_{max} (µM/min)	K_m (µM)	k_{cat} (s^{-1})	k_{cat}/K_m (s^{-1}µM^{-1})
phlorizin	5720 ± 250	2280 ± 230	1.7	0.001
UDP	4290 ± 130	70 ± 11	1.015	0.015

3.3.4.1 UDP

The kinetic parameters for UDP in the coupled reaction of *Pc*OGT and *Os*CGT were determined by variation of UDP concentrations (5- 2000 µM) and constant substrate concentrations (5 mM phlorizin). Initial reaction rates were measured with HPLC; the exact data are given in the appendix. The mass balance deviation was calculated to be around 15 %.

For calculation of the apparent K_m- value of UDP concentrations of phloretin and nothofagin were summarized and the increase thereof was plotted against applied UDP concentrations; exact calculations were done with SigmaPlot 9.0 resulting in an apparent K_m of 70 µM and a maximum reaction rate of 4290 µM/min. The turnover number (k_{cat}) was calculated to be 1.015 s^{-1}.
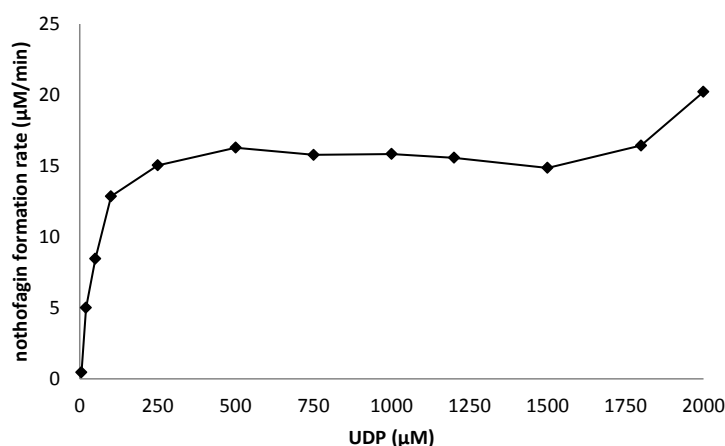
Figure 41: Nothofagin formation rate depending on different UDP concentrations The linear increase of the product concentration was used for calculating the initial reaction rates
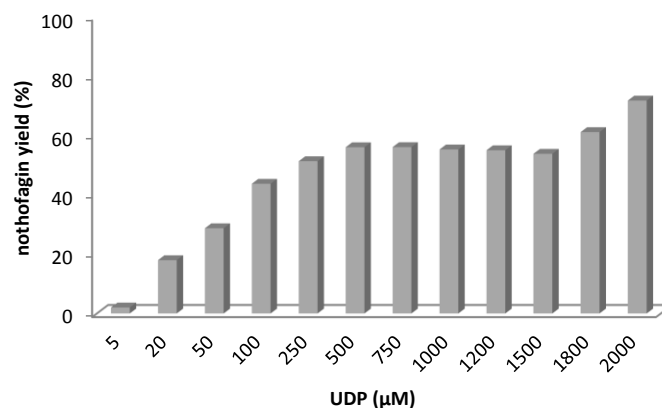
Figure 42: Final yield of nothofagin with varying concentrations of UDP The yield was determined after 180 min of incubation by using the initial concentration of substrate (5 mM phlorizin) as reference.

For UDP concentrations higher than 100 µM an overall substrate conversion of about 65 % was observed; a decrease in the overall substrate conversion could be detected for UDP concentrations below 100 µM. Maximum conversion of phlorizin was obtained for a UDP concentration of 2 mM, verifying this concentration to be optimal for all further coupled assay experiments as also the product formation rate and the final product yield as well as the ratio of product to substrate were determined to be optimal at this UDP concentration. Concentrations lower than 50 µM UDP did not lead to sufficient conversion of phlorizin into neither the intermediate phloretin nor the final product nothofagin
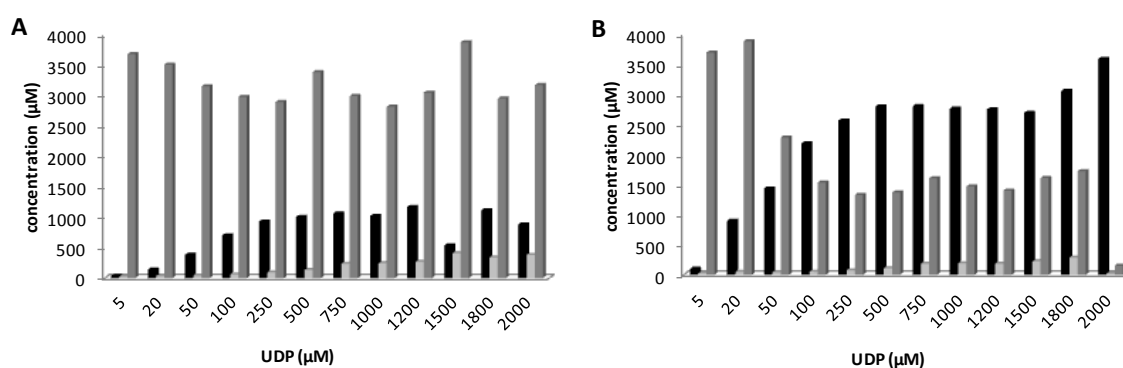
Figure 43: Concentrations of nothofagin, phloretin and phlorizin with varying concentrations of UDP and 5 mM phlorizin (A) Concentrations after 40 min of reaction, (B) Concentrations after 180 min of reaction (Nothofagin is shown in black, phloretin is shown in light- grey, phlorizin is shown in dark- grey)

It was determined that with increasing concentration of UDP, also the final concentration of phloretin was increasing. This could be explained by a higher activity of *Pc*OGT due to higher concentrations of available UDP usable for the formation of phloretin out of phlorizin.

The more UDP was present at the start of the reaction, the more phloretin and UDP-glucose were produced. One could assume that the acceleration of *Pc*OGT reverse reaction from phlorizin to phloretin by increasing UDP concentration could not be equalized by *Os*CGT as the *C*-glycosylation occurred still with constant but an overall lower reaction rate, leading to the accumulation of the intermediate product. Maximum intermediate concentrations were determined for 1800- 2000 µM UDP (~370 µM phloretin). As the increase of the concentration of phloretin with increasing concentrations of UDP was overall linear, saturation of *Os*CGT with substrate could be assumed and a limitation of the reactions by the *C*-glycosyltransferase could be excluded. The concentration of the intermediate was observed to never reach the inhibition constant of *Os*CGT, but remaining in a range to allow sufficient product formation.
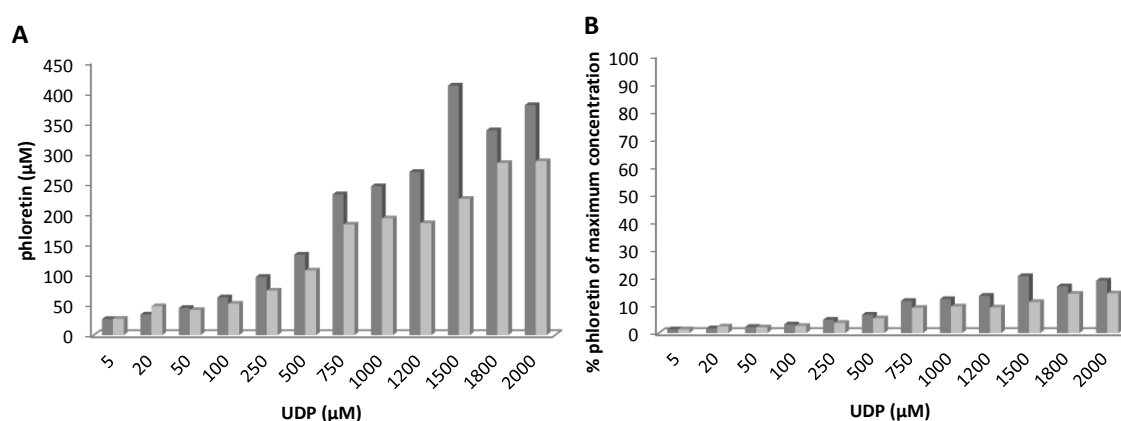
Figure 44: Concentrations of phloretin depending on different UDP concentrations (A) Concentrations of phloretin at 40 min and 180 min of reaction, (B) Representation of phloretin concentration as percentage of maximally obtainable phloretin concentration after 40 min and 180 min (40 min values shown in dark- grey, 180 min values shown in light- grey)

Considering the increase of the concentration of the intermediate product phloretin with increasing UDP concentration; it could be supposed that a higher concentration of UDP accelerated the reverse reaction of *Pc*OGT, whereas the activity of *Os*CGT did not increase accordingly, leading to the accumulation of phloretin. *Pc*OGT seemed to reach saturation for UDP concentrations of 500- 600 µM, up to this concentration the rate of the reverse O-glycosyltransfer was observed to increase.

An eventual influence of the *O*-glycosyltransferase forward reaction could not be clearly demonstrated, but it could be suggested that due to the increase of UDP, a higher concentration of the intermediates phloretin and UDP-glucose would be reached. Higher concentrations of phloretin and UDP-glucose were suspected to accelerate the forward reaction causing a regeneration of phlorizin. This could explain the observed incomplete substrate conversion as remaining or newly- generated phlorizin was detected at the end of reactions.

The conversion of substrate during the initial reaction rate, i.e. after 60 min, was evaluated to reflect the influence of the cofactor concentration on conversion kinetics. It could be proposed that UDP concentrations higher than 100 µM did not influence the conversion rate, whereas lower concentrations caused a decrease in the conversion velocity. This was consistent with the lower overall conversion at comparably low concentrations of cofactor.

Table 22: Conversion of phlorizin with varying concentrations of UDP

UDP (µM)	% conversion (60 min)	% conversion (300 min)
5	22.5	26.1
20	31.3	22.3
50	41.5	54.0
100	50.8	69.3
250	54.2	73.4
500	53.6	72.7
750	47.1	67.9
1000	55.1	70.7
1200	53.8	72.0
1800	52.7	65.6
2000	46.1	97.0
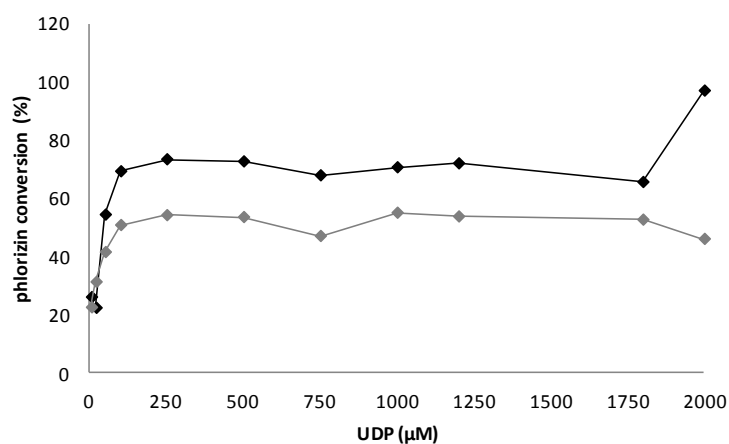
Figure 45: Comparison of phlorizin conversion Conversion was calculated by comparing the substrate concentration at defined time points with the 5 mM initial concentration of substrate (Percentage of converted substrate after 1 h of reaction is shown in black, conversion after 3 h of reaction is shown in grey)

For all reactions except for that with 2000 µM UDP, the formation rate of the final product nothofagin was shown to decrease with incubation time, as the final conversion of phlorizin (after 300 min of reaction) was not drastically higher than the conversion determined after 60 min of reaction. Albeit the incubation time was three times longer between the first and second representation (Figure 45), the overall increase of substrate conversion did not increase accordingly. This indicated a significant deceleration of the reaction, which could presumably be caused by enzyme inactivation.

By comparing the apparent Michaelis- Menten constants of PcOGT for UDP in the single (K_m= 470 µM) and in the coupled system (K_m= 70 µM), the O-glycosyltransferase was excluded from contributing to limitation of the system performance when combined with OsCGT. If the O-glycosyltransferase would have been the rate limiting factor the same or at least a similar K_m would have been determined for the single and the coupled reaction.

The lower K_m in the coupled system could be explained by: due to the equilibrium reaction of PcOGT, it could not be expected that in spite of an excessive phloretin concentration more than 50 % of UDP could be converted to UDP-glucose. According to this assumption half of the calculated concentration of UDP (35 µM) were present as UDP-glucose. A concentration of 35 µM UDP-glucose in the system fits to the measured K_m of 23 µM for UDP-glucose of OscGT and demonstrates the limitation by the C-glycosyltransferase.

3.3.4.2 Phlorizin

Kinetic parameters for phlorizin in the coupled reaction system were determined by incubating pure enzymes with increasing concentrations of substrate (0- 10000 µM) and constant UDP concentration (2 mM). The initial reaction rates at different concentrations of phlorizin were determined over time and used for the calculation of kinetic parameters. Exact values and figures are given in the appendix. The average deviation from the mass balance was determined to be about 4 %.

An apparent Michaelis- Menten constant of 2280 µM and a maximum reaction rate of 5720 µM/min were determined. A turnover number of 1.7 s^{-1} was calculated.

Considering half- saturation constants of 10 µM for phloretin and 25 µM for UDP-glucose for OsCGT in the single reaction, it could be concluded that the maximum reaction rate was reached already for low concentrations of 100 µM phloretin, which related to 100 µM UDP-glc. 80 % of v_{max} were reached at this concentration. Analyzing the reaction with 10 mM phlorizin, it was observed that 300 µM of phloretin were generated immediately after starting the reaction by enzyme addition, and phloretin increased further with time although the optimal concentration for conversion by OsCGT already has been present.

The fact that up to 1 mM phloretin is produced (50 % conversion of UDP), demonstrated the approximation to the equilibrium of the O-glycosyltransferase reaction directions, albeit the forward reaction should not have been favored at the used conditions.
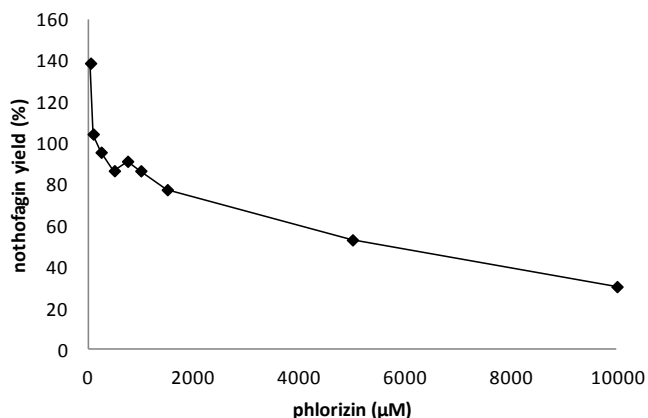
Figure 46: Final yield of nothofagin depending on different concentrations of phlorizin

The conversion of phlorizin was nearly complete (~98 %) for concentrations from 250 to 1500 µM, concentrations below and above this range showed a decrease in the overall level of conversion. An increase of the concentration of phlorizin could exhibit inhibitory effects on *Pc*OGT activity. For the determination of apparent Michaelis- Menten parameters of the coupled system a lower concentration of enzymes was used than it was the case for the experiment with increasing substrate concentrations, which could explain the appearance of inhibitory effects for lower concentrations than determined beforehand. Substrate concentrations lower than 100 µM caused a significant decrease of the overall conversion, presumably due to inefficient enzyme saturation and/ or substrate degradation as degradation reactions were shown to particularly occur in the low concentration range.
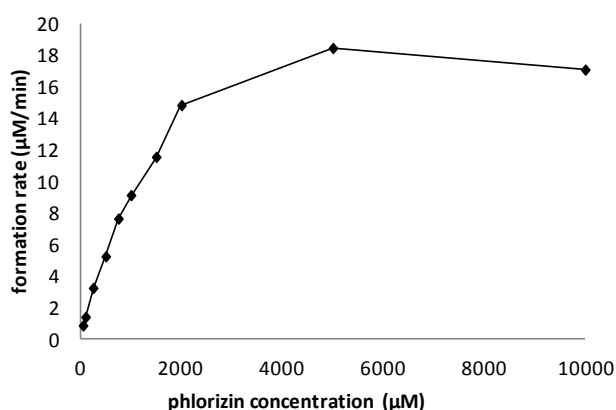
Figure 47: Nothofagin formation rate depending on different phlorizin concentrations

An increase in the phlorizin concentration caused an increase in the rate of product formation. A linear increase of the formation rate could be observed for substrate concentrations from 0 to 5000 µM, demonstrating this concentration to be optimal for product generation. A

phlorizin concentration of 10 mM led to a slight decrease in the production rate, which could be related to inhibition of *Pc*OGT. An inhibitory effect of phlorizin on *Pc*OGT would reduce the concentration of the intermediate product, which should serve as substrate for *Os*CGT for the formation of nothofagin.
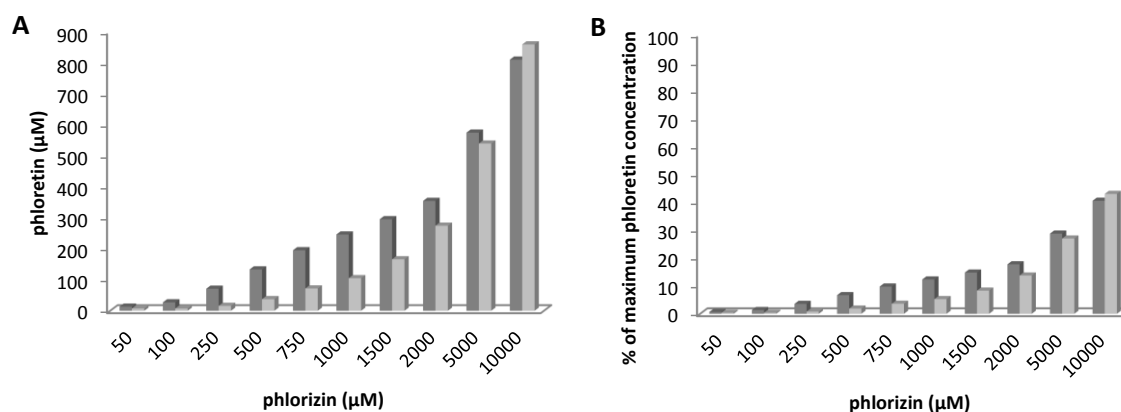
Figure 48: Concentrations of phloretin depending on different substrate concentrations (A) Graphical representations of phloretin concentrations after 25 min and 180 min of reaction, (B) Representation of phloretin concentration as percentage of maximum obtainable phloretin concentration (25 min values are given in dark- grey, 180 min values are given in light- grey)

Increasing the concentration of phlorizin provoked a nearly linear increase of the concentration of the intermediate product due to acceleration of *Pc*OGT´ s activity by providing more substrate for the reaction. The increase in the rate of the reverse *O*-glycosylation reaction was suspected to exceed the *C*-glycosylation activity thereby causing an accumulation of phloretin, as it was not sufficiently converted to the final product nothofagin. The linear increase of the phloretin concentration also verifies *Pc*OGT as not being the limiting factor of the coupled reaction system. Considering the variation of the concentration of phlorizin for the single *O*-glycosyltransferase, it can be observed that the increase of the intermediate concentration approaches a quasi- steady concentration reflected by a sigmoid curve of concentration increase. A slow-down of phloretin increase in the coupled system was not achieved. The accumulation of phloretin was also suspected to be due to phlorizin somehow exhibiting inhibitory effects on *Os*CGT; wrong binding into the active site could cause enzyme inactivation.

3.3.5 Increase of Initial substrate concentration

The concentration of phlorizin was varied from 5- 100 mM and incubated along with UDP (2 mM), 100 mU/mL *Pc*OGT and 50 mU/mL *Os*CGT in buffer (25 mM Tris/HCl, pH 7.0). The final substrate conversion and product yield was evaluated over time.

The overall substrate conversion was observed to be nearly 100 % for initial phlorizin concentrations of 5-10 mM, for higher concentrations the overall conversion was linearly decreasing. Deviations from the mass balance were determined to be about 15 %, where the highest deviation was observed for samples with relatively high initial phlorizin concentrations (>30 mM).
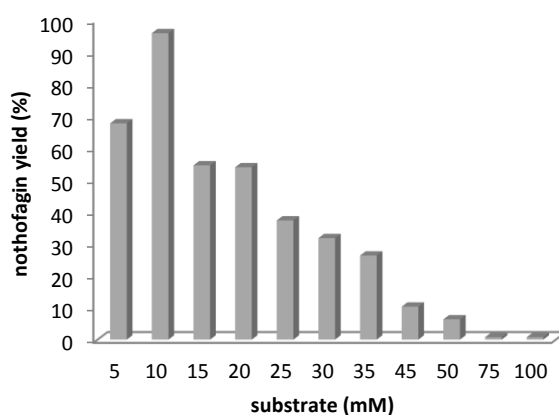
Figure 49: Final yield of nothofagin depending on different concentrations of substrate The yield was determined after 24 h of reaction using the initial concentration of substrate phlorizin as reference (shown on y-axis)

Highest product yield was obtained from 10 mM substrate and the final ratio of formed nothofagin depending on the used substrate concentration was also determined to be highest for that condition.
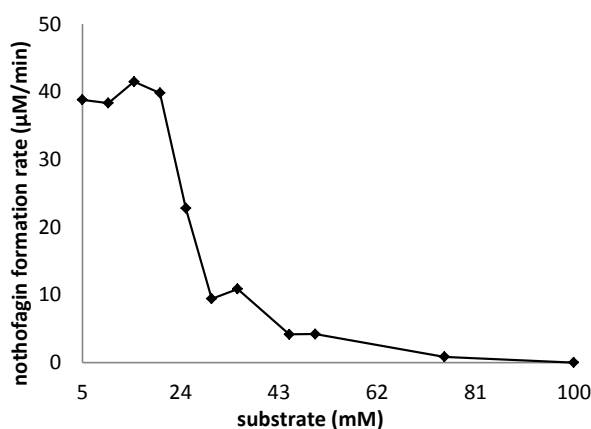
Figure 50: Rate of nothofagin formation depending on initial substrate concentration The linear increase of the product concentration was used for calculating the initial nothofagin formation rates.

Consistent with the very high nothofagin yield at a phlorizin concentration of 10 mM, also the rate of product formation was determined to be highest at this concentration. Although the overall yield was determined to decline for phlorizin concentrations of 15- 35 mM, the initial rate of product formation was not impaired. For an initial phlorizin use of more than 20 mM a drastic decrease of the nothofagin formation rate was determined; at substrate concentrations of 75-100 mM the enzymatic activity was completely lost.
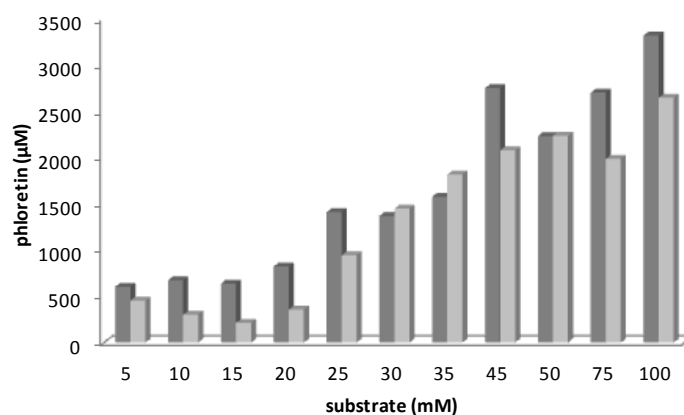
Figure 51: Final concentration of phloretin depending on substrate concentration Concentrations of phloretin were evaluated upon 1 h (dark grey bars) and upon 24 h of incubation (light-grey bars)

For phloretin it was observed that the concentration of the intermediate product increased along with the initial substrate concentration. For concentrations higher than 30 mM phlorizin a concentration of ~1500 µM and higher was measured. At comparably high phloretin concentrations a possible inhibition of OsCGT (K_i = 1500 µM) could be an explanation for a decreased conversion and product yield with increasing phlorizin concentrations. The lowest phloretin concentration was measured for a substrate concentration of 15 mM. As the product formation rate continued decreasing with increasing phlorizin concentration although the inhibitory concentration of phloretin (K_i~ 1500µM) was already reached, one could suggest additional inhibition of OsCGT by the O-glycoside. This could be due to binding of phlorizin into the active site- of the C-glycosyltransferase thereby rendering the enzyme inactive.

Increasing phloretin concentrations could also shift the reaction equilibrium of PcOGT from the reverse to the forward direction as more substrate (phloretin and UDP-glucose) would be provided. An increase of PcOGT forward reaction would also explain the apparently lower conversion of substrate as a regeneration of phlorizin was not detectable with the applied method.

3.3.6 Fed- batch conversion

To raise the final yield of nothofagin, phlorizin was converted in a fed-batch mode by regular addition of substrate to the final reaction volume over a prolonged incubation time of 70 h. Feeding with 10 mM substrate was performed twice and reached an overall concentration of 30 mM. For sample 1 (S1) only substrate was added, whereas for sample 2 (S2) additional enzymes were fed into the reaction together with fresh substrate. An additional sample (S3) was incubated solely with substrate, but no enzymes, as a control to monitor eventual precipitation reactions.
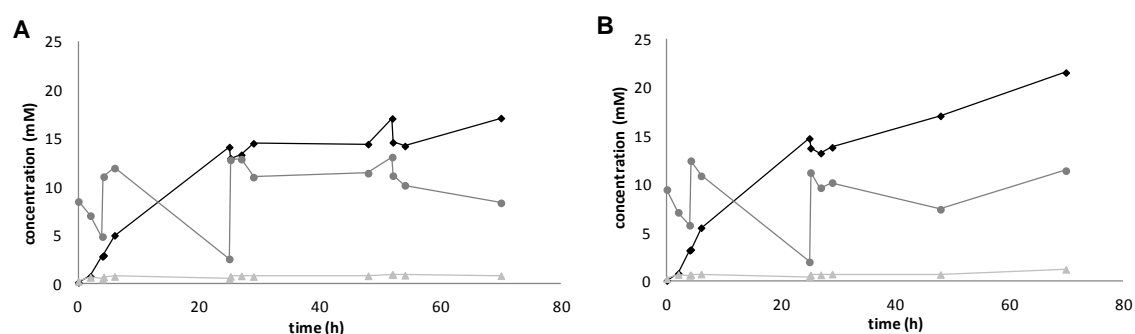
Figure 52: Concentration curves for nothofagin, phloretin and phlorizin (A) sample 1, (B) sample 2 (Nothofagin is shown in black, phloretin is shown in light- grey, phlorizin is shown in dark- grey)
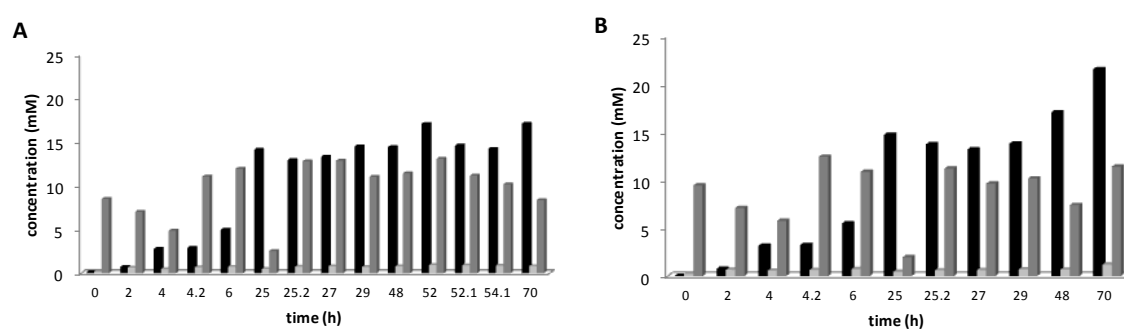
Figure 53: Concentrations in fed-batch conversions (A) sample 1, (B) sample 2 (Nothofagin is shown in black, phloretin is shown in light grey, phlorizin is shown in dark grey)

For S1 the concentration of nothofagin was constantly increasing over time, reaching a final value of about 17 mM. Final concentrations of phlorizin and phloretin were measured to be about 8.3 mM and 0.8 mM, respectively.

From Figure 52 an inactivation of enzymes with time could be assumed, as the rate of conversion was determined to decrease with increasing incubation time. Addition of enzymes at t= 50 h was shown to restart the formation of nothofagin.

For S2 fresh enzyme was appended with each round of substrate addition. A final product concentration of about 21.5 mM nothofagin was reached, with 11.4 mM of remaining phlorizin

and about 1.2 mM of the intermediate phloretin by the end of the reaction. It was observed that, compared to S1, the overall substrate conversion and product formation rate was rather constant over the whole incubation period, presumably by virtue of the regular addition of fresh enzyme along with substrate addition. It was detected that with increasing reaction time the concentration of phloretin was slightly increasing which could have provoked an inhibition of *Os*CGT (substrate inhibition by phloretin). An inhibition of the *C*- glycosyltransferase could explain the incomplete conversion of phlorizin and the overall yield of nothofagin of just 72 %.

For the control reaction (S3), substrates were incubated in buffer, but without enzymes. Fresh phlorizin was fed along with S1 and S2 and the concentrations and eventual precipitation reactions were monitored over time.

Table 23: Final concentrations of substrate, intermediate and product of fed-batch samples

sample no	phlorizin (mM)	phloretin (mM)	nothofagin (mM)
1 [a]	8.3	0.8	17.1
2 [b]	11.4	1.2	21.6

[a] substrate feed
[b] substrate and enzyme feed
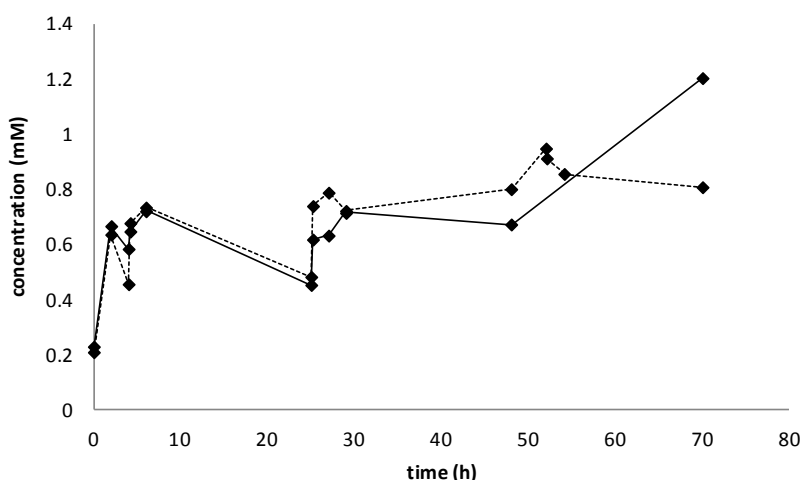
Figure 54: Phloretin concentrations of fed-batch samples 1 and 2 Sample 1 is shown by a dashed line, sample 2 is shown by a continuous line

The concentration of the intermediate product was determined to increase for both samples with time, depending on addition of substrate. Higher phloretin concentrations were measured to be achieved for S2, where fresh enzyme was added along with each substrate feed. Feeding of phlorizin also led to a higher concentration of phloretin as the intermediate concentration peaked with every feeding of substrate and was then reduced again prior next feeding (Figure 54).

The accumulation of phloretin could be explained by inhibition or inactivation of the *C*-glycosyltransferase. No limitation by one of the two enzymes would have resulted in a continuous conversion of phlorizin to phloretin by *Pc*OGT and to nothofagin by *Os*CGT. As phloretin accumulates in all reactions, one could assume an insufficient conversion into the final product, either due to a higher activity of the *O*-glycosyltransferase that is not balanced by the *C*-glycosylation reaction, or due to the beforehand reduction of *Os*CGT activity caused by substrate inhibition by phloretin as it was determined for the single enzyme ($K_i \sim 1500$ µM).

Destabilization and related inactivation of enzymes by degradation due to long incubation time could also be the reason for the accumulation of phloretin over time.
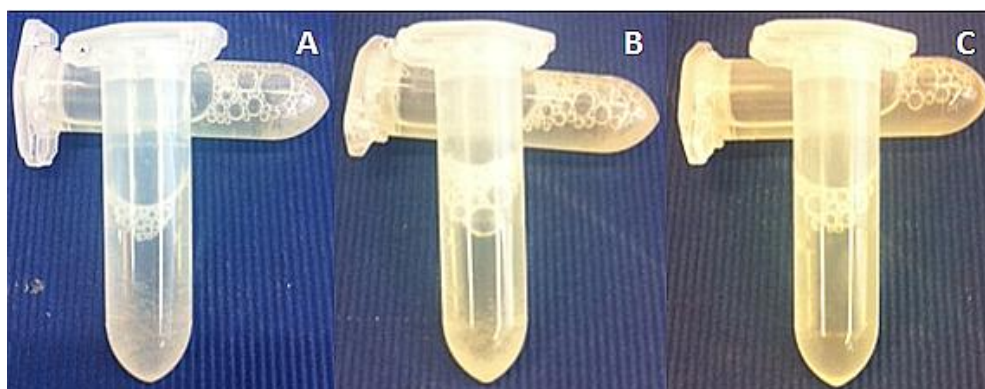
Figure 55: Photographies of fed-batch conversion samples 1-3 (A) Sample 1 – Conversion with substrate feed; (B) Sample 2 – Conversion with substrate and enzyme feed; (C) Sample 3 (control) – No conversion, but substrate feed

S3 (Figure 55, C) was incubated without enzymes but with regular substrate feed in order to monitor eventual precipitation of phlorizin with increasing concentration. No precipitation of substrate was detectable although the final concentration reached 30 mM of phlorizin by the end of the incubation time. For S1 and S2 the formation of precipitates was observed. As no precipitation could be detected for the control sample 3, precipitates in sample 1 and 2 (Figure 55, A and B) were suggested to be protein, resulting from the overall high concentration. As to S2 fresh enzyme was added with each feeding of substrate, for this sample a higher degree of precipitation was observed when compared to S1. Precipitation of protein could be the explanation for the incomplete conversion of substrate and for a lower final nothofagin yield than it was expected. Accumulated phloretin and nothofagin were assumed to contribute to the high degree of precipitation.

The incomplete conversion of substrate could be explained by inactivation of the enzymes due to the prolonged incubation time. Upon stop of the reaction, unfortunately it was not possible to close the mass overall mass balance, as the sum of all final concentrations deviated from the expected 30 mM were retrieved. The gap in the balance could be either due to oxidative

side reactions inducing product degradation or unexpected rearrangement reactions leading to a change in absorption of products in HPLC analysis.

3.4 Oxidative side reactions

It was observed that the balance of remaining substrate and generated product did not close the overall mass balance, especially when high substrate concentrations (>20 mM) were used or incubation times were prolonged (>24 h). For phlorizin concentrations higher than 15 mM a loss of up to 20 % was observed. This could be explained either by degradation of the product nothofagin or the intermediate phloretin, by solubility problems of phlorizin either in DMSO or in the reaction mixture as well as by precipitation of phlorizin due to the addition of acetonitrile prior HPLC measurement. It was detected that upon addition of acetonitrile, the reaction turned slightly turbid, the degree of which varied with varying substrate concentration in the reaction mixture. After centrifugation higher amounts of precipitate were observed for samples with higher substrate concentration.

From the theoretically used concentrations it was calculated that the gap in the balances was higher either for samples taken earlier in the reaction, which could be caused by impairment of substrate solubility. For samples that were taken after time spans of longer than 12 h it was determined that with increasing reaction time the gap in the concentration balance was also increasing, which was presumably related to nothofagin and phloretin degradation.

The gap in the final concentration balance can then be explained also by nothofagin and phloretin degradation during sample incubation. It was likely that eventual degradation products did not absorb UV- light at a wavelength of 288 nm to the same extend and therefore could not be detected during HPLC analysis. Phlorizin was not suspected to undergo degradation reaction as only two hydroxyl groups of the ring structure could participate in oxidation reactions, thereby rendering the substance more stable.

Although the amount of detectable product degradation tended to increase with incubation times higher than 12 h, the degradation reactions started coincidentally. Reasons for different degree of this phenomenon could be non- controllable concentrations of unknown oxidizing agents such as O_2 or UV- derived generation of radical species. Being antioxidants nothofagin and phloretin function as radical scavengers and are thereby occasionally degraded by long or high exposure to UV- light (33). As the reaction vessels were supposed to show high absorption, light- induced degradation could be neglected.

To verify the assumption of product degradation, the antioxidant activity and the effect of oxidation of phloretin and its glycosides was examined by incubating samples of known concentrations in aqueous solution and with oxidizing agent. The decrease of the respective peak area reflecting substance decomposition was monitored with HPLC.
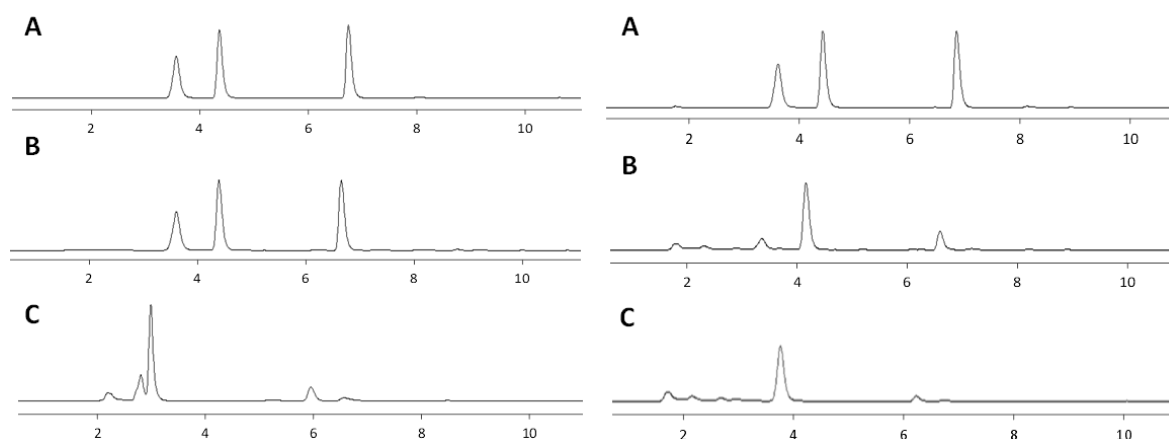
Figure 56: Oxidation of dihydrochalcones nothofagin and phlorizin and the aglycon phloretin Left graph shows the progress of oxidation reactions of sample incubated in H_2O, right graph shows the progress of oxidation reactions of sample incubated with additional oxidizing agent H_2O_2 ((A)chromatogram after 1 h, (B) chromatogram after 20 h, (C) chromatogram after 72 h of incubation); Distinction of substances according to retention time: 3.5 min nothofagin, 4.2 min phlorizin, 6.5 min phloretin

It was detected that due to the addition of H_2O_2 the degradation rate of phloretin and nothofagin was greatly enhanced. It can be seen in Figure 56 that due to the oxidation more peaks representing degradation products could be detected by HPLC analysis. Phlorizin was hardly affected by oxidation. Comparing the samples with and without oxidizing agent it can be seen that the same degree of degradation was reached with H_2O_2 even after 20 h of incubation, whereas it took 3 days for the sample without additional oxidizing agent to show the same degree of product degradation.

Table 24: Decrease of peak areas due to oxidation

	nothofagin (peak area)		phloretin (peak area)		phlorizin (peak area)	
time (h)	H_2O	H_2O_2	H_2O	H_2O_2	H_2O	H_2O_2
0	1891.9	1891.9	2774.6	2774.6	2476.4	2774.6
1	1978.0	1811.1	2727.6	2509.8	2550.4	2509.8
20	1766.0	496.4	2479.5	594.8	2467.0	594.8
72	498.8	128.4	568.0	151.5	568.0	151.5

From Table 24 the decrease or peak areas of nothofagin and phloretin can be clearly observed, which was more significant for the samples incubated with H_2O_2. Phlorizin was affected by oxidation reactions mainly by the oxidizing agent and only after long incubation times.
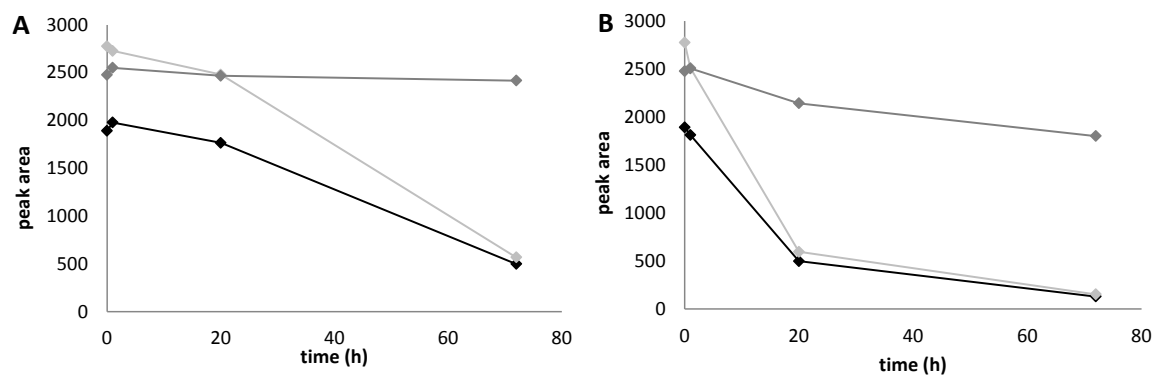
Figure 57: Oxidative degradation of nothofagin, phloretin and phlorizin (A) Product degradation in presence of H_2O, (B) Product degradation in presence of oxidizing agent H_2O_2 (Nothofagin is shown in black, phloretin is shown in light-grey, phlorizin is shown in dark-grey)

4 CONCLUSION

Nothofagin is a member of the group of phenolic antioxidants and comprises one of the principal components of rooibos tea. In nature, the substance is thought to be generated via phloretin glycosylation catalyzed by a *C*-glycosyltransferase related to *Os*CGT (rice) employing UDP-glucose as sugar donor. As nothofagin is hardly commercially available and its difficult chemical synthesis is associated with high costs, an enzyme- based route of synthesis would be of great benefit, albeit using only *Os*CGT would require high financial effort due to high costs of the nucleotide sugar donor.

Exploiting the reversibility of glycosyltransferases allows the synthesis of valuable rare NDP-sugars and allows increasing the diversity of natural products. Based on this, the basic objective of the present thesis was to establish a "two-enzyme in one-pot" system to allow the conversion of the *O*-glycoside phlorizin into the *C*-glycoside nothofagin via the intermediate aglycon phloretin. The inherent ability of *Pc*OGT to catalyze reverse glycosylation was exploited to produce phloretin and UDP-glucose from the bulk substrate phlorizin and UDP, thereby pushing the reaction towards the irreversible *C*-glycosylation catalyzed by *Os*CGT. UDP is added to the system as chemical initiator only at catalytic amounts as the *C*-glycosylation reaction facilitates UDP recovery.

Generation of the sugar donor UDP-glucose for synthesis of the final product nothofagin by the reverted *O*-glycosylation reaction makes the addition of expensive donor substrates gratuitous and the absence of side products eases the purification and processing of the final *C*-glycoside.

Coupling of two enzymes in one reaction requires assessment of reaction conditions suitable for both to allow sufficient activity in both reaction directions with high substrate conversion and high product yield. For the described system of *Pc*OGT and *Os*CGT it was determined, that factors such as pH, the concentrations of the bulk substrate phlorizin and UDP as well as the enzyme activity ratio were significantly influencing the progress and overall performance of the system. Both enzymes were determined to differ in their optimum operation range regarding pH, therefore it was important to determine the intermediate condition that allowed high conversion of phlorizin into phloretin by *Pc*OGT on the one hand and on the other sufficient activity of the *C*-glycosyltransferase to form nothofagin from phloretin. Suitable pH conditions were also determining the reaction direction of PcOGT, as for high pH the forward reaction (phloretin to phlorizin) was favored, whereas for low pH the equilibrium was shifted towards the backward reaction (phlorizin to phloretin).

Also the used solvent was demonstrated to be a determinant for sufficient product synthesis. For the single enzymes and especially in the coupled set- up DMSO was shown to be superior to EtOH; stabilizing effects by higher protein concentrations were demonstrated.

Excess phlorizin as starting material was shown to strongly inhibit the overall conversion efficiency and also elevated amounts of UDP exhibited negative effects regarding the yield of final product as accumulation of the intermediate aglycon was caused. Accumulation of phloretin was suspected to presumably decrease the yield of the final product by exhibiting inhibitory effects on the *C*-glycosyltransferase.

The *C*-glycosylation reaction was identified as the main limiting parameter of the whole system, as an increase of the applied *Os*CGT activity caused an increase in yields of nothofagin. It could be suggested that besides this other factors seemed to have influence, although these have not been clearly identified. From fed-batch conversions it could be assumed that long- term stability of the enzymes also needs to be considered, as incubation for more than 48 h caused a high level of inactivation reflected by a decrease in the product formation rate and a related lower yield.

Due to the antioxidant nature and the ability of scavenging radical oxygen species, objectionable side reactions such as product or substrate degradation were to be taken into account, although no clear trend for the occurrence thereof was observable. It could be suggested that light- or oxygen- induced reactions caused deterioration as well as precipitation of substrate and/ or products, which potentially exerted negative influence on the systems overall performance. These effects were suspected to occur with a higher frequency for prolonged incubation times and in the high concentration range for either substrate or products.

To sum up, the combination of two glycosyltransferases, one reversible (*Pc*OGT) and one irreversible (*Os*CGT), allows the sufficient conversion of *O*- into *C*-glycosides via one intermediate product. As mentioned beforehand, this system is advantageous with regard of bulk substrate and sugar donor usage as well as product purification and processing.

5 ABBREVIATIONS

GT	glycosyltransferase
UGT	UDP-dependent glycosyltransferase
UDP	uridine diphosphate
PSPG- motif	putative secondary plant glycosyltransferase motif
O-GT	*O*- glycosyltransferase
C-GT	*C*- glycosyltransferase
LDL	low density lipoprotein
SGLT2	sodium glucose linked transporter 2
NDP	nucleotide diphosphate
UDP-glc	uridine disphosphate glucose
UDP-gal	uridine diphosphate galactose
*Pc*OGT	*Pyrus communis O*-glycosyltransferase
*Os*CGT	*Oryza sativa C*-glycosyltransferase
OE-PCR	overlap- extension polymerase chain reaction
SOC- medium	super optimal broth medium
PEG	polyethylene glycol
LiAc	lithium acetate
IPTG	isopropyl-β-D-galactopyranoside
SDS PAGE	sodium dodecyl sulphate polyacrylamide gel
DMSO	dimethyl sulphoxide
EtOH	ethanol
EDTA	ethylenediaminetetraacetic acid
HABA	hydroxyl-azo-benzoic acid
BCA	bicinchoninic acid
BSA	bovine serum albumin
PK/LDH	pyruvate kinase/ lactic acid dehydrogenase
AcN	acetonitrile
TFA	trifluoracetic acid
HPLC	high performance liquid chromatography

6 LIST OF FIGURES

7 LIST OF TABLES

8 REFERENCES

1. **Gachon, C. M., Langlois-Meurinne, M. and Saindrenan, P.** Plant secondary metabolism glycosyltransferases: the emerging functional analysis. *Trends Plant Sci.* 2005, 10, pp. 542- 549.

2. **Jones, P. and Vogt, T.** Glycosyltransferases in secondary plant metabolism: tranquilizers and stimulant controllers. *Planta.* 2001, 213, pp. 164- 174.

3. **Koeller, K. M. and Wong, C. H.** Emerging themes in medicinal glycoscience. *Nat Biotechnol.* 2000, 18, pp. 835- 841.

4. **Harborne, J. B. and Baxter, H.** The Handbook of Natural Flavonoids. Chichester : Wiley, 1999.

5. **Griffith, B. R., Langenhan, J. M. und Thorson, J. S.** "Sweetening" natural procuts via glycorandomization. *Curr Opin Biotechnol.* 2005, 16, S. 622- 630.

6. **Thibodeaux, C. J., Melancon, C. E. and Liu, H. W.** Unusual sugar biosynthesis and natural product glycodiversification. *Nature.* 2007, 446, pp. 1008- 1016.

7. **Mackenzie, P. I.; Owens, I. S.; Burchell, B.; Bock, K. W.; Bairoch, A.; Belanger, A.; Fournel-Gigleux, S.; Green, M.; Hum, D. W.; Iyanagi, T.; Lancet, D.; Louisot, P.; Magdalou, J.; Chowdhury, J. R.; Ritter, J. K.; Schachter, H.; Tephly, T. R.; Tipton, K. F. and Nebert, D. W.;.** The UDP glycosyltransferase gene superfamily: recommended nomenclature update based on evolutionary divergence. *Pharmacogenetics.* 1997, 7, pp. 255- 269.

8. **Campbell, J. A.; Davies, G. J.; Bulone, V. and Henrissat, B.** A classification of nucleotide-diphospho- sugar glycosyltransferases based on amino acid sequence similarities. *Biochem J.* 1997, 326 (Pt3), pp. 929- 939.

9. **Coutinho, P. M.; Deleury, E.; Davies, G. J. and Henrissat, B.** An evolving hierarchial family classification for glycosyltransferases. *J Mol Biol.* 2003, 328, pp. 307- 317.

10. **Hughes, J. and Hughes, M. A.** Multiple secondary plant product UDP-glucose glucosyltransferase genes expressed in cassava (*Manihot esculenta* Crantz) cotyledons. *DNA Seq.* 1994, 5, pp. 41-49.

11. **Osmani, S. A., Bak, S. and Moller, B. L.** Substrate specificity of plant UDP-dependent glycosyltransferases predicted from crystal structures and homology modeling. *Phytochemistry.* 2009, 70, pp. 325- 347.

12. **Lim, E. K. and Bowles, D. J.** A class of plant glycosyltransferases involved in cellular homeostasis. *EMBO J.* 2004, 23, pp. 2915-2922.

13. **Paquette, S., Moller, B. L. and Bak, S.** On the origin of family 1 plant glycosyltransferases. *Phytochemistry.* 2003, 62, pp. 399- 413.

14. **Hefner, T.; Arend, J.; Warzecha, H.; Siems, K. and Stockigt, J.** Arbutin synthase, a novel member of the NRD1beta glycosyltransferase family, is a unique multifunctional enzyme

converting various natural products and xenobiotics. *Bioorg Med Chem.* 2002, 10, pp. 17341- 17414.

15. **Miller, K. D.; Guyon, V.; Evans, J. N.; Shuttleworth, W. A. and Taylor, L. P.** Purification, cloning and heterologous expression of a catalytically efficient flavonol-3-*O*-galactosyltransferse expressed in the male gametophyte of *Petunia* hybrid. *J Biol Chem.* 1999, 274, pp. 34011- 34019.

16. **Modolo, L. V.; Blount, J. W.; Achnine, L.; Naoumkina, M. A.; Wang, X. and Dixon, R. A.** A functional genomics approach to (iso)flavonoid glycosylation in the model legume *Medicago truncatula*. *Plant Mol Biol.* 2007, 64, pp. 499- 518.

17. **Sawada, S.; Suzuki, H.; Ichimaida, F.; Yamaguchi, M.; Iwashita, T.; Fukui, Y.; Hemmi, N.; Nishino, T. and Nakayama, T.** UDP-glucoronic acid:anthocyanin-glucoronosyltransferase from red daisy (*Bellis perennis*) flowers: enzymology and phylogenetics of a novel glycosyltransferase involved in flower pigment biosynthesis. *J Biol Chem.* 2005, 280, pp. 899- 906.

18. **Yonekura-Sakakibara, K.; Tohge, T.; Niida, R. and Saito, K.** Identification of a flavonol-7-O-rhamnosyltransferase gene determining flavonoid pattern in *Arabidopsis* by transcriptome coexpression analysis and reverse genetics. *J Biol Chem.* 2007, 164, pp. 574- 580.

19. **Shao, H.; He, X.; Achnine, L.; Blount, J. W.; Dixon, R. A. and Wang, X.** Crystal structure of a multifunctional triterpene/flavonoid glycosyltransferase from *Medicago truncatula*. *Plant Cell.* 2005, 17, pp. 3141- 3154.

20. **Offen, W.; Martinez-Fleites, C.; Yang, M.; Kiat-Lim, E.; Davis, B. G.; Tarling, C. A.; Ford, C. M.; Bowles, D. J. and Davies, G. J.** Structure of a flavonoid glycosyltransferase reveals the basis for plant natural product modification. *EMBO J.* 2006, 25, pp. 1396- 1405.

21. **Li, L.; Modolo, L. V.; Escamilla-Trevino, L. L.; Achnine, L.; Dixon, R. A. and Wang, X.** Crystal structure of *Medicago truncatula* UGT85H2- insights into the structural basis of a multifunctional (iso)flavonoid glycosyltransferase. *J Mol Biol.* 2007, 370, pp. 951- 963.

22. **Brazier-Hicks, M.; Offen, W. A.; Gershater, M. C.; Revett, T. J.; Lim, E. K.; Bowles, D. J.; Davies, G. J. and Edwards, R.** Characterization and engineering of the bifunctional *N*- and *O*-glycosyltransferase involved in xenobiotic metabolism in plants. *Proc Natl Acad Sci.* 2007, 104, pp. 20238- 20243.

23. **Hu, Y. and Walker, S.** Remarkable structural similarities between diverse glycosyltransferases. *Chem Biol.* 2002, 9, pp. 1287- 1296.

24. **Lim, E. K.** Plant glycosyltransferases: their potential as novel biocatalysts. *Chemistry.* 2005, 11, S. 5486- 5494.

25. **Breton, C.; Bettler, E.; Joziasse, D. H.; Geremia, R. A. and Imberty, A.** Sequence function relationships of prokaryotic and eukaryotic galactosyltransferases. *J Biochem.* 1998, 123, pp. 1000- 1009.

26. **Breton, C. and Imberty, A.** Structure function studies of glycosyltransferases. *Curr Opin Struct Biol.* 1999, 9, pp. 563- 571.

27. **Lairson, L. L.; Henrissat, B.; Davies, G. J. and Withers, S. G.** Glycosyltransferases: Structures, Functions and Mechanisms. *Annu Rev Biochem.* 2008, 77, pp. 521- 555.

28. **Durr, C.; Hoffmeister, D.; Wohlert, S. E.; Ichinose, K.; Weber, M. and von Mulert, U.;.** The glycosyltransferase UrdGT2 catalyzed both *C*- and *O*-glycosidic sugar transfers. *Angewandte Chemie- International Edition.* 2004, 43(22), pp. 2962- 2965.

29. **Gutmann, A. and Nidetzky, B.** Switching between *O*- and *C*-glycosyltransferase through exchange of active- site motifs. *Angew Chem Int Ed.* 2012, 51, pp. 1- 6.

30. **Hammerstone, J. F., Lazarus, S. A. and Schmitz, H. H.** Procyanidin content and variation in some commonly consumed foods. *J Nutr.* 2000, 130, pp. 2086S-2092S.

31. **Cook, N. C. and Samman, S.** Flavonoids: chemistry, metabolism, cardioprotective effects and dietary sources. *J Nutr Biochem.* 1996, 7, S. 66- 76.

32. **Heim, K. E., Tagliaferro, A. R. and Bobilya, D. J.** Flavonoid antioxidants: chemistry, metabolism and structure-activity relationships. *Journal of Nutritional Biochemistry.* 2002, 13, pp. 572- 584.

33. **Rice- Evans, C. A., Miller, N. J. and Paganga, G.** Antioxidant properties of phenolic compounds. *Trends in plant science: reviews.* 1997, 4, 2, pp. 152- 159.

34. **Rezk, B. M.; Haenen, G. R.; van der Vijgh, W. J. and Blast, A.** The antioxidant activity of phloretin: the disclosure of a new antioxidant pharmacophore in flavonoids. *Biochem Biophys Res Commun.* 2002, 295, pp. 9- 13.

35. **Ferrali, M.; Signorini, C.; Ciaciotti, B.; Sugherini, L.; Ciccoli, L.; Giochetti, D. and Comporti, M.** Protection against oxidative damage of erythrocyte membranes by the flavonoids quercetin and its relation to iron chelating activity. *FEBS Lett.* 1997, 416, pp. 123- 129.

36. **Kondo, K.; Hirano, R.; Matsumoto, A.; Igarashi, O. and Itakura, H.** Inhibition of LDL oxidation by cocoa. *Lancet.* 1996, 348, pp. 1514- 1518.

37. **Mazur, A.; Bayle, D.; Lab, C.; Rock, E. and Rayssiguier, Y.** Inhibitory effect of procyanidin- rich extracts on LDL oxidation in vitro. *Atherosclerosis.* 1999, 145, pp. 421- 422.

38. **Plumb, G. W., Price, K. R. and Williamson, G.** Antioxidant properties of flavonol glycosides from tea. *Redox Rep.* 1999, 4, pp. 13- 16.

39. **Nakamura, Y.; Watanabe, S.; Miyake, N.; Kohno, H. and Osawa, T.** Dihydrochalcones: Evaluation as novel radical scavenging antioxidants. *J Agric Food Chem.* 2003, 51, pp. 3309- 3312.

40. **Watts, K. T., Lee, P. C. and Schmidt-Dannert, C.** Exploring recomninant flavonoid biosynthesis in metabolically engineered *Escherichia coli. Chembiochem.* 2004, 5, pp. 500- 507.

41. **Pontais, I.; Treutter, D.; Paulin, J. P. and Brisset, M. N.** *Erwinia amylovora* modifies phenolic profiles of susceptible and resistant aplle through it type III secretion system. *Physiol Plant.* 2008, 132, pp. 262- 271.

42. **Burda, S., Oleszek, W. and Lee, C. Y.** Phenolic compounds and their changes in apples durimg maturation and cold storage. *J Agric Food Chem.* 1990, 38, pp. 945- 948.

43. **Williams, A. H.** Dihydrochalcones of *Malus* species. *J Chem Soc.* 1961, 155, pp. 4133- 4136.

44. **Valenta, C.; Cladera, J.; O´Shea, P. and Hadgraft, J.;.** Effect of phloretin on the percutaneous absorption of lignocaine across human skin. *J Pharm Sci.* 2001, 90, pp. 485- 492.

45. **Gaudot, D.** Phloridzin-rich phenolic fraction and use thereof as a cosmetic, dietary of nutraceutical agent. US2006073223 2006.

46. **Gosch, C.; Halbwirth, H.; Schneider, B.; Hölscher, D. and Stich, K.** Cloning and heterologous expression of glycosyltransferases from *Malus* x *domestica* and *Pyrus communis*, which convert phloretin to phloretin 2-*O*-glycoside (phloridzin). *Plant Science.* 2010, 178, pp. 299- 306.

47. **Ehrenkranz, J. R.; Lewis, N. G.; Kahn, C. R. and Roth, J.** Phlorizin: a review. *Diabetes Metab Res Rev.* 2005, 21, pp. 31- 38.

48. **Williams, A. H.** Dihydrochalcones: their occurence and use as indicators in chemical plant taxonomy. *Nature.* 1964, 202, pp. 824- 825.

49. **White, J. R.** Apple trees to sodium glucose co-transporter inhibitors: a review of SGLT2 inhibition. *Clinical Diabetes.* 2010, 28(1), pp. 5- 10.

50. **Joubert, E. and Schultz, H.** Production and quality aspects of rooibos tea and related products: a review. *J Appl Bot Food Qual.* 2006, 80, pp. 138- 144.

51. **Hillis, W. E. and Inoue, T.** The polyphenols of *Nothofagus* species II- The heartwoodof Nothofagus fusca. *Phytochemistry.* 1967, 6, pp. 59- 67.

52. **van der Merwe, J. D.; Joubert, E.; Manley, M.; de Beer, D.; Malherbe, C. J. and Gelderblom, W.C. A.** In vitro hepatic biotransformation of aspalathin and nothofagin, dihydrochalcones of rooibos (*Aspalathus linearis*) and assessment of metabolite antioxidant activity. *J Agric Food Chem.* 2010, 58, pp. 2212- 2220.

53. **Krafcyk, N., Woyand, F. and Glomb, M. A.** Structure-antioxidant relationships of flavonoids from fermented rooibos. *Mol Nutr Food Res.* 2009, 53, pp. 635- 642.

54. **Snijman, P. W.; Joubert, E.; Ferreira, D.; Li, X. C.; Ding, Y.; Green, I. R. and Gelderblom, W.C. A.** Antioxidant activity of the dihydrochalcones aspalathin and nothofagin and their corresponding flavones in relation to other rooibos (*Aspalathus linearis*) flavonoids epigallocatachin, gallate and Trolox. *J Agric Food Chem.* 2009, 57, pp. 6678- 6684.

55. **Koeppen, B. H. and Roux, D. G.** *C*-glycosylflavonoids: the chemistry of aspalathin. *Biochem J.* 1966, 99, pp. 604- 609.

56. **Ypremyan, A., Salehani, B. and Minehan, T.** Concise total synthesis of aspalathin and nothofagin. *Organic Letters.* 2010, 12(7), pp. 1580- 1582.

57. **Koeller, K. M. and Wong, C. H.** Synthesis of complex carbohydrates and glycoconjugates: Enzyme- based and programmable one- pot strategies. *Chem Rev.* 2000, 100, pp. 4465- 4493.

58. **Zhang, C.; Griffith, B. R.; Albermann, C.; Fu, X.; Lee, I. K.; Li, L. and Thorson, J. S.** Exploiting the reversibility of natural product glycosyltransferase- catalyzed reactions. *Science.* 2006, 313, S. 1291- 1294.

59. **Bode, H. B. and Müller, R.** Reversible sugar transfer by glycosyltransferases as a tool for natural product (bio)synthesis. *Angew Chem Int Ed.* 2007, 46, pp. 2147- 2150.

60. **Minami, A., Kakinuma, K. und Eguchi, T.** Aglycon switch approach toward unnatural glycosides from natural glycoside with glycosyltransferase VinC. *Tetrahedron Letters.* 2005, 46, S. 6187- 6190.

61. **Yang, J.; Hoffmeister, D.; Liu, L.; Fu, X. and Thorson, J. S.** Natural product glycorandomization. *Bioorg Med Chem.* 2004, 12, S. 1577- 1584.

62. **Williams, G. J.; Yang, J.; Zhang, C. and Thorson, J.S.** Recombinant *E.coli* prototype strains for in vivo glycorandomization. *ACS chemical biology.* 2010, 6(8), pp. 95-100.

63. **Brazier-Hicks, M.; Evans, K. M.; Gershater, M. C.; Puschmann, H.; Steel, P. G. and Edwards, R.** The *C*-glycosylation of flavonoids in cereals. *Journal of Biological Chemistry.* 2009, 284, pp. 17926- 17934.

64. **Gietz, R. D. und Woods, R. A.** Transformation of yeast by the LiAc/SS-carrier DNA/ PEG method. *Methods in Enzymology.* 2002, 350, S. 87- 96.

65. **Studier, W. F.** Protein production by auto-induction in high-density shaking cultures. *Prot Expr Pur.* 2005, 41, S. 207- 234.

9 APPENDIX

9.1 Components of ZYM 5052- Medium

Table 25: Components of solution M

component	concentration (M)
$Na_2HPO_4*2H_2O$	1.25
KH_2PO_4	1.25
NH_4Cl	2.50
Na_2SO_4	0.25

Table 26: Components of solution 5052

component	concentration (%)
glycerol	25.0
glucose	2.5
α-D-lactose	10.0

Table 27: Components of trace element solution

component	concentration (M)
$FeCl_3$	0.1
$CaCl_2$	2.0
$MnCl_2$	2.0
$ZnSO_4$	2.0
$CoCl_2$	2.0
$CuCl_2$	2.0
$NiCl_2$	1.0
Na_2MoO_4	1.0
Na_2SeO_3	2.0
H_3BO_3	0.2

9.2 Kinetic characterization of single enzymes

9.2.1 *Pc*OGT

9.2.1.1 Forward reaction: Phloretin

Table 28: Initial reaction rates of *Pc*OGT forward reaction depending on different phloretin concentrations

phloretin concentration (µM)	initial reaction rate (µM/min)
0	0.0
5	0.0
10	0.0
20	108.6
30	333.3
50	506.7
75	681.0
100	666.2
125	628.6
250	557.6
500	456.2
750	252.3

Figure 58: Graphical representation of Michaelis- Menten parameters for phloretin in *Pc*OGT forward reaction Phloretin concentrations were varied from 5- 750 µM, UDP-glucose concentration was kept constant (2 mM); Calculations were performed using SigmaPlot 9.0

Table 29: Apparent kinetic parameters for phloretin in *Pc*OGT forward reaction

v_{max} (µM/min)	K_m (µM)	K_i (µM)	k_{cat} (s^{-1})	k_{cat}/K_m (s^{-1}µM^{-1})
3846.760 ± 4486.534	310.747 ± 425.221	59.207 ± 80.736	2.734	0.009

9.2.1.2 Forward reaction: UDP-glucose

Table 30: Initial reaction rates of *Pc*OGT forward reaction depending on different UDP-glucose concentrations

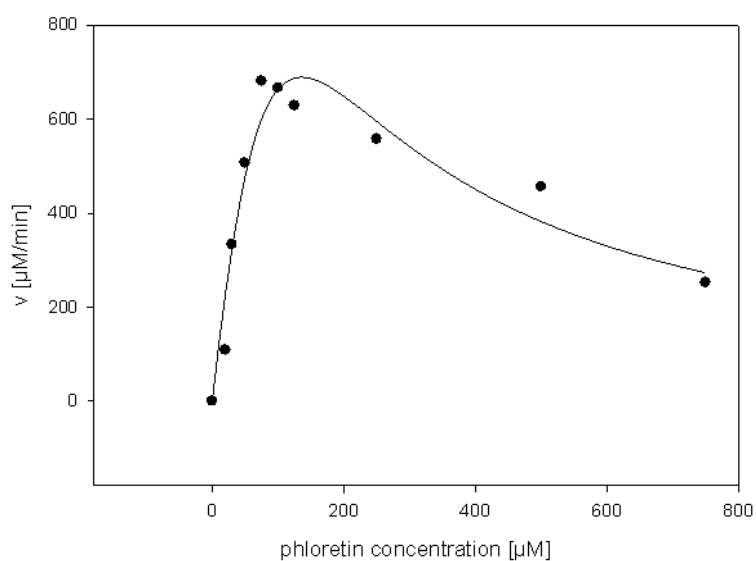| UDP-glucose concentration (µM)	initial reaction rate (µM/min)
0.00	0.0
25.00	2301.7
37.50	2494.7
56.25	5016.9
75.00	5517.4
93.75	5291.6
187.50	7329.7
375.00	8197.9
562.50	8203.6
750.00	7950.9
1125.00	8425.4
2250.00	8349.1
3750.00	8411.3

Figure 59: Graphical representation of Michaelis- Menten parameters for UDP-glucose in *Pc*OGT forward reaction UDP-glucose concentration was varied from 25 to 3750 µM, phloretin concentration was kept constant (250 µM); Calculations were performed using SigmaPlot 9.0

Table 31: Apparent kinetic parameters for UDP-glucose in *Pc*OGT forward reaction

v_{max} (µM/min)	K_m (µM)	k_{cat} (s^{-1})	k_{cat}/K_m (s^{-1}µM^{-1})
8851.402 ± 247.783	56.329 ± 7.214	6.291	0.112

9.2.1.3 Forward reaction: UDP-galactose

Table 32: Initial reaction rates of *Pc*OGT forward reaction depending on different concentrations of UDP-galactose

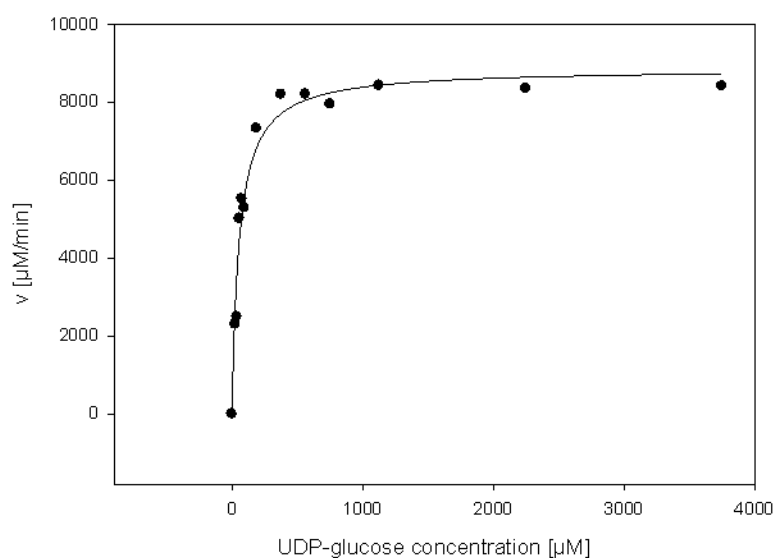| UDP-galactose concentration (µM)	initial reaction rate (µM/min)
0	0
10	14.5
25	21.2
50	39.4
100	51.5
500	308.7
1000	318.6
2500	504.4
5000	743.4
10000	701.9
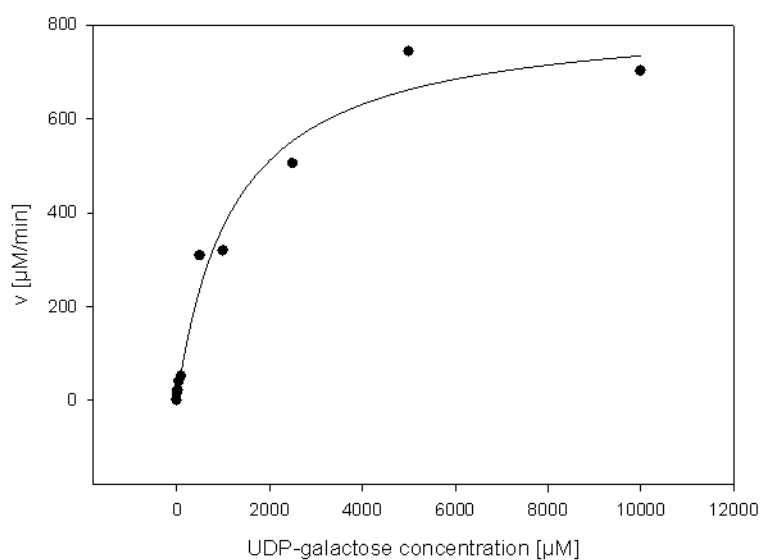
Figure 60: Graphical representation of Michaelis- Menten parameters for UDP-galactose in *Pc*OGT forward reaction UDP-galactose concentration was varied from 0 to 10000 µM, phloretin concentration was kept constant (200 µM); Calculations were performed using SigmaPlot 9.0

Table 33: Apparent kinetic parameters for UDP-galactose in *Pc*OGT forward reaction

v_{max} (µM/min)	K_m (µM)	k_{cat} (s^{-1})	k_{cat}/K_m (s^{-1}µM^{-1})
824.007 ± 57.339	1222.855 ± 285.968	0.245	0.0002

9.2.1.4 Reverse reaction: Phlorizin

Table 34: Initial reaction rates of *Pc*OGT reverse reaction depending on different phlorizin concentrations

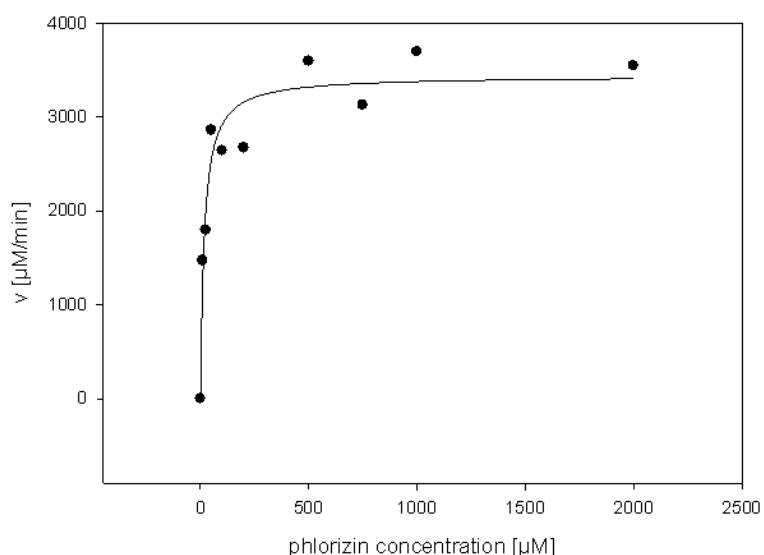| phlorizin concentration (µM)	initial reaction rate (µM/min)
0	0
10	1469.8
25	1794.1
50	2859.3
100	2640.7
200	2671.2
500	3594.6
750	3126.2
1000	3693.9
2000	3546.1
5000	2781.5

Figure 61: Graphical representation of Michaelis- Menten parameters for phlorizin in *Pc*OGT reverse reaction Phlorizin concentration was varied from 10 to 5000 µM, UDP concentration was kept constant (2 mM); Calculations were performed using SigmaPlot 9.0

Table 35: Apparent kinetic parameters for phlorizin in *Pc*OGT reverse reaction

v_{max} (µM/min)	K_m (µM)	k_{cat} (s^{-1})	k_{cat}/K_m (s^{-1}µM^{-1})
3435.795 ± 151.573	17.667 ± 4.746	1.022	0.058

9.2.1.5 Reverse reaction: UDP

Table 36: Initial reaction rates of *Pc*OGT reverse reaction depending on different concentrations of UDP

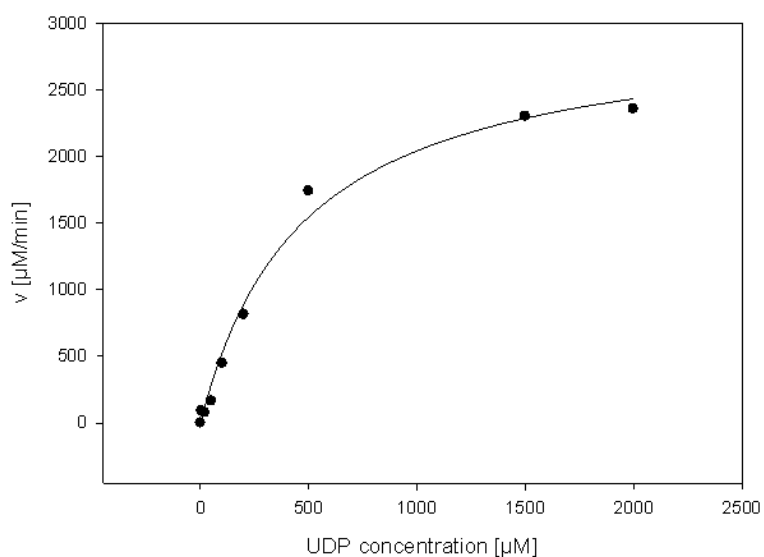| UDP concentration (µM)	initial reaction rate (µM/min)
0	0
5	91.5
20	79.4
50	164.7
100	447.7
200	814.6
500	1740.6
750	2528.0
1000	4384.2
1500	2300.8
2000	2356.1

Figure 62: Graphical representation of Michaelis- Menten parameters for UDP in *Pc*OGT reverse reaction
UDP concentration was varied from 5 to 2000 µM, phlorizin concentration was kept constant (5 mM); Calculations were performed using SigmaPlot 9.0

Table 37: Apparent kinetic parameters for UDP in *Pc*OGT reverse reaction

v_{max} (µM/min)	K_m (µM)	k_{cat} (s^{-1})	k_{cat}/K_m (s^{-1}µM^{-1})
3005.346 ± 168.300	471.955 ± 76.750	0.895	0.002

9.2.2 *Os*CGT

9.2.2.1 Phloretin

Table 38: Initial reaction rates of *Os*CGT depending on different concentrations of phloretin

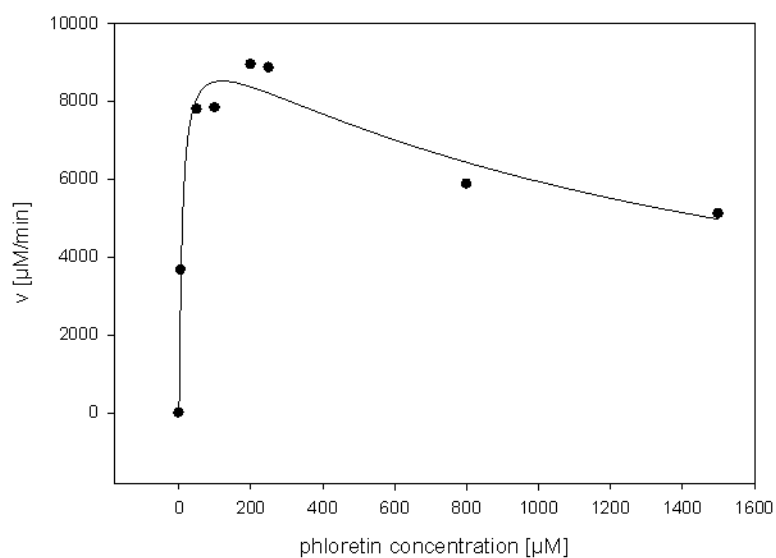| phloretin concentration(µM)	initial reaction rate (µM/min)
0	0
5	3664.2
25	13571.2
50	7788.5
100	7828.4
200	8934.3
250	8852.5
600	32109.9
800	5871.7
1500	5105.7
5000	188.8

Figure 63: Graphical representation of Michaelis- Menten parameters for phloretin for *Os*CGT reaction
Phloretin concentration was varied from 0 to 5000 µM, UDP-glucose concentration was kept constant (2 mM); Calculations were performed using SigmaPlot 9.0

Table 39: Apparent kinetic parameters for phloretin in *Os*CGT reaction

v_{max} (µM/min)	K_m (µM)	K_i (µM)	k_{cat} (s^{-1})	k_{cat}/K_m ($s^{-1}µM^{-1}$)
9830.398 ± 593.490	9.229 ± 2.752	1543.260 ± 401.641	22.074	2.392

9.2.2.2 UDP-glucose

Table 40: Initial reaction rates of *Os*CGT depending on different concentrations of UDP-glucose

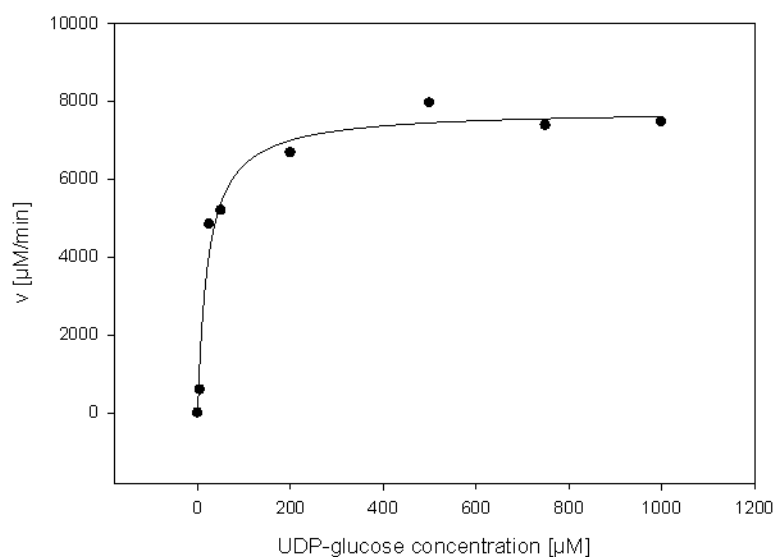| UDP-glucose concentration (µM)	initial reaction rate (µM/min)
0	0
5	588.1
25	4840.4
50	5196.6
100	9946.5
200	6675.1
500	7950.1
750	7372.4
1000	7461.5
1500	12045.7
2000	6161.6

Figure 64: Graphical representation of Michaelis- Menten parameters for UDP-glucose of *Os*CGT reaction
UDP-glucose concentration was varied from 5 to 2000 µM, phloretin concentration was kept constant (1 mM); Calculations were performed using SigmaPlot 9.0

Table 41: Apparent kinetic parameters for UDP-glucose in *Os*CGT reaction

v_{max} (µM/min)	K_m (µM)	k_{cat} (s^{-1})	k_{cat}/K_m (s^{-1}µM^{-1})
7769.742 ± 318.814	22.206 ± 5.040	17.448	0.786

9.3 Kinetic characterization of coupled system

9.3.1 Phlorizin

Table 42: Apparent initial reaction rates of the coupled system depending on different concentrations of phlorizin

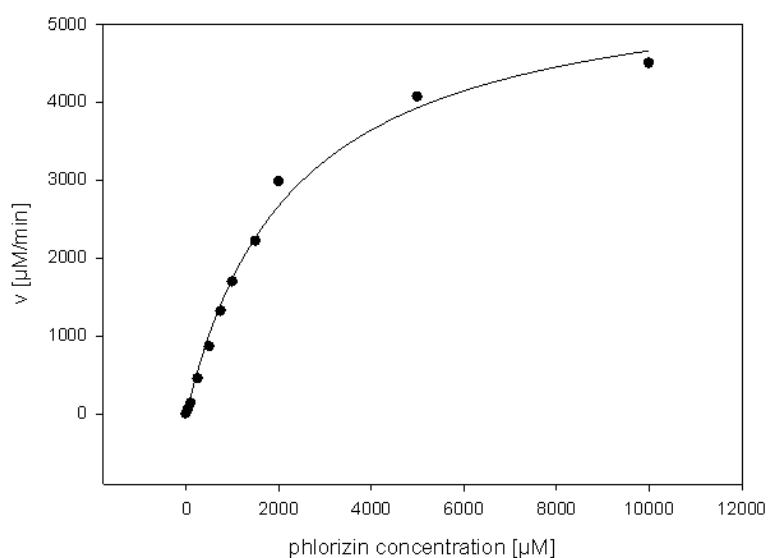| phlorizin concentration (µM)	initial reaction rate (µM/min)
0	0.0
50	64.9
100	136.3
250	450.8
500	863.3
750	1316.2
1000	1693.3
1500	2214.0
2000	2981.4
5000	4065.7
10000	4496.3

Figure 65: Graphical representation of apparent Michaelis- Menten characteristics of the coupled reaction system Phlorizin concentration was varied from 0 to 5000 µM, UDP concentration was kept constant (2 mM). Parameters were calculated via the rate of overall product formation (sum of phloretin and nothofagin); Calculations were performed using SigmaPlot 9.0

Table 43: Apparent kinetic parameters for phlorizin in coupled reaction system

v_{max} (µM/min)	K_m (µM)	k_{cat} (s^{-1})	k_{cat}/K_m (s^{-1}µM^{-1})
5718.572 ± 246.838	2279.852 ± 234.999	1.702	0.001

9.3.2 UDP

Table 44: Apparent initial reaction rates of the coupled system depending on different concentrations of UDP

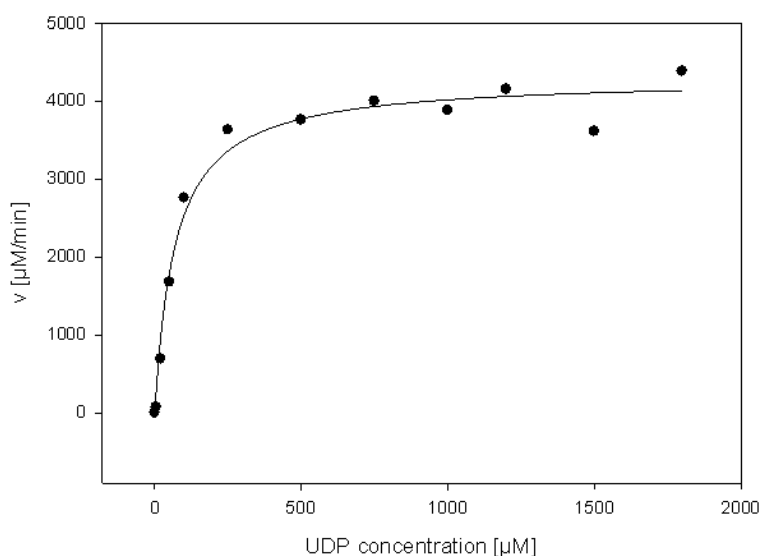| UDP concentration (µM)	initial reaction rate (µM/min)
0	0.0
5	75.1
20	693.1
50	1677.5
100	2758.6
250	3631.1
500	3757.4
750	3999.1
1000	3880.6
1200	4152.3
1500	3610.2
1800	4380.7
2000	3546.7

Figure 66: Graphical representation of apparent Michaelis- Menten characteristics of the coupled reaction system UDP concentration was varied from 5 to 2000 µM, phlorizin concentration was kept constant (5 mM). Parameters were calculated via the rate of overall product formation (sum of phloretin and nothofagin); Calculations were performed using SigmaPlot 9.0

Table 45: Apparent kinetic parameters for UDP in coupled reaction system

v_{max} (µM/min)	K_m (µM)	k_{cat} (s^{-1})	k_{cat}/K_m (s^{-1}µM^{-1})
4293.853 ± 128.488	69.443 ± 11.543	1.015	0.015